Aus der Medizinischen Klinik und Poliklinik V,
Klinik der Ludwig-Maximilian-Universität München

Sektion Pneumologie Innenstadt und Thorakale Onkologie

Vorstand: Prof.Dr.med.Jürgen Behr

PD-L1 enhanced cisplatin resistance in Non-Small Cell Lung Cancer through PI3K/AKT/mTOR

Dissertation
zum Erwerb des Doktorgrades der Medizin
an der Medizinischen Fakultät der
Ludwig-Maximilians-Universität zu München

vorgelegt von
Yinhui Xu
aus Xuchang, Henan, China
2022

Mit Genehmigung der Medizinischen Fakultät der
Ludwig-Maximilians-Universität München

Berichterstatter:	Prof.Dr. Rudolf M.Huber
Mitberichterstatter:	Prof. Dr. David Anz
Mitbetreuung durch die promovierten Mitarbeiter:	PD Dr. Amanda Tufman Dr. Diego Kauffmann-Guerrero
Dekan:	Prof. Dr. med. Thomas Gudermann
Tag der mündlichen Prüfung:	29.09.2022

Table of Contents

List of figures

List of abbreviations

Full name	Abbreviation
Programmed cell death 1 ligand 1	PD-L1
Programmed cell death protein 1	PD-1
Non-small cell lung cancer	NSCLC
Small cell lung cancer	SCLC
Phosphoinositide 3-kinase	PI3K
Protein kinase B	AKT
Phospho-Protein kinase B	p-AKT
Mammalian target of rapamycin	mTOR
Phospho-Mammalian target of rapamycin	p-mTOR
Ribosomal protein S6	S6
Phospho-ribosomal protein S6	p-S6
PI3K/AKT/mTOR signaling pathway	PATSP
Real-time reverse transcription PCR	qRT-PCR
Flow cytometry	FCM
Major pathological remission	MPR
Immunohistochemistry	IHC
Body surface area	BSA
Fetal bovine serum	FBS
Phosphate-buffered saline	PBS
Half maximal inhibitory concentration	IC50
Concentration for 50% of maximal effect	EC50
Computed tomography	CT
Magnetic resonance imaging	MRI
Positron emission tomography	PET

Cisplatin (cis-diamminedichloroplatinum II)	DDP
Major histocompatibility complex class I	MHC-I
Phosphatase and tensin homolog deleted on chromosome10	PTEN
Carcinoembryonic antigen	CEA
Cancer testis antigens	CTA
Food and Drug Administration	FDA
Epidermal growth factor receptor	EGFR
EGFR-tyrosine kinase inhibitor	EGFR-TKI
Tumor microenvironment	TME
Tumor associated antigens	TAA
Immunogenic cell death	ICD
Myeloid-derived suppressor cells	MDSC
Glycogen synthase kinase 3 beta	GSK-3β
Phosphoinositide-dependent kinase	PDK
Dimethyl sulphoxide	DMSO
Analysis of Variance	ANOVA
Adenosine triphosphate	ATP

Abstract-Summary

Objective:
Non-small cell lung cancer (NSCLC) is a disease with high morbidity and mortality. Cisplatin (DDP) is one of the most widely used chemotherapy regimens. However, patients who take cisplatin-based drugs for a long time are prone to develop side effects such as ototoxicity, nephrotoxicity and drug resistance, and these side effects seriously affect patients' quality of life and treatment outcomes. The current findings suggest that chemotherapeutics can suppress tumor immune responses and achieve tumor immune escape by remodeling immune cells and altering PD-L1 expression in tumor cells. Therefore, it is of clinical concern whether cisplatin may limit the anti-tumor effect of the organism by inducing immunosuppression in lung cancer or not. Studies on the effects of cisplatin on PD-L1 expression in NSCLC cell lines are scarce, and the intracellular regulatory mechanisms are unclear. Our study focused on unraveling the effects and on clarifying whether the PI3K/Akt/mTOR signaling pathway (PATSP) also played a regulatory role in this process. We also compared the difference in PD-L1 expression between NSCLC cisplatin-resistant cell lines (NSCLC/DDP) and NSCLC naïve cell lines. This study aimed to reveal that NSCLC/DDP cell lines contribute to tumor immune escape. This phenomenon might be caused by the high expression of PD-L1 regulated by PATSP. Our research also provided new evidence that low concentrations of cisplatin promote tumor immune evasion in NSCLC cell lines. Providing a new direction for better immunotherapy in cisplatin-resistant patients is the clinical significance of this study.

Methods:
We successfully induced A549/DDP cells that were not available in the laboratory by incrementing the concentration method. Therefore, A549, HCC827, H1975 cell lines, and A549/DDP, HCC827/DDP, H1975/DDP cell lines were selected for this research. Cisplatin, XL-765 (dual PI3K/mTOR inhibitor), and 740Y-P (PI3K agonist) were selected as stimulating drugs. We first detected the IC50s and EC50s of the above six cell lines stimulated by the above drugs with CCK-8 kit and determined the optimal concentration range of the drugs. After that, we detected the invasion capability, migration capability, proliferation rate and apoptosis rate of the cell lines after drug stimulation by Transwell, Wound healing, CellTiter-Glo ® 2.0 and Flow cytometry assays. These experiments were able to show the variations in cellular function after stimulation of NSCLC cell lines with cisplatin, XL-765 and 740Y-P. In the following experiments, we initially detected the expression differences of PD-L1 in the above cells before and after drug stimulation by Immunohistochemistry and then the differences in expression of PD-L1, p-AKT (phosphorylated AKT), AKT, p-S6 (phosphorylated S6) and S6 proteins were then detected by Western blot. Finally, we also compared PD-L1 mRNA and membrane PD-L1 expression differences in the cell lines before and after drug stimulation by qRT-PCR and Flow cytometry.

Results:

There are five primary outcomes that we can learn. 1. The cell activity, invasion capability, and migration capability of NSCLC/DDP cell lines were higher than those of the corresponding NSCLC naïve cell lines, but the apoptosis rates of NSCLC/DDP cell lines were lower than that of the corresponding NSCLC naïve cell lines. Cisplatin and 740Y-P both had a promoting effect on the cellular function of NSCLC naïve cell lines, while XL-765 had an inhibitory effect. 2. Low concentrations of cisplatin significantly up-regulated the expression of cell membrane PD-L1 and total PD-L1 in NSCLC naïve cell lines, and the expression levels tended to increase with increasing concentrations of cisplatin.3. PD-L1 expression was significantly higher in NSCLC/DDP cells than in NSCLC naïve cells but was significantly reduced after stimulation with XL-765. 4.In H1975 and H1975/DDP cell lines, a low concentration of cisplatin and 740Y-P could increase the expression of p-AKT, AKT, p-S6, S6, and PD-L1, while XL-765 could decrease the expression. 5. The degree of increase and decrease in the expression of p-AKT, AKT, p-S6, S6, and PD-L1 correlated with the drugs' treatment time and treatment concentration.

Conclusion:

Our results suggested that low concentrations of cisplatin could promote PD-L1 expression in NSCLC cells, leading to cisplatin resistance and immune escape in NSCLC cell lines. The over-activated PATSP was involved in cisplatin-induced up-regulation of PD-L1 expression. Inhibition of this signaling pathway resulted in decreased expression of PD-L1 and, to some extent, reversed immune escape caused by cisplatin resistance in NSCLC cell lines.

Abstrakt-Zusammenfasung

Zielsetzung:
Nichtkleinzelliger Lungenkrebs (NSCLC) ist eine Krankheit mit hoher Morbidität und Mortalität. Cisplatin (DDP) ist eines der am häufigsten eingesetzten Chemotherapieschemata. Patienten, die Cisplatin-haltige Medikamente über einen langen Zeitraum einnehmen, neigen jedoch dazu, Nebenwirkungen wie Ototoxizität, Nephrotoxizität und Arzneimittelresistenz zu entwickeln, und diese Nebenwirkungen beeinträchtigen die Lebensqualität der Patienten und die Behandlungsergebnisse erheblich. Die aktuellen Erkenntnisse deuten darauf hin, dass Chemotherapeutika die Immunreaktion von Tumoren unterdrücken und durch den Umbau von Immunzellen und die Veränderung der PD-L1-Expression in Tumorzellen eine Flucht des Tumorimmunsystems ermöglichen können. Daher ist es von klinischem Interesse, ob Cisplatin die Anti-Tumor-Wirkung des Organismus durch Induktion von Immunsuppression bei Lungenkrebs einschränken kann oder nicht. Es gibt nur wenige Studien über die Auswirkungen von Cisplatin auf die PD-L1-Expression in NSCLC-Zelllinien, und die intrazellulären Regulationsmechanismen sind unklar. Unsere Studie konzentrierte sich darauf, die Auswirkungen zu entschlüsseln und zu klären, ob der PI3K/Akt/mTOR-Signalweg (PATSP) bei diesem Prozess ebenfalls eine regulatorische Rolle spielt. Außerdem verglichen wir den Unterschied in der PD-L1-Expression zwischen cisplatinresistenten NSCLC-Zelllinien (NSCLC/DDP) und naiven NSCLC-Zelllinien. Ziel dieser Studie war es, zu zeigen, dass NSCLC/DDP-Zelllinien zur Immunflucht des Tumors beitragen. Dieses Phänomen könnte auf die hohe Expression von PD-L1 zurückzuführen sein, die durch PATSP reguliert wird. Unsere Forschung lieferte auch neue Beweise dafür, dass niedrige Konzentrationen von Cisplatin die Umgehung des Tumorimmunsystems in NSCLC-Zelllinien fördern. Die klinische Bedeutung dieser Studie liegt darin, dass sie eine neue Richtung für eine bessere Immuntherapie bei cisplatinresistenten Patienten aufzeigt.

Methoden:
Wir haben erfolgreich A549/DDP-Zellen induziert, die im Labor nicht verfügbar waren, indem wir die Konzentrationsmethode erhöht haben. Daher wurden die Zelllinien A549, HCC827, H1975 und A549/DDP, HCC827/DDP, H1975/DDP für diese Untersuchung ausgewählt. Cisplatin, XL-765 (dualer PI3K/mTOR-Inhibitor) und 740Y-P (PI3K-Agonist) wurden als stimulierende Medikamente ausgewählt. Zunächst wurden die IC50- und EC50-Werte der oben genannten sechs Zelllinien, die durch die oben genannten Medikamente stimuliert wurden, mit dem CCK-8-Kit ermittelt und der optimale Konzentrationsbereich der Medikamente bestimmt. Danach haben wir die Invasionsfähigkeit, die Migrationsfähigkeit, die Proliferationsrate und die Apoptoserate der Zelllinien nach Medikamentenstimulation durch Transwell-, Wundheilungs-, CellTiter-Glo ® 2.0- und Durchflusszytometrie-Assays ermittelt. Diese Experimente konnten die Veränderungen der Zellfunktionen nach Stimulation der NSCLC-Zelllinien mit Cisplatin, XL-765 und 740Y-P aufzeigen. In den folgenden Experimenten wiesen

wir zunächst die Unterschiede in der Expression von PD-L1 in den oben genannten Zellen vor und nach der Medikamentenstimulation durch Immunhistochemie nach. Anschließend wurden die Unterschiede in der Expression von PD-L1, p-AKT (phosphoryliertes AKT), AKT, p-S6 (phosphoryliertes S6) und S6-Proteinen durch Western Blotting nachgewiesen. Schließlich verglichen wir auch die Unterschiede in der PD-L1-mRNA- und Membran-PD-L1-Expression in den Zelllinien vor und nach der Medikamentenstimulation mittels qRT-PCR und Durchflusszytometrie.

Ergebnisse:
Es gibt fünf Hauptergebnisse, die wir lernen können. 1. Die Zellaktivität, Invasionsfähigkeit und Migrationsfähigkeit der NSCLC/DDP-Zelllinien waren höher als die der entsprechenden naiven NSCLC-Zelllinien, aber die Apoptoseraten der NSCLC/DDP-Zelllinien waren niedriger als die der entsprechenden naiven NSCLC-Zelllinien. Cisplatin und 740Y-P hatten beide eine fördernde Wirkung auf die zelluläre Funktion der naiven NSCLC-Zelllinien, während XL-765 eine hemmende Wirkung hatte. 2. Niedrige Konzentrationen von Cisplatin führten zu einer signifikanten Hochregulierung der Expression von PD-L1 an der Zellmembran und des Gesamt-PD-L1 in naiven NSCLC-Zelllinien, und die Expressionsniveaus tendierten dazu, mit steigenden Konzentrationen von Cisplatin zuzunehmen.3. die PD-L1-Expression war in NSCLC/DDP-Zellen signifikant höher als in naiven NSCLC-Zellen, wurde aber nach Stimulation mit XL-765 signifikant reduziert. In den Zelllinien H1975 und H1975/DDP konnte eine niedrige Konzentration von Cisplatin und 740Y-P die Expression von p-AKT, AKT, p-S6, S6 und PD-L1 erhöhen, während XL-765 die Expression verringern konnte. 5. Der Grad der Zunahme und Abnahme der Expression von p-AKT, AKT, p-S6, S6 und PD-L1 korrelierte mit der Behandlungszeit und der Behandlungskonzentration der Medikamente.

Schlussfolgerung:
Unsere Ergebnisse deuten darauf hin, dass niedrige Konzentrationen von Cisplatin die Expression von PD-L1 in NSCLC-Zellen fördern können, was zu Cisplatin-Resistenz und Immun-Escape in NSCLC-Zelllinien führt. Der überaktivierte PATSP war an der Cisplatin-induzierten Hochregulierung der PD-L1-Expression beteiligt. Die Hemmung dieses Signalwegs führte zu einer verringerten PD-L1-Expression und kehrte in gewissem Maße die durch Cisplatin-Resistenz verursachte Immunflucht in NSCLC-Zelllinien um.

1. INTRODUCTION

1.1 Lung cancer

Due to environmental pollution and the increased number of smokers, lung cancer has become one of the fastest-growing malignancies [1]. In 2020, there were approximately 2.2 million new lung cancer diagnoses and 1.8 million lung cancer deaths [2]. Lung cancer is a prominent cause of cancer mortality in men. Among women, its incidence ranks third, after breast cancer and colorectal cancer, and its mortality ranks second, after breast cancer. Women's morbidity and mortality rates are approximately half that of men [3]. Lung cancer originates in the lung tissue and usually develops from genetic mutations in the epithelial cells of the airways. It is divided into small cell lung cancer (SCLC) and non-small cell lung cancer (NSCLC). NSCLC accounts for about 80-85% of lung cancers and it usually progresses more slowly than SCLC [4]. As for an early-stage NSCLC patient, he or she can be cured by surgery, radiotherapy, or chemotherapy and immunotherapy. However, if a patient is diagnosed with SCLC, the patient often cannot be cured. This is because SCLC grows rapidly and by the time it is diagnosed, the cancer cells have already spread through the blood and lymphatic systems [5]. Therefore, the treatment options for SCLC patients are molecular targeted therapy, chemotherapy, or combination therapy [6].

1.2 Symptoms of lung cancer

Early-stage patients are usually asymptomatic, but as the cancer cells grow, patients may experience common symptoms including increasingly severe or chronic cough, shortness of breath, dyspnea, chest pain, hemoptysis, hoarseness, recurrent lung infections, feeling tired all the time, and unexplained weight loss [7].

1.3 Diagnosis

If symptoms consistent with lung cancer are present, the patient will need to undergo tests such as blood samples and X-rays. When the results suggest a high likelihood of lung cancer, doctors need to collect additional samples through sputum cytology, bronchoscopy, fine needle aspirations, and open biopsies to find definitive diagnosis evidence. To design the best treatment plan for a patient, doctors need to know not only the type of cancer but also the stage of the tumor. Lung tumors can be initially staged by PET (Positron emission tomography), CT (Computed tomography) and MRI (Magnetic resonance imaging) [8]. These techniques can be used to clarify how the mediastinal involvement is and whether tumor cells have metastasized or not. Lung cancer cells tend to metastasize to lymph nodes, brain, liver, etc. [9].

1.4 Treatment

Treatment goals depend on the stage. For early-stage patients, the goal of treatment is to cure the patient; for advanced-stage patients, treatment is aimed at controlling the tumor progression, prolonging their lives or alleviating their discomfort symptoms to improve their quality of life. Treatment options may be administered singularly or in combination [10].

1.4.1 Localized NSCLC

For patients with localized NSCLC, treatment options include surgery, chemotherapy and immunotherapy, radiotherapy, and a combination of systemic therapy and radiotherapy [11]. During lung cancer surgery, tissue containing tumor cells and lymph nodes near the tumor will be removed. Radiotherapy uses precise radiation to kill cancer cells. This treatment will only kill the cells in the area being irradiated [12]. Chemotherapy uses anti-cancer drugs given by intravenous infusion to kill cancer cells. When chemotherapeutics enter the bloodstream, they will kill cancer cells throughout the body without selection. [13].

1.4.2 Advanced NSCLC

When NSCLC has metastasized, the goal of treatment is to control tumor growth, reduce discomfort symptoms and prolong life. Chemotherapy, targeted therapy and immunotherapy are the treatment options [14]. Targeted therapy is more effective in treating patients with advanced NSCLC. As for advanced NSCLC, EGFR-TKIs (Epidermal growth factor receptor tyrosine kinase inhibitors) have a good effect. Its representative first generation drugs are gefitinib and erlotinib [15]. Second generation drugs are Afatinib, Dacomitinib and Osimertinib. Immunotherapy is a treatment that kills cancer cells by strengthening specific mechanisms of the body's immune system. Cancer cells can "disguise" themselves so that the body's immune system cannot identify these "rogue cells" and digest them. Immunotherapy helps boost the immune system, making it easier for immune cells to identify and digest these "rogue cells " [16, 17]. As a result, immunotherapy has been shown to inhibit tumor progression over time compared to other therapeutic approaches.

1.5 PD-L1

PD-L1 (B7-H1, CD274) is regulated by the CD274 gene, with a molecular size of 40 kDa, which can also be expressed in the cytoplasm [18]. In a normal immune response, the presence of antigens in the lymph nodes or spleen activates T cells in the immune system [17]. In recent years, the PD-L1/PD-1 signaling axis has been extensively studied to provide an inhibitory effect on T cell proliferation [19]. In cancer cells of tumor tissue, gamma-interferon-gamma (IFN-γ) secreted by T cells can induce PD-L1 expression and play a role in eliminating tumor cells [20]. Tumor cells in different tissues can express different levels of PD-L1. Overexpressed PD-L1 can bind PD-1 to

transmit signals that inhibit T cell proliferation so that tumor cells can escape T cell immune attack and directly affect the treatment results and clinical prognosis of cancer patients [21].

1.6 Immunotherapy

In recent years, with the maturity of related technologies such as antibody preparation, immuno-oncology (I-O) therapy has developed rapidly and has become another effective treatment for cancer after surgery, radiotherapy, chemotherapy, and targeted therapy. Immunotherapy is being developed as a therapy against advanced NSCLC. It can be used as a stand-alone therapy or combined with chemotherapy or targeted therapy [22]. At present, immune checkpoint drugs for the treatment of malignant tumors have been approved for marketing by the FDA (U.S. Food and Drug Administration) [23]. Pembrolizumab, nivolumab and ipilimumab are PD-1 inhibitors, while atezolizumab is a PD-L1 inhibitor, and they are all approved to treat metastatic cancers [24]. Chemotherapy drugs plus Pembrolizumab are a kind of standard therapy explicitly used to treat patients with metastatic NSCLC [25]. In February 2018, durvalumab (anti-PD-L1) became available for treating patients who are inoperable and whose disease is stable after chemo- and radiation therapy [26]. Immunotherapy for lung cancer is mostly performed every three weeks for a more extended period, and each procedure takes only one hour [27]. The introduction of immunotherapy has opened up new avenues of cancer treatment, allowing patients to extend their lives while maintaining their quality of life effectively.

The second group of immunotherapeutic drugs, called PD-L1 inhibitors, have the exact mechanism as the first generation of PD-1 inhibitors, both blocking signals that inhibit T cell apoptosis [22]. The differences between these two groups of drugs are that PD-L1 inhibitors are effective in restarting the normal function of T cells and in activating T cells in lymph nodes. PD-L1 inhibitors act on cancer cells rather than T cells, making PD-L1 inhibitors safer than PD-1 inhibitors [28]. Clinical studies have also confirmed that PD-L1 inhibitors have a lower immune response to normal cells and a lower chance of immune response-related side effects [28]. Immunotherapy is currently available for NSCLC, uroepithelial cancer, bladder cancer and melanoma, with NSCLC being more established. For NSCLC cases without specific genetic variants or who have become resistant to chemotherapy, immunotherapy will be considered. Immunotherapy will be treated for patients assessed by physicians as suitable, such as smokers, the elderly, or those in poor health with high PD-L1 expression. In addition, there is also an emerging trend to combine immunotherapy with chemotherapy as a first-line treatment [29].

Three recombinant fully-humanized anti-PD-L1 monoclonal antibodies are currently available globally. Atezolizumab, the world's first monoclonal antibody targeting PD-L1 developed by Genentech, was approved in May 2016 as a breakthrough drug for bladder cancer [30]. It has now been approved for bladder cancer, uroepithelial cancer, NSCLC and extensive-stage SCLC (ES-SCLC) [31]. What is more, the use of platinum-based drugs plus atezolizumab for ES-SCLC patients has been agreed upon by the FDA, making it the first new FDA-approved first-line treatment regimen for SCLC in more

than 20 years [32].
Durvalumab is a PD-L1 inhibitor developed by AstraZeneca. In May 2017, the FDA accelerated the approval process for durvalumab in metastatic uroepithelial cancer and approved the commercialization of PD-L1 Assay Kit-SP263 [33]. In February 2018, durvalumab was approved as a breakthrough therapy for advanced NSCLC by the FDA [34]. In a study involving 713 NSCLC patients, median progression-free survival (PFS) time was three times longer in the durvalumab group than in the control group [35].
Avelumab is a PD-L1 antibody developed by Merck in Germany and commercialized by Merck and Pfizer. The FDA approved avelumab as the first immunotherapy drug for metastatic Merkel cell carcinoma in March 2017. There are currently 30 clinical research projects on avelumab. Among them, the results of the Phase Ib trial conducted by Verschraegen unraveled the effectiveness and safety of avelumab monotherapy for stage III-IV NSCLC patients, providing important reference data for further studies. The research results of Verschraegen will also shed light on the effectiveness of avelumab in treating NSCLC [36].

1.7 Chemotherapy combined with Immunotherapy for advanced NSCLC

In recent years, treatments for advanced NSCLC have been diversified. Traditional chemotherapy has an unshakable status as a treatment for advanced NSCLC. However, with extensive research on the uncontrolled energy metabolism of tumor cells, immune escape, tumor pro-inflammatory effect, and gene mutation, emerging therapies such as targeted therapy, gene therapy, and immunotherapy are becoming more and more important. More and more precision therapies are applied in tumor treatment. Now immunotherapy has become a hot research area for NSCLC treatment. With the application of immunotherapy in NSCLC, how to increase the rationality of immune monotherapy or combination-therapy for NSCLC patients has become another hot topic.

1.7.1 Current status of chemotherapy in advanced NSCLC

About 80% of NSCLC patients are found at a late stage when surgery cannot be performed [2, 37]. Only 20-25% of patients are candidates for surgery, but the postoperative recurrence rate and metastasis rate are still above 50% [38]. Despite advances in targeted therapy and immunotherapy, platinum-based drugs remain the first-line drugs in clinical use for approximately 85% of NSCLC patients without targeted genetic mutations [39]. Cisplatin has apparent benefits for advanced NSCLC patients. As for the selection of first-line chemotherapy agents, various preliminary clinical trials have confirmed the efficacy of third-generation chemotherapy agents plus cisplatin or carboplatin for advanced NSCLC [40]. These drugs include paclitaxel, docetaxel, gemcitabine, pemetrexed, vincristine, etoposide, and paclitaxel. Despite the results achieved by platinum-based drugs for NSCLC patients, the emergence of drug resistance is an important limitation to their clinical application. Many patients are

susceptible to chemotherapeutic drugs at the beginning of platinum-based chemotherapy. The tumor size becomes smaller during the treatment, and the symptoms associated with the tumor are also reduced [41]. However, in the later stages of treatment, the results are often unsatisfactory. Multiple studies have shown that drug resistance in tumor cells often leads to failure of chemotherapy in NSCLC. Cisplatin diffuses passively into cells via transporters. If the transporters are reduced or an increase in efflux, it will lead to fewer platinum drugs entering the cells, making the tumor cells resistant to the drug after two or three courses of treatment. In some cisplatin-resistant cancer cells, metallothionein and glutathione-related metabolic enzymes such as Glutathione S-transferases inactivate cisplatin [42]. Despite numerous mechanisms of cisplatin resistance having been investigated and the application of multiple strategies to address these resistance factors in clinical trials, the prognosis of NSCLC remains the poorest of all malignancies [43]. This suggests that there are other signaling networks in the response of NSCLC cells to chemotherapy. In recent years, the effects of chemotherapeutic agents on immune responses have been extensively studied. There are growing evidence that chemotherapy regimens and immunotherapy are effective, since chemotherapeutic agents induce new or restore existing tumor-specific immune responses [44]. This mechanism is known as immunogenic cell death (ICD), which means chemotherapeutics can stimulate immune cells to destroy malignant cells. Several common chemotherapy drugs can cause ICD, such as doxorubicin, cyclophosphamide and oxaliplatin. In addition to inducing immunogenic cell death, it is reported that oxaliplatin can also inhibit PD-L2 [45]. In breast cancer treatment, paclitaxel and etoposide can up-regulate PD-L1 expression and activate inhibitory cell proliferation factors. During the experiment, Yang observed that leukemia cells after decitabine treatment, the expression of PD-L1 increased with the increase of decitabine concentration [46]. In hepatocellular carcinoma H22 cells, studies have shown that cisplatin can up-regulate PD-L1 expression with the cisplatin concentration is lower than IC50 [47, 48]. In summary, chemotherapeutics, such as cisplatin, can alter PD-L1 expression, but the expression levels depend on the cell lines and the chemotherapeutics being studied.

1.7.2 Mechanisms of Chemotherapy combined with Immunotherapy

Chemotherapy combined with Immunotherapy can improve the efficacy of treating advanced NSCLC, and the mechanisms of how these two pathways act synergistically are unclear [49]. It has been suggested that systemic chemotherapy can increase antigenicity and immunogenicity. Antigenicity can cause the overexpression of tumor-associated surface antigens and stimulate immune surveillance to achieve antitumor effects. Immunogenicity increases the likelihood that tumor cells will be recognized and killed by immune effectors. Therefore, chemotherapy is also indirect immunotherapy and closely relates to tumor immunotherapy [50].

Combining immunologic agents with chemotherapeutic drugs seems to obtain higher MPR (Major pathological remission) rates than neoadjuvant immune single or double drugs. This reason may be that the combination regimen not only kills tumor cells

directly but also is involved in regulating immune processes [45]. This course mainly consists of the regulation of immune cells and the suppression of immune escape of tumor cells. There are four main mechanisms by which chemotherapeutic drugs stimulate immune cells as follows. ①Tumor cells release a large amount of tumor-specific antigens during chemotherapy. On the one hand, chemotherapy can stimulate tumor cells to express tumor-specific antigens, such as carcinoembryonic antigen (CEA) and cancer-testis antigens (CTA). On the other hand, tumor cells can release large amounts of tumor antigens upon apoptosis [51]. ②Chemotherapeutic agents can increase the up-regulation of tumor cell surface calreticulin, up-regulate the MHC-I (major histocompatibility complex I), and promote tumor-specific antigen delivery to CD8+ cytotoxic T cells, which can promote T cell activation [52]. In the tumor microenvironment (TME), laboratory studies have shown that some chemotherapeutic agents can destroy tumors by influencing immune cells. For example, pemetrexed can increase tumor-infiltrating lymphocytes, making PD-L1 inhibitors effective [53].③The stimulation of tumor cells by some chemotherapeutic agents causes tumor cells to secrete immune-related factors. These factors promote the immune response by activating processes such as dendritic cells (DC) differentiation and maturation [54].④ Reduction in the number of immune suppressor cells. Gemcitabine and cisplatin can specifically reduce MDSC (myeloid inhibitory cells) and Treg. The percentage of Treg cells decreased in peripheral blood of NSCLC patients receiving immunotherapy + docetaxel + cisplatin. In vivo, immunotherapy combined with chemotherapy synergistically enhances the anti-tumor effect through multiple mechanisms mentioned above. In experiments conducted on mice, gemcitabine promoted TSA release, enhanced CD8+ T cell activity, and significantly reduced MDSC levels [45, 55]. Nolan et al. found satisfactory results in a mouse model by first treating BRCA1-mutated breast cancer with cisplatin and then combining it with two different immune check inhibitors to improve the treatment effect [56]. The above results suggest that an approach similar to the above may apply to patients.

1.7.3 Immunogenic activation

Studies have shown that chemotherapeutic drugs may work through immune stimulation mechanisms. For example, in the TME, anthraquinone drives a regulated ICD phenotype and directly blocks the immunosuppressive pathway [57]. ICD can produce large amounts of tumor-associated antigen (TAA) and release ATP and type I interferon to communicate dangerous situations. The damage-related molecular pattern induces the antigen-presenting ability of DC, activates immune response cells and produces anti-tumor immune responses [58]. Oxaliplatin combined with cyclophosphamide were used to treat tumors lacking T-cell infiltration in a transgenic mouse lung adenocarcinoma model. The results showed enhanced sensitivity of PD-L1 and CTLA4 antibodies, resulting in enhanced anti-tumor effects [59]. These data are consistent with clinical observations that adding ipilimumab and carboplatin as the preferred option for patients with NSCLC significantly improves overall survival. In a lung adenocarcinoma model with Kras and Trp53 mutations, Pfirschke et al.found that

chemotherapeutic agents induce PD-1 expression and increase the tumor-eliminating effect of immune checkpoint drugs. [60]. Therefore, the appropriate application of chemotherapeutic drugs can make tumor cells more sensitive to immune checkpoint therapy and improve clinical outcomes.

1.8 PI3K/AKT/mTOR signaling pathway

Various growth factors act on transmembrane receptors and activate them, thereby activating the PI3K signaling pathway. The increased PIP3 in the cytoplasm can act as a secondary signal to fully activate AKT by phosphorylating Thr308 and Ser473 [61]. Activated AKT can phosphorylate mTOR and its downstream molecules p70S6K and 4E-BP1, thereby transmitting biological signals into cells. (Figure 1 for details)

1.8.1 PI3K

PI3K is composed of p85 and p110. P85 contains SH2 and SH3 structural domains that bind to the corresponding target proteins [62]. P110 can be divided into three categories, among which the function of the category IA is of the most important. Category IA PI3K is closely associated with human cancer. Cells maintain survival and proliferation through this pathway, which is one of the most dysregulated pathways in tumors. The PI3K described below refers to PI3K of category IA [63]. Numerous extracellular signals can activate PI3K.Activated PI3K promotes phosphorylation of membrane phosphatidylinositol, and phosphorylated membrane phosphatidylinositol catalyzes phosphatidylinositol (3,4)-bisphosphate (PI-3,4P2) and phosphatidylinositol (3,4,5)-trisphosphate (PI-3,4,5P3). They act as second messengers in the cell and mediate various cellular functions in which PI3K is involved [64]. The expression of PTEN (Phosphatase and tensin homolog deleted on chromosome10) induces dephosphorylation of 3-phosphatidylinositol, which negatively regulates the PI3K signaling pathway [65].

1.8.2 AKT

AKT (Protein kinase B) is an essential subordinate signal for PI3K. It includes at least three forms, Akt1, Akt2 and Akt3. They are involved in cell proliferation, migration and glucose metabolism [66]. PI-3,4P2 and PI-3,4,5P3 promote phosphorylation of Akt at Ser473 and Thr308 under the catalysis of phosphoinositol-dependent protein kinases (PDKs) [67]. Phosphorylation of Ser473 or/and Thr308 sites is necessary for Akt activation, which is an essential prerequisite for its cellular functions. Activated Akt plays a biological role in anti-apoptotic and pro-proliferative functions, mainly by promoting phosphorylation of downstream substrates such as Bad, mTOR, and glycogen synthase kinase-3 (GSK-3) [68].

1.8.3 mTOR

mTOR (mammalian Target of Rapamycin) is a member of the phosphatidylinositol kinase 3-associated kinase family. mTOR does not have kinase activity but can phosphorylate Ser/Thr residues of protein substrates [69]. It is the downstream

signaling center of AKT and can initiate translation by altering 4E-BP1 (eukaryotic initiator 4E binding protein) and p70S6k (ribosomal protein S6 kinase beta-1).The dephosphorylated state of 4E-BP1 can inactivate eIF-4E [70]. However, phosphorylated 4E-BP1 dissociates and releases eIF-4E, which binds to the 5' cap of mRNA and initiates translation. The translation process can be initiated by phosphorylation of ribosomal protein S6 [71]. The proliferation and survival of normal cells and tumor cells have different degrees of PI3K/Akt/mTOR signaling pathway (PATSP) activation. Anti-tumor drugs based on PATSP inhibition are in the preliminary stage of research, and it will take some time for clinical application.

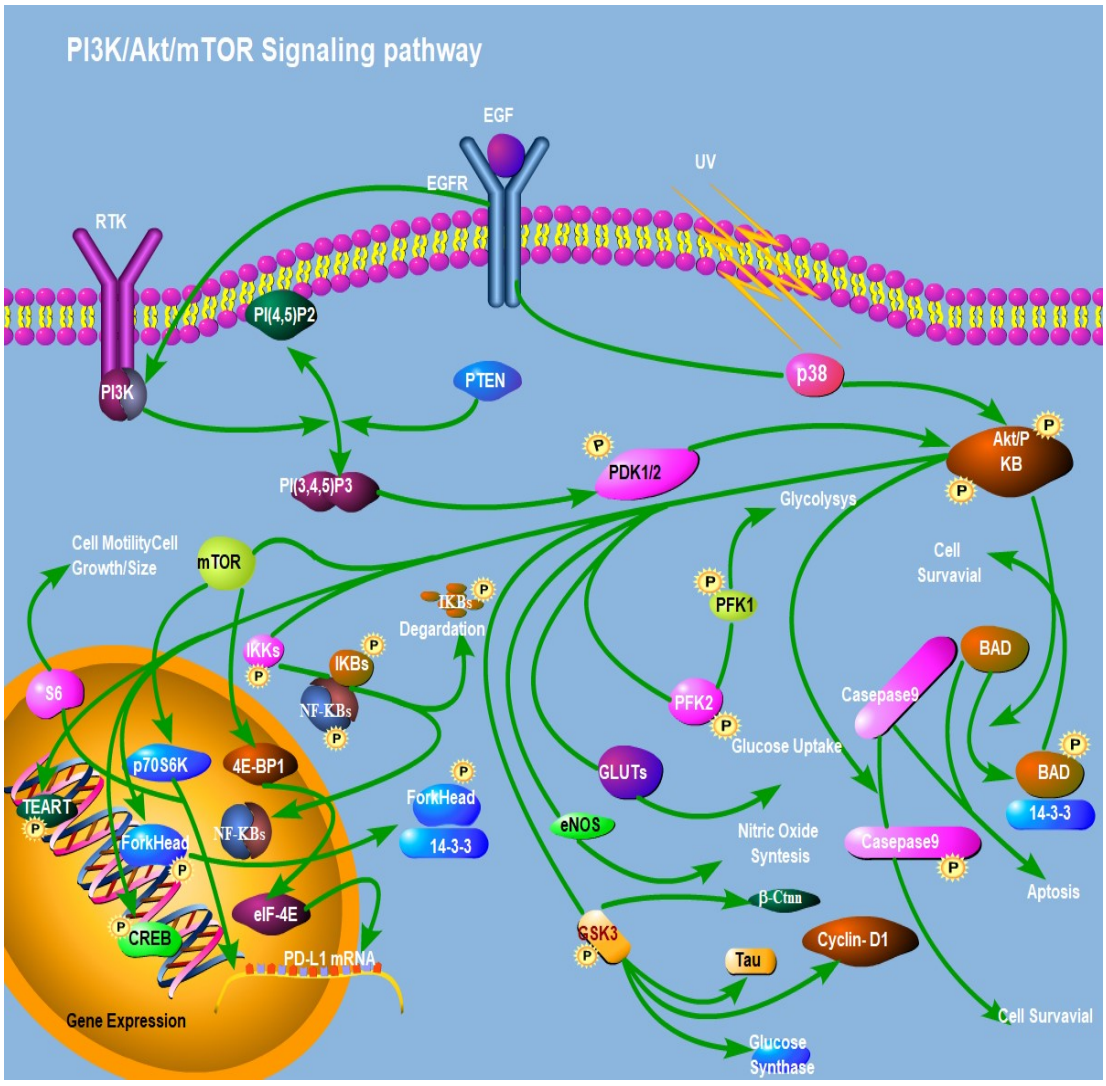

Figure 1. Schematic diagram of the PATSP activation process.
Created with Pathway Builder Tool 2.0 software (Protein Lounge Inc. USA)

1.9 Role of PATSP in tumors

1.9.1 Inhibition of apoptosis

The anti-apoptotic effect of the PATSP may be associated with several mechanisms. (i) Regulation of Bcl-2 activity. The Bcl-2 protein family includes two major groups. One group is a protein that inhibits apoptosis, such as Bcl-xL, and the other group is a protein that promotes apoptosis, such as Bad. The interaction of the two proteins determines cell survival or apoptosis. AKT can phosphorylate Ser136/Ser112 residues of Bad. Phosphorylated Bad first depolymerizes with Bcl-xL and then binds to the anti-apoptotic protein 14-3-3. In addition, the dissociated state of Bcl-2 also plays a pro-growth role. Inhibition of apoptosis by phosphorylation and inactivation of the Ser184 residues of Bax is one of the activated PI3K/Akt pathways [72]. (ii) Caspase-9 and caspase-3 can initiate apoptosis. Activated AKT can inactivate caspase-9 and caspase-3 by phosphorylating them [73]. (iii) Directly or indirectly affects transcription factor families such as Forkhead, NF-κB, p53, etc. (iiii) By phosphorylating mTOR and its downstream molecules p70S6K and 4E-BP1, AKT can inhibit p53-independent apoptosis and promote cell survival [74, 75].

1.9.2 Promoting cell proliferation

Cyclin-dependent kinases (CDK) and CDK inhibitors (CKIs) form a network system that coordinates the control of the cell cycle [76]. AKT prevents downregulation of cyclin D1 by regulating the cyclin D1 kinase glucose synthase kinase 3β (GSK3β), which directly phosphorylates GSK3β and prevents kinase activation, allowing cyclin D1 accumulation. (Figure 1). In addition, Akt inhibits the expression of CKIs, p27KIP1 and p21CIP1/WAF1. It also regulates p27 and p21 activation directly or indirectly through phosphorylation [77].

1.9.3 The importance of the PATSP in NSCLC

1.9.3.1 The activation state of PATSP in NSCLC

The role of PATSP is gradually being demonstrated. Many experimental results have shown that PATSP is involved in a variety of cellular activities in NSCLC. PIK3CA mutation/amplification or PTEN deletion/downstream molecular activation can activate the pathway. Mutations or abnormal amplification of PIK3CA are commonly seen in NSCLC patients. In a study of tumor tissue from 1144 NSCLC patients, PIK3CA mutations were found to be more common [78]. There is much evidence for abnormal activation of PATSP in NSCLC, for example, phosphorylation of Akt is present in approximately 50%-70% of NSCLC cases [79]. A study of 110 NSCLC specimens measured by immunohistochemistry showed increased activity of Akt in 51% specimens [80]. Another study showed that four patients out of a sample of 219 NSCLC patients had Akt mutations [81]. Activation of Akt was attributed to mutations in PTEN or EGFR or PIK3CA [82]. David et al. found that phosphorylated Akt was associated with tumor invasion after analyzing samples from NSCLC patients [83]. One study found persistent Akt and mTOR phosphorylation in 51% NSCLC patient samples and 74% NSCLC cell lines [84]. There is evidence of mTOR up-regulation in most NSCLC specimens. For example, p-mTOR was elevated in 90% adenocarcinomas, 60% large cell carcinomas, and 40% squamous cell carcinomas [85]. In addition, the downstream products S6K and 4E-BP1, activated by mTOR, were also found in 58% and 25% of

NSCLC patient specimens, respectively. p-S6K and p-mTOR were also strongly correlated [86]. High expression of mTOR in bronchial adenocarcinoma was associated with eIF-4E [87]. Dysregulation of PATSP promotes NSCLC progression, while the application of LY294002 (inhibition of PI3K) enabled the effects of chemotherapy and increased apoptosis [88]. Based on the above studies, it can be seen that PATSP has an important role in both NSCLC cell proliferation and resistance to radiotherapy or chemotherapy.

1.9.3.2 The role of PATSP in the invasion and metastasis of NSCLC

Grille et al. told us that a squamous carcinoma cell line (SCC15) transfected with activated Akt (myr-Akt) lost the morphological features of squamous epithelial cells and showed fibroblast-like characteristics [89]. This indicates that Akt directly affects the morphological characteristics, tumorigenicity, cell migration capability and invasive capability of epithelial cells. Thus, the PATSP promotes the metastasis of tumor cells by attenuating intercellular adhesion. It was also found that in A549 cell line, TGF-β1 (Transforming growth factor-β1) and CC chemokine ligand 5 (CCL5) up-regulated the expression of β1 integrin and avβ3 integrin by stimulating the p85α subunit of PI3K and phosphorylating Ser473 of Akt, causing increased metastatic capacity of A549 cells [90]. Chemokine receptor 4 (CXCR4) is closely associated with mTOR-regulated tumor metastasis. A preclinical study showed that CXCR4 significantly up-regulated A549 cells and H157 cells of NSCLC on the cell surface after incubation in a hypoxic environment. Both tumor cells were found to have an enhanced migration capability. The increased CXCR4 expression by hypoxia and EGR-promoted PI3K/Akt activation suggested that the mTOR pathway is closely related to CXCR4 up-regulation [91]. In addition, the expression of some matrix metalloproteinases can be up-regulated through the PATSP to promote tumor cell migration. Zhang et al. found that Lewis lung carcinoma (highly invasive) cell subline H-59 highly expressed MT1-MMP, but in the presence of Rapamycin (dual inhibitor of PI3K and mTOR) or dominant-negative mutant of Akt or overexpression of PTEN, MT1-MMP expression could be reduced [92]. They also reduced the invasion ability of H-59 cells.

1.9.3.3 Drugs targeting PATSP

The development of drugs targeting PATSP has received increasing attention. A series of specific drugs targeting this pathway have been developed one after another. These drugs can directly inhibit the over-activated signaling molecules in the PATSP, thus acting as a blocker of tumor progression.

As first-generation PI3K inhibitors, Wortmannin and LY294002 can inhibit the reactivity of the p110 subunit. Combining Wortmannin or LY294002 with chemotherapy can effectively increase the effect and reduce the toxicity of chemotherapeutic drugs [93]. It can be seen that the combination of PI3K inhibitors with traditional chemotherapeutic drugs provides a better choice for tumor patients who have developed resistance to chemotherapeutic drugs. PX-866 and PWT-458 are newly discovered derivatives of Wortmannin that have efficient PI3K inhibition. The combination of PX-866 with cisplatin or radiotherapy in lung cancer models enhances

the antitumor effect [94, 95].
Currently, Akt inhibitors are celecoxib and its derivatives, OSU-03012 and OSU-03013. Celecoxib is a COX-2 inhibitor that prevents Akt phosphorylation by inhibiting PDK [96].Clinical trials showed that celecoxib alone or combined with docetaxel and zoledronate showed good therapeutic effects [97, 98]. Perifosine is a synthetic alkyl phospholipid Akt inhibitor that inhibits the tumor cells growth by inhibiting the membrane translocation of Akt and reducing the activity of Akt [99].
There have been a variety of evidence that the antitumor effects of mTOR inhibitors (including NSCLC) can alleviate the disease or prolong the stability of patients with cancer. Rapamycin and docetaxel have complementary effects on inhibiting the growth of NSCLC cells [100]. Konstantinidou et al. found that BEZ235(an inhibitor of PATSP) combined with radiotherapy could benefit NSCLC patients with K-RAS mutations [101]. This suggests that mTOR inhibitors may have better efficacy with radiotherapy or chemotherapy in lung cancer treatment.
Second-generation mTOR inhibitors not only block mTORC1 and mTORC2 but also have the ability to inhibit class I PI3K. Results from clinical trials of XL-765 plus erlotinib for NSCLC patients showed good clinical outcomes [87, 102]. In a phase Ib clinical trial, GDC-0980 (PI3K inhibitor) combined with chemotherapy also showed an acceptable safety profile for NSCLC patients [103]. This suggests that chemotherapy or immunotherapy combined with multi-targeted therapy of the PATSP may be a better strategy for NSCLC patients.

1.10 The aim of this dissertation

Platinum-based drugs are frequently used in clinical applications. However, long-term use of platinum-based drugs often produces side effects such as ototoxicity, nephrotoxicity and drug resistance, which seriously affect patients' treatment outcomes. As for advanced NSCLC, the efficacy of chemotherapy has reached a plateau, and checkpoint inhibitors plus chemotherapy have shown synergistic. Based on the above analysis, chemotherapeutic agents can inhibit the clearance of tumor cells by the immune system through affecting the composition of immune cells in TME and by altering the expression status of autoimmune molecules (e.g., PD-L1) in tumor cells. However, this modulation can both promote and suppress tumor immunity. How this phenomenon develops depends on the cell line and the chemotherapeutic agent and its concentration. Thus, platinum-based chemotherapeutic agents can limit the antitumor effects of lung cancer cells by inducing immunosuppression, which is of great clinical interest. Moreover, acquired resistance to platinum-based chemotherapeutic agents was also found to be associated with an increase in PD-L1. Currently, most studies have focused on the therapeutic effects and reduction of side effects of anti-PD-1 or anti-PD-L1 antibody plus traditional platinum-containing chemotherapeutic agents. Fewer studies have been conducted on the impact of cisplatin on PD-L1 expression in NSCLC cells, and its regulatory mechanism is still unknown. Therefore, we investigated the effects of cisplatin on PD-L1 expression in NSCLC cells, and explored whether PATSP participated in the regulation of this process or not.

2 METHODS AND MATERIALS

We performed experiments to study cell proliferation, apoptosis, metastasis and invasion in NSCLC naïve cells and NSCLC/DDP cells to clarify the biological characteristics of naïve cells and DDP cells in vitro.

A549 cell line (Human-derived, ATCC CCL-185).

A549/DDP cell line was derived from A549 cells induced in our laboratory.

HCC827, HCC827/DDP, H1975, H1975/DDP cell lines were obtained from our laboratory and these cells were grown in good status in vitro.

2.1 Thawing cells

2.1.1 Apparatus and reagents

Culture flasks: corning, 25 cm^2, REF 3289; corning 75 cm^2, REF 430720U

RPMI-1640 Medium: R0883-500ML, RNBH7512, Sigma

DMEM (high glucose): D5671-500ML, RNBJ5134, Sigma

Gibco™ FBS: REF 10270106, LOT 42Q4467K

1 ml blue tips

200μl yellow tips

50 ml centrifuge tube: RÖHRCHEN

Ultra-clean Bench: KS 12, Thermo Fisher Scientific

Centrifuge: Rotofix 32A

CO_2 incubator: Thermo Scientific Heracell 150i

99.9 % Isopropanol: 10L, Höfer Chemie GmbH

2.1.2 Experimental Procedure

(1) The items were sterilized with 75% isopropanol and placed on the ultra-clean bench. Freeze tubes containing A549, HCC827, HCC827/DDP, H1975, and H1975/DDP cells from the -80°C freezer and thaw quickly in a 37°C atmosphere. Keep the cap of the freezing tube higher than the water bath liquid level to prevent the water from entering

the lyophilization tube and causing cell contamination.
(2)Transfer the cryopreservation solution containing the cells into a 50ml RÖHRCHEN. Add 10 ml cell culture medium and centrifuge for 5 min.
(3) Discard the cell culture medium directly from the centrifuge tube and retain the cell precipitate. Add 5ml 1640 medium containing 10% FBS to A549, HCC827, HCC827/DDP. Add 5ml DMEM medium containing 10% FBS and 1% Na Pyruvate to H1975 and H1975/DDP and mix gently with a pipette.
(4) Carefully add 5ml cell mixture to a 25cm^2 culture flask and gently shake the flask to distribute the cells evenly at the bottom of the flask to avoid uneven cell density, affecting the uniform growth of cells. Finally, transfer the cells to a constant 37°C, 5% CO_2 cell incubator.

2.2 Induction A549/DDP cell line by increasing the concentration of cisplatin

2.2.1 Apparatus and reagents

Cisplatin: Apotheke-LMU Klinikum

2.2.2 Optimal cisplatin concentration NSCLC/DDP cell lines

The average height of German (man) is 1.80m and the average weight is 88.7kg [104]. According to Dubois's calculation formula of human body surface area [105], we can conclude that the average BSA of the Germans is 2.09m^2. According to Nadler equation [106], the average blood volume of an adult German is 5600.00ml. The maximum dose of cisplatin is 120mg/m^2. According to the formula: Molarity=mol solute/L of the solution, the average blood concentration is 149.261μmol/L. Therefore, the cisplatin resistance concentration of A549 cells cultured in vitro should be >149.261μmol/L.

BSA = 0.007184 * (Height in cm) $^{0.725}$ * (Weight in kg) $^{0.425}$
Blood Volume = (0.3669 × H^3) + (0.03219 × W) + 0.6041

2.2.3 Experimental Procedures

A549 cells were induced to be resistant to cisplatin by regular gradient of cisplatin concentration. At the beginning of the experiment, A549 was incubated in the medium containing 50 nmol/L cisplatin for 48 h. After the cells resumed normal growth, they were treated again with 50 nmol/L cisplatin for 48 h. After three replicates, the concentration of cisplatin was doubled. During the induction of cisplatin resistance in A549 cells, the cisplatin concentration was adjusted to promote cell growth until A549 cells were able to grow well in medium containing 300μmol/L cisplatin.

2.3 Subculture cells

2.3.1 Apparatus and reagents

In addition to the reagents and equipment used for cell thawing, there were also Dulbeccos Phosphatgepufferte Kochsalz lösung: D8537-500ML: Sigma-Aldrich.

Trypsin/EDTA: L2143, Bio & Sell

2.3.2 Experimental Procedure

(1) Select cells with a fusion rate of around 80% and in well growth status for passaging. Discard 5ml original medium from the culture flasks. Add 5ml PBS solution to each culture flask, wash twice, and discard the PBS solution.
(2) Add 1ml trypsin to 5ml culture flask to trypsinize HCC827 cells for 6-8 minutes, A549 and H1975 cells were trypsinized for 4 minutes. NSCLC/DDP cells for 1-2 minutes longer than HCC827, A549, and H1975 with trypsin. When the cells were observed to flow in a quicksand manner by gently tapping the side of the cell culture flask, the trypsinization could be terminated by adding 10 ml DMEM medium or 1640 medium containing 10% FBS to avoid over-trypsinization.
(3) Transfer the cell mix suspension from the 5ml cell culture flask to the tube and centrifuge for 5min.
(4) Pour out the liquid in the centrifuge tube directly and keep the cell precipitate. Add 15ml 1640 medium or DMEM medium containing 10% FBS. Blow gently without air bubbles. Passage at a ratio of 1:3, and add 5 ml cell suspension to each flask.
(5) The culture flasks were gently shaken to distribute the cells in the culture flasks evenly and then incubated in the cell incubator.

2.4 Cell Cryopreservation

2.4.1 Apparatus and reagents

In addition to the reagents and equipment used for cell subculture, we also used these following consumables below.
CRYO.S, 2 ML, PP, RUNDER BODEN, Art. Nr.: 122263, Greiner Bio-One GmbH

Freezing Container Mr. Frosty™ Freezing Container: Catalog Number, 5100-0001, Thermo Scientific™

2.4.2 Experimental Procedure

(1) Cells with 90% cell fusion and in well growth status were removed from the cell culture flask, sterilized with isopropanol, and placed in the ultra-clean bench. Discard the original medium and wash each cell culture flask twice with 5ml PBS, respectively.
(2) Add 1 ml trypsin to the cell culture flasks and trypsinize HCC827 cells for 6-8 min, A549 and H1975 cells for 4 min, HCC827/DDP, A549/DDP and H1975/DDP cells for 1-2 min longer than the corresponding naïve cells. Gently tap the side of the cell culture flask and terminate the enzymatic digestion when cells were observed to flow like

quicksand.
(3) Carefully transfer the cell suspension to a 10 ml pipette and centrifuge.
(4) Pour off the liquid directly from the centrifuge tube, retaining the cell precipitate. Add cell lyophilization solution (DMSO: FBS=1:9), and blow the cell lyophilization solution gently, then carefully add 1ml cell mixture to the lyophilization tube. Place the lyophilized tubes in a Freezing Container and store them in the freezer at -80°C.

2.5 Cell Counting

2.5.1 Apparatus and reagents

Zählkammer Neubauer: mTiefe 0,100mm

Motic Microscope AE31E bino: Infinity, 40x-400x, phase, Hal, 100W

2.5.2 Experimental Procedure

After cells were treated with trypsin and centrifuged, 1 ml 1640 medium or DMEM medium was added to the sediment. Aspirate 100μl cell suspension into another centrifuge tube, add 900μl PBS to the centrifuge tube, and then aspirate 100μl cell suspension into the Neubauer Chamber. The cells were counted under an inverted microscope after standing still for 1 min. The counting area was four squares. The formula was calculated as Cell concentration = (N/4) $\times 10 \times 10^4$ cells/ml, and N was the total number of cells observed in the four big squares.

2.6 IC50 and EC50 values

IC50 is a measure of an antagonist's ability to inhibit a specific biological or biochemical function. It can be interpreted as the concentration of a specific drug required to induce apoptosis in 50% of tumor cells in the culture medium. The purpose of measuring IC50 is to know the appropriate dose of the inhibitory drug to be added to the cells. The half-maximum effect concentration (EC50) is when a drug induces a maximum cellular effect in half of the cells. EC50 is used to describe the efficacy (both agonistic and antagonistic) of a drug at the cellular level.

2.6.1 Apparatus and reagents

Enzyme Marker iMark Microplate Reader: Catalog Number, 1681135, Bio-Rad

CCK-8: 96992-100TESTS-F, Sigma

2.6.2 Experimental Procedure

The proliferation rates of cisplatin, Voxtalisib (XL-765) (PI3K/mTOR inhibitor), and 740 Y-P (PDGFR 740Y-P) (PI3K agonist) on A549,A549/DDP,HCC827, HCC827/DDP, H1975, 1975/DDP cell lines were assayed with the CCK-8 kit.
(1) Pre-experiments to determine the following parameters. 1. Factors affecting the cells

spread on the plate and the appropriate number of inoculations by setting different cell density gradients; 2. Time for cells to adhere to the bottom of the wells; 3. The incubation time after adding cisplatin, XL-765, and 740Y-P; 4. Dose of CCK-8 (WST-8) reagent and incubation time after adding CCK-8.
(2) Add 100μl PBS to the outer ring wells and leave the control wells blank according to the experimental design (add only culture medium without cells). Exploratory wells were added with 4~5×10^4 cells per well for a total culture volume of 100μl.
(3) Prepare medium containing different concentrations of cisplatin, XL-765, 740Y-P. Add them to a 96-well plate and continue to incubate in the incubator for 48 hours.
(4) Before the Microplate reader started to read the absorbance values, add 10μl CCK-8 reagent per well and incubate for 0.5-4h. In the initial experiments, the absorbance values were measured every 0.5 h by the Microplate reader to determine the optimal reaction time. For subsequent experiments, only the absorbance values at the optimal reaction time were measured.
(5) The absorbance values of each well of the 96-well plate were measured at 450 nm. We analyzed the inhibitory effects of cisplatin and XL-765 at different concentrations on cell lines and the promoting effects of 740Y-P at different concentrations. The cell survival curves of different concentrations of cisplatin, XL-765 and 740Y-P treatment were plotted and the corresponding IC50s and EC50s were figured out.

2.7 Wound Healing assay

It is an easy and inexpensive way to study tumor cell invasion in vitro. The experiment imitates the migration process of cells in the human body and can be used to test the migration capability of cells. When the cells grow into a monolayer at the bottom of the 6-well plate, a blank area, called a "scratch", is artificially created on the fused monolayer. Cells on both sides of the scratch will slowly cover the blank area during proliferation, making the "scratch" spacing smaller, which mimics the migration process of tumor cells in vivo to some extent.

2.7.1 Apparatus and reagents

RPMI-1640 Medium: R0883-500ML, RNBH7512, Sigma

DPBS: D8537-500ML, Sigma

Corning Falcon 353502 6 Well Plate with Lid: TC Treated Polystyrene Permeable Support Companion, Sterile, Corning

Marker pen

120mm Straightedge

100μl Pipette Tips (sterilized)

2.7.2 Experimental Procedure

1. All sterilizable instruments should be sterilized, and the straightedge and marker pen should be fully sterilized before being placed on the ultra-clean bench.
2. We used the marker pen and straightedge to draw a horizontal line evenly on the back of the 6-well plate with lines spaced between 0.5~1 cm. Draw at least 5 lines in each hole, each line evenly perpendicular and parallel to the edge of the 6-well plate.
3. Each well was inoculated with approximately (5-10)*10^5 cells. The rate of cell proliferation in the culture flask determined the cells number, and the inoculated cells must be evenly distributed.
4. The next day, we used a 100μl pipette tip to scrape vertically along the black line at the back of the 6-well plate. When scratching, the 100μl pipette tip should be vertical and not tilted.
5. Cells were washed 2-3 times with sterile PBS so that the blank area was visible to the naked eye. The cells were then cultured with fresh serum-free medium.
6. Cells were incubated for 24-48 hours and then removed for observation under a microscope and photographed.
7. Data analysis

These images were processed with Image J software, 6-8 horizontal lines were randomly selected, and the average distance between the edges of the both sides was calculated. The experimental group was presented as a ratio after comparison with the control group.

2.8 Cellular Activity assay

CellTiter-Glo ® 2.0 Assay is a method for detecting the cell number in the culture medium based on the quantification of ATP to indicate metabolically active cells. The assay procedure can be performed by simply adding the reagent directly to the cultured cell medium. This process does not require washing the cells, and the optical density values can be directly measured by removing the medium. This reagent has the characteristics of rapid and sensitive, and it can be completed in less than 10 minutes. The reagent detects the amount of intracellular ATP after cell lysis and the number of cells determines the luminescence signal. This method can detect as low as 15 cells per well.

2.8.1 Apparatus and reagents

CellTiter-Glo® 2.0 Reagent: G9241, Promega GmbH

Edmund Bühler Plattformschüttler Kleinschüttler: KM-2 , Art.-ID: 14902

Black 96-well plate: Product Number, 353376

2.8.2 Experimental Procedure

1. A549, A549/DDP, HCC827, HCC827/DDP, H1975, H1975/DDP were cultured in 96-well plates with opaque walls and cell volumes and numbers were optimized

according to experimental parameters.
2. A549, A549/DDP, HCC827, HCC827/DDP, H1975, H1975/DDP cell lines that grew well in 96-well plates were selected. XL-765 stimulation group and 740Y-P stimulation group were established. The cells were incubated for 0h, 2h, 6h, 12h, 24h and 48h.
3. A549, HCC827 and H1975 cell lines were grown well in 96-well plates. The stimulation concentrations of cisplatin added to the cell lines were DMSO(0μM), 2μM, 4μM, 6μM, 8μM, 16μM. Then the cell lines were incubated for 12 h.
4. Thaw the reagent in a 4°C refrigerator overnight. Equilibrate it in a 25°C environment before use. Gently shake the 96-well plate to obtain a homogeneous solution.
5. Prepare control wells without cell culture medium to determine background luminescence.
6. Add 100μl reagent to 100μl cell culture wells.
7. Put the 96-well plate on a shaker for 2 minutes.
8. Incubate the plate for 10 minutes at 25°C to stabilize the luminescence signal.
9. Record luminescence values, and analyze data with Graphpad Prism 8.02.

2.9 Transwell assay

Transwell invasion assay was performed by separating high-nutrient cultures from low-nutrient cultures using a polycarbonate membrane and then inoculating cells into low-nutrient cultures. The polycarbonate membrane pores are covered with matrix gel that mimics the extracellular matrix. Tumor cells must secrete hydrolases and move by deformation to cross the membrane covered with matrix gel. This assay reflects the invasive capacity of tumor cells by the number of cells that enter the lower chamber.

2.9.1 Apparatus and Reagents

Transwell (6.5 mm, 8.0 μm): Product Number 3422, Corning®

Cotton swabs

1640 or DMEM medium with or without 10% FBS

DPBS: D8537-500ML,Sigma

Trypsin/EDTA: L2143, Bio & Sell

Corning™ Matrigel™ Membrane matrix Corning™: Product Number, 354234

Paraformaldehydlösung,4% in PBS: Thermo Scientific™ Thermo Scientific J19943.K2

Crystal violet solution HT901-8FOZ: Sigma-Aldrich

Gibco™ Fetal Bovine Serum, FBS: REF 10270106, LOT 42Q4467K

2.9.2 Experimental Procedure

1. Cisplatin, XL-765, 740Y-P stimulated for 12 hours and then passaged for 2-3 generations. This step was to ensure whether the cell status was normal or not.
2. Dissolve the matrix gel in a 4℃ refrigerator.
3. Pre-cool the pore polycarbonate membrane inserts, 24-well plates and pipette tips in the 4°C refrigerator. All items need to be pre-cooled to prevent the gel from solidifying.
4. Dilute Matrigel matrix with FBS-free medium and add to the upper chamber. Dilute Matrigel matrix at a ratio of 1:6, this step was done on ice.
5. Place the inserts with dilution Matrigel matrix in the incubator overnight to allow them to fully solidify.
6. Dilute each cell line to 100μl with FBS-free cell culture medium and add to the upper chamber.
7. Add 600μl medium to the lower chamber.
8. Place 24-well plates in the incubator for 24-72 hours to induce cells to cross the matrix gel. Observe and plot the incubation time while in culture.
9. Remove inserts from the 24-well plate, aspirate excess liquid from the upper and lower chambers, wash the upper chamber (200μl)/lower chamber (600μl) with PBS three times, then carefully wipe off the cells inside the upper Pore Polycarbonate layer with a cotton swab. In 24-well plates, cells were added with 4% paraformaldehyde for 20 min and then placed in crystal violet solution for 15 min.

2.10 Cell Immunohistochemistry assay

Immunohistochemistry (IHC) is the application of the basic principles of immunology. Antigens bind specifically to antibodies by labeling them with chromogenic agents (fluorescein, enzymes, metal ions, isotopes). Target proteins can be located, characterized and relatively quantified by IHC.

2.10.1 Apparatus and reagents

Eppendorf Pipette: 1ml, 200μl, 10μl

Pipette Tips: 1ml, 200μl, 10μl

Circular Microscope Slide Coverslip, Size: Diameter 25mm, Thickness: 0.15mm

Eppendorf Safe-Lock Tubes: 1.5 mL

Cultrex Poly-L-Lysine: 3438-200-01, Bio-Techne GmbH

Cell Immunohistochemistry Staining Kit: CTS008, Bio-Techne GmbH

Falcon® 24-well Plate: Product Number 353047, CORNING

Hematoxylin Solution, Mayer′s: MHS32-1L, Sigma-Aldrich

ddH_2O

2.10.2 Experimental Procedure

Items to be sterilized: 24-well plates, cell crawl sheets (Cultrex poly-L-lysine treated and sterilized with ethylene oxide) and other regular cell culture equipment.

1. Soak the sterilized circular microscope slide coverslip with 4% Cultrex Poly-L-Lysine overnight. Rinse twice with PBS, and then air dry under aseptic conditions.
2. Cells were trypsinized and resuspended with 5 ml complete medium (cell density: (1-5) $x10^6$/ml)).
3. Put the coverslips into a 24-well plate with sterile tweezers. Take a drop of cell suspension onto the disc separately. Control the suspension not to fall outside the disc, and let the cells adhere to the walls for 30 min.
4. After 30min, the medium was gently added to the 24-well plate, then incubated for 48h.
5. Discard the medium and rinse twice with PBS for 2 minutes each time.

2.10.3 Follow the kit instructions

1. Cover cell slides with 2 drops of the Peroxidase Blocking Reagent for 2 minutes.
2. Rinse cell slides with buffer and then wash in the buffer for 5 minutes gently.
3. Incubate cell slides with 2 drops of Serum Blocking Reagent D for 15 minutes. Drain slides and carefully wipe off excess Serum Blocking.
4. Incubate cell slides with 2 drops of Avidin Blocking Reagent for 15 minutes.
5. Rinse cell slides with buffer, drain slides and carefully wipe off excess buffer before the next step.
6. Incubate cell slides with 2 drops of Biotin Blocking Reagent for 15 minutes.
7. Rinse with buffer, drain slides and carefully wipe off excess buffer before the next step.
8. Incubate cell slides with primary antibody.
9. Rinse cell slides with buffer. Wash three times in buffer for 15 minutes each time.
10. Drain slides and carefully wipe off excess buffer before the next step.
11. Incubate cell slides with 2 drops of Biotinylated Secondary Antibody (Vial A) for 60 minutes.
12. Repeat step 9.
13. Drain slides and carefully wipe off excess buffer before the next step.
14. Incubate cell slides with 2 drops of HSS-HRP for 30 minutes.
15. Rinse with buffer. Wash three times in buffer for 2 minutes each time.
16. Drain slides and carefully wipe off excess buffer before the next step.
17. Add two drops of DAB Chromogen to 2 mL DAB Chromogen Buffer. Add 100µL DAB Chromogen solution on a single slide.
18. Mix DAB Chromogen and the DAB Chromogen Buffer in the empty Dropper Bottle.
19. Add 3 drops of freshly prepared DAB Chromogen solution from the Dropper Bottle to cover the entire sample and incubate for 20 minutes. Monitor intensity of staining under a microscope to ensure the proper intensity of tissue staining.
20. Rinse with distilled water and then wash in a fresh portion of distilled water for 5 minutes.
21. Cell slides stained with DAB will be mounted after staining with hematoxylin.
22. Place slides vertically on a filter paper to drain excess mounting medium and let them dry.
23. Slides were ready for observation under the microscope.
24. Analyze cell staining intensity with ImageJ software.

Kit instructions are available: https://www.rndsystems.com/products/anti-goat-hrp-dab-cell-tissue-staining-kit_cts008#product-details

2.11 Scheme for detecting PATSP involved in PD-L1 expression

1. The reagents and equipment required for the passage of H1975 and H1975/DDP cell lines were prepared on the ultra-clean bench, and the UV lamp was turned on for 30 minutes. The well-grown cells were removed from the cell incubator and spread evenly in 6-well plates with appropriate proportions. They were then placed in the incubator overnight.
2. The control group, cisplatin stimulation group, XL-765 stimulation group, and 740Y-P stimulation group were established according to the experimental design. As for groups stimulated with increasing concentrations of cisplatin, H1975 cells were first in normal medium for 48 h and then boosted with (0-16) μM cisplatin for an additional 24 h. As for groups stimulated with cisplatin at different times, H1975 cells were first cultured in normal medium for 48 h, then boosted with 16μM cisplatin for (0-48) h.
3. For the XL-765 stimulation group, H1975 cells were first cultured in medium containing 16μM cisplatin for 48 h, then boosted with 10μM XL-765 for (0-8) h. For the 740Y-P stimulation group, H1975 cells were first cultured in medium containing 16μM cisplatin for 48 h and then stimulated with 20μM 740Y-P for (0-24) h.
4. We also established another XL-765 stimulation group using the H1975/DDP cell line. In this group, H1975/DDP cells were first in medium containing 16μM cisplatin for 48 h, then stimulated with 10μM XL-765 for (0-8) h.
To demonstrate the involvement of PATSP in PD-L1 expression, we need to detect the expression of PD-L1, P-Akt, AKT, P-S6 and S6 proteins by Western blot assay.

2.12 Western Blot assay

Western Blot mainly involves transferring proteins from cells or tissues isolated by gel electrophoresis to PVDF membranes, which are then labeled with specific antibodies. The intensity of labeled proteins is recorded using an imaging system. By analyzing the location and intensity of the antibody signal, the expression level of a specific protein in cells or tissues can be determined.

2.12.1 Apparatus and Reagents

Primary antibody

PD-L1: AF156, Bio-Techne GmbH (2 μg/ml)

S6: MAB5436, Bio-Techne GmbH (0.5 μg/ml)

Akt: MAB2055, Bio-Techne GmbH (0.2 μg/ml)

p-S6: AF3918, Bio-Techne GmbH (0.5 μg/ml)

p-Akt: MAB887, Bio-Techne GmbH (0.2 µg/ml)

Fluorescent labeled secondary antibody

Goat IgG HRP-conjugated Antibody: HAF017 Bio-Techne GmbH

Pre-stained Protein Marker

Precision Plus Protein™ WesternC™ Blotting: Standards #1610376, Bio-Rad

PVDF Membrane: Immun-Blot® PVDF Membrane: 1620175, Bio-Rad

ECL Chemiluminescence Kit: Clarity™ Western ECL Substrate: 1705060, Bio-Rad

BCA Protein Quantitative Kit: BCA Protein Assay Kit, ab102536, Abcam

18 well Protein Gel: 30 µl #5671124, AnykD™

26 well Protein Gel: 15 µl #5671125, AnykD™

Tris-Glycine Electrophoresis Buffer: 30.3g Tris, 188g Glycine, 10g SDS, dissolve them in distilled water to 1000ml, and dilute it 10 times before use. pH≈8.3

Transfer buffer	2.9g glycine 5.8g Tris base 0.37g SDS	200ml methanol (added before use), add water to a total of 1L. pH≈8.3
Running buffer	25 mM Tris base 190 mM glycine 0.1% SDS	Check the pH and adjust to 8.3

TBST:
Tris base 4.84 g
NaCl 16g
Add the above two substances to a beaker and add deionized water to fix the volume to 1900 ml. Adjust the pH to 7.6 (add 3 ml concentrated hydrochloric acid to the solution). Add 2 ml 0.1% Tween20 and finally deionized water to 2000 ml. Stir the solution with a glass rod to mix thoroughly.
5% skim milk powder:
Weigh 1g skim milk powder and add 1x TBST to 20 ml.

Cell lysis solution:
The components of 1 ml RIPA lysis solution were

Cell lysis solution	50 mM Tris (pH 7.4) 150 mM NaCl 1% NP-40 0.5% sodium deoxycholate	20ml RIPA lysate was mixed with 2 tablets PhosSTOP™ and 2 tablets Protease Inhibitor Cocktail

Cryogenic high-speed benchtop centrifuges: Eppendorf 5417R, 5415R, Germany

NanoDrop™ 2000/2000c Spektralphotometer: Thermo scientific, USA

SDS-PAG electrophoresis system: Bio-Rad, USA

Controlled Circumferential Oscillator: Kleinschüttler KM 2, Germany

LI-COR Odyssey® FC LI-COR: Bioscience, USA

Corning® Small Cell Scraper: Product Number 3010

2.12.2 Experimental steps
2.12.2.1 Extraction of total protein from monolayers of adherent cells
1. After the cell culture was completed in the 6-well plate, discard the medium, add 1ml cold PBS to wash the 6-well plate twice, gently shake the 6-well plate each time, and use the pipette to suck up the remaining liquid. Meanwhile, turn on the 4℃ low-temperature centrifuge to pre-cool.
2. Add 200μl RIPA lysis solution to each well of the 6-well plate, and gently shake the 6-well plate so that the lysis solution evenly covers the bottom of the 6-well plate. Shake the 6-well plate back and forth on the ice to make the cells fully lysed. After cell lysis was complete, scrape off the protein lysate with a clean cell spatula and transfer it all

to an EP tube.
3. The EP tubes were placed in a cryogenic centrifuge and centrifuged at 12,000 rpm for 20min.
4. Protein lysates were determined by a nanodrop spectrophotometer according to A260/A280. Add 1/4 volume of 5× loading buffer according to the volume of protein samples, and store them in a refrigerator at -80℃ to avoid repeated freezing and thawing.

2.12.2.2 Protein concentration determination

(1) Prepare an appropriate amount of BCA solution (Reagent A: Reagent B=50:1).
(2) Take 10μl standard solution (5mg/ml) and dilute it to 100μl (concentration = 0.5mg/ml).
(3) Prepare a 96-well plate and sequentially add 20, 19, 18, 16, 12, 8, 4, and 0μl of PBS to the protein standard wells. Take the newly configured standard solution and add 0, 1, 2, 4, 8, 12, 16, 20μl to the corresponding wells, respectively, ensuring 20μl standard substance per well. The equivalent concentrations of the standards were 0, 0.025, 0.05, 0.1, 0.2, 0.3, 0.4, 0.5 mg/ml, respectively.
(4) According to the number of samples to be tested, add 18μl PBS (for diluting protein samples) to the protein sample test wells, and add 2μl sample solution to the above PBS dilution to prepare 20μl protein sample solution.
(5) Add 200μl BCA solution to each of the standard wells and protein wells to be tested, mix well, and stand still at 37℃ for 30 minutes.
(6) After cooling to 25°C, the protein concentration was measured by nanodrop, and the values were recorded.
(7) Take the protein concentration (μg) as the abscissa, the absorbance value as the ordinate, and draw a standard curve in an excel sheet. Select "XY scatterplot" for the chart type, add a trend line, linear regression, select the display formula y=ax+b (y=absorbance value, x=protein concentration) in the options, display R_2. R_2 should be higher than 0.99.
(8) According to the standard curve, the actual concentrations of the samples (μg/μl) to be measured were calculated from the absorbance value of the protein samples by the formula: x=10(absorbance value y-b)/a. According to the formula, all the above data could be uniformly calculated in an excel document.

2.12.2.3 Protein sample preparation

(1) According to the measured protein concentrations, dilute each group of proteins with RIPA lysate to a uniform concentration.
(2) Add 5×sample loading buffer containing 10% β-mercaptoethanol to each tube and mix well.
(3) Boil the proteins in 100°C Schüttel-Trockenbad for 5 minutes.
(4) The denatured protein samples were centrifuged instantaneously at low speed to allow them to mix well and then added to the gel well using a micropipette.
(5) Freeze the remaining protein samples at -20°C. When using the samples again, boil the samples in a Schüttel-Trockenbau at 100°C for 1-2 minutes to thaw completely, then

centrifuge immediately and mix thoroughly before operation.

2.12.2.4 Protein electrophoresis

a. Assemble the purchased SDS-PAGE gels into the electrophoresis system.
b. Add electrophoresis buffer with a loading volume of 20μl per well and 5μl for protein marker loading.
c. Turn on the Gel Electrophoresis, set the power supply voltage to 80V, and set the time to 20 min. After the protein indicator has disappeared, set the power supply to 120 V for 1 hour.

2.12.2.5 Transfer membranes

Carefully pry off the electrophoresis plate, cut out the gel containing the target protein according to the position of the protein indicator, and place the gel on the transfer filter paper. Cut the PVDF membrane according to the area of the gel. Soak the PVDF in anhydrous methanol for 10s, then gently cover the gel. Cover and clamp the transfer clip with filter paper. The transfer sequence was "sponge-filter paper-sample gel-PVDF membrane-filter paper-sponge". The power supply voltage was set to 120V and the membrane was transferred using a Trans-Blot Turbo (Bio-Rad) for 80 min.

2.12.2.6 Blocking protein antigen

Remove the membrane strips at the end of the transfer and rinse once with TBST buffer. The rinsed membranes were placed in a prepared blocking buffer with 5% skim milk powder and then slowly shaken in a shaker at 25°C for 2 hours.

2.12.2.7 Antigen-antibody reaction

a. Rinse the PVDF membrane 3 times with 0.1% TBST. Each time lasted 5 minutes.
b. Dilution of primary antibody:

Antibody	Concentration (μg/mL)
PD-L1	2
S6	0.5
AKT	0.2
p-S6	0.5
p-AKT	0.2

c. Incubate the above antibody overnight.
d. Recover the antibodies and store them at -20°C for reuse. The PVDF membrane was rinsed with 0.1% TBST 3 times.
e. Incubate the secondary antibody: 0.1% TBST dilute the corresponding species of HRP-labeled secondary antibody at a ratio of 1:1000 and incubate on a shaker at 25°C for 120 minutes.
f. Clean the PVDF 3 times.

2.12.2.8 Exposing the images

Prepare the ECL luminescent solution (1:1 mixture of liquid A and liquid B, available on demand) and place it away from light before use. Place the PVDF strips in the luminescent solution for approximately 10 seconds, then put them on the exposure table of the Li-COR Odyssey® Fc Imaging System. Adjust the appropriate exposure parameters and save the images. The grayscale values in the images were analyzed using ImageJ software.

2.13 qRT-PCR assay

qRT-PCR can detect the total amount of product after each polymerase chain reaction (PCR) cycle in the amplification reaction of a specific DNA sequence in a sample. qRT-PCR can be used as the basis for specific mRNA quantification. The number of cycles conducted for the fluorescence signal to reach the set domain value is the Ct value. qRT-PCR has a plateau period in amplification, before which PCR amplification is a simple 2^{Ct} exponential growth. The smaller the Ct value, the fewer cycles required to reach a plateau and the higher the starting concentration of the target gene.

2.13.1 Apparatus and Reagents

ROCHE Light Cycler® 480: Switzerland

Trizol Pure ZOL™ RNA Isolation Reagent: Bio-rad

Vortex Genie 2, universeller Kleinschüttler: Scientific industries

Centrifugation Of RNA And Protein Samples At 4 Degree: Celsius, Catalog Number: 5424R

Invitrogen™ UltraPure™ DEPC-behandeltes Wasser: Invitrogen™ ,750024

Ethanol, 1L, glass: Art. No. 9065.1

0.2 ml 8-Tube Strips: TBC0802, Bio-Rad

2.13.2 Experimental Procedures

2.13.2.1 Extraction of total RNA from monolayers of adherent cells

(1) The following measures should be paid attention to during the experiment.Wear clean disposable gloves; Use a unique laboratory bench for RNA manipulation; Avoid talking during the operation.
(2) Prepare the icebox in advance, spread the ice, and turn on the 4°C centrifuge to pre-cool.
(3) Add an appropriate amount of PBS to the 6-well plate, gently wash and discard the PBS, repeat washing the cells 2 times, and aspirate the residual PBS.
(4) Add 500μl Trizol to each well of the 6-well plate, shake gently to cover the entire bottom of the wells, and keep the 6-well plate on ice for 5 minutes.

(5) Transfer the Trizol and cell mixture to a new EP tube and add 100μl chloroform. Cap tightly and label the groups. Shake with a Vortex-Genie 2 for 15 seconds, then place the EP tube on ice for 5 minutes.
(6) The EP tubes were placed in the 4°C centrifuge for 15 min. After centrifugation, the solution was observed in three layers: a colorless solution in the upper layer, a thin white solution in the middle, and a pink solution in the lower layer.
(7) Carefully remove the centrifuge tube, avoid shaking, gently aspirate the upper colorless layer, transfer it to another new EP tube, avoid aspirating the middle layer as much as possible, and record the volume of colorless liquid aspirated.
(8) Add an equal volume of isopropanol to the EP tube as aspirate and cover the tube with a cap. Gently invert the tube about 10 times to mix the liquid well and continue to stand still on ice for 10 minutes.
(9) Place them in the 4°C centrifuge and centrifuge for 10 min, and then add 1 ml 75% ethanol to the precipitate and gently rotate the EP tube up and down to float the white residue.
(10) After waiting for the precipitate to float, place the EP tube in the 4°C centrifuge. Discard the supernatant after centrifugation and wash twice with pre-chilled 75% ethanol.
(11) Dry upside down at 25°C for 5-10 min. Add 15μl-50μl DEPC to the EP tube and mix it gently.
(12) The RNA concentration was measured by nanodrop. The OD260/OD280 of qualified RNA was between 1.8 and 2.0. After the concentration measurement was completed, store it in a -20°C refrigerator.

RNA extraction	Trizol Chloroform Isopropanol Ethanol The red blood cell lysate DEPC dNTP mix (10mM)
Reverse Transcription	RNA reverse transcriptase RNase inhibitor Oligo $(dT)_{18}$
qPCR	2×SYBR Green qPCR Mix

2.13.2.2 Reverse transcription reaction

(1) Prepare 200μl PCR reaction tubes and mix the reverse transcription reaction system for PCR according to the following components (operation was performed on ice). "Con" represents the RNA concentration (ng/μl) measured during the RNA extraction.

Reagents	Volume
5×PrimeScript@ RT Master Mix for Real-Time	2μL
Total RNA	500ng/Con
DEPC	Up to 10μL

(2) The components were gently mixed and reverse transcribed into cDNA according to the following conditions.

React in a 37°C environment.

Water bath at 85°C for 10 seconds.

Place the PCR reaction tubes on ice.

(3) After reverse transcription, 40μl DEPC water was added to dilute it for 5 times and then used it as a PCR template.

2.13.2.3 Polymerase chain reaction

PD-L1 primers were designed for RT-PCR detection using Primer Premier 5 software.

PD-L1 primer sequence

Forward: 5'-TGTACCGCTGCATGATCAG-3'

Reverse: 5'-AGTTCATGTTCAGAGGTGACTG-3'

β-Actin primer sequence

Forward: 5'- CATGTACGTTGCTATCCAGGC -3'

Reverse: 5'- CTCCTTAATGTCACGCACGAT -3'

(1) Prepare the reaction system according to the following components, 8-Tube Strips for PCR reactions. The operation was performed on ice.

(2) The reaction system was centrifuged briefly, and the reaction solution was mixed. Turn on the PCR amplification function, set the reaction parameters, and perform the PCR reaction.

cDNA Template	2μL
2×SYBR Green qPCR Mix	10
10μM Primer Forward	0.4
10μM Primer Reverse	0.4
ddH_2O	7.2
Total volume	20

2.13.2.4 Amplification cycle temperature and time

Pre-denaturation	95℃ 300s	
Denaturation	95℃ 20s	n=40 Cycles
Annealing	55℃ 20s	
Extend	72℃ 20s	

At the end of the amplification cycle, the reaction system was cooled to 60°C and then heated to 95°C to denature the DNA.

2.13.2.5 Results analysis method

Results were analyzed using the relative quantification method: - ΔΔCt.

Ct (target gene in experimental group) − Ct (internal reference gene in experimental group) = ΔCt (experimental group)

Ct (target gene in control group) − Ct (internal reference gene in control group) = ΔCt (control group)

ΔCt (experimental group) − ΔCt (control group) = ΔΔCt

Fold difference = $2^{-\Delta\Delta Ct}$

2.14 Flow Cytometry assay

Flow cytometry (FCM) is a technique that uses monoclonal antibodies with fluorescence to label cells or other biological particles for rapid multi-parameter quantitative assays. It is a contemporary advanced technique for measuring cell parameters, such as the number of antigens on the cell surface.

2.14.1 Apparatus and Reagents

Flow cytometer: BD LSRFortessa™, USA

PD-L1 antibody: 374512, Bio Legend

RM 5 Rotating mixer REF: 14340/0348, Mini tube

EdU Staining: ab219801, Abcam

2.14.2 Experimental Procedure

Detection expression of PD-L1.

(1) A549, A549/DDP, HCC827, HCC827/DDP, H1975, H1975/DDP cells were inoculated in 6-well plates according to the experimental design incubated overnight in the incubator. Different drug concentrations of cisplatin, 740Y-P and XL765 were added to the cells.

(2) Aspirate the original medium, transfer the medium to an EP tube, add 2 ml PBS, gently shake the 6-well plate to rinse the cells, discard the buffer, and repeat the washing 2 times.

(3) Cells were digested by adding sterile trypsin solution in a 6-well plate according to the dose of 200μl/well. The changes in cell morphology were observed under the microscope. If cells were observed to change from shuttle or polygonal to oval, this indicates that the digestion could be terminated. Trypsin digestion reaction was terminated by adding medium containing serum from the previous step to each corresponding well.
(4) Gently aspirate the medium with a 1 ml pipette and rinse the cells until all cells were suspended. The digested cell suspension was transferred to a new EP tube and the control group was divided into two tubes. The cells were then centrifuged.
(5) Discard the supernatant, resuspend the cells with 1 ml PBS, and mix well.
(6) After centrifugation, discard the upper layer of PBS, add 500μl PBS Buffer containing 0.5% BSA to the cell precipitate, resuspend and mix well.
(7) Add an equal amount of 4% paraformaldehyde at 25°C to fix the cells.
(8) Wash twice with PBS containing 0.5% BSA. Then block the antigen with 3% BSA.
(9) Sample labeling: (0.5-1)*10^6 cells in 100μl of 1 x PBS with 0.5% BSA.
We established different groups: a) no-labeled cell sample group; b) isotype control group; c) labeled primary antibody group.
(10) Add PD-L1 antibody and incubate on a rotating mixer for 1-2h at 25°C.
(11) After centrifugation, the supernatant was discarded, and 1 mL PBS (0.5% BSA) was added again to resuscitate the cells. Wash the cells 3 times, and resuspend the cells with 500μl PBS.
(12) Wrap the samples in tin foil. When the samples were transferred to the flow cytometry core, the cell suspension in each sample was transferred from the EP tube to a new flow cytometry tube for determination.

2.14.3 Detection of apoptosis rates of different cell lines before and after drug treatment

Steps 1-6 were as above, and the remaining steps were conducted according to the kit instructions. Cells needed to be washed between steps.

7. Add EdU solution to the cells to be stained.
8. Incubate the cells for 2-4 hours under optimal growth status.
9. Add fixative solution and incubate for 15 min.
10. Add permeability buffer and incubate for 20 min.
11. Add a reaction mixture of fluorescently labeled EdU and incubate for 30 min.
12. Analyze by flow cytometer.

Kit instructions are available: https://www.abcam.com/edu-assay--edu-staining-proliferation-kit-ifluor-488-ab219801.html

3. STATISTICAL METHODS

The results of the Wound Healing assay, Transwell assay, Cell Immunohistochemistry and Western Blot were analyzed by Image J software. The results of the Cellular Activity Assays were analyzed by Graphpad Prism 8.02. Flow cytometry results were processed by Flowjo-V10 software (FlowJo Software, USA). Each group of experiments was independently repeated three times, and all data were analyzed by SPSS version 25.0 software. For data that obeyed a normal distribution with consistent variance, the mean ± standard deviation (mean ± SD) was used to describe the data. Independent samples t-test were used for comparison between two separate groups of data, and one-way ANOVA was used for comparison between multiple groups. All data were plotted using GraphPad Prism 8.02 software. $P<0.05$ stands for statistical differences.

4. RESULTS

4.1 Induction of A549/DDP cell line in vitro

After culturing the A549 cell line by increasing cisplatin concentration over 9 months, they could grow well in medium containing 300μM cisplatin, which we labeled as A549/DDP cell line. A549/DDP cells had a round cell morphology and larger cell nucleus. A549 cells had a lower adhesion capacity than A549/DDP cells.

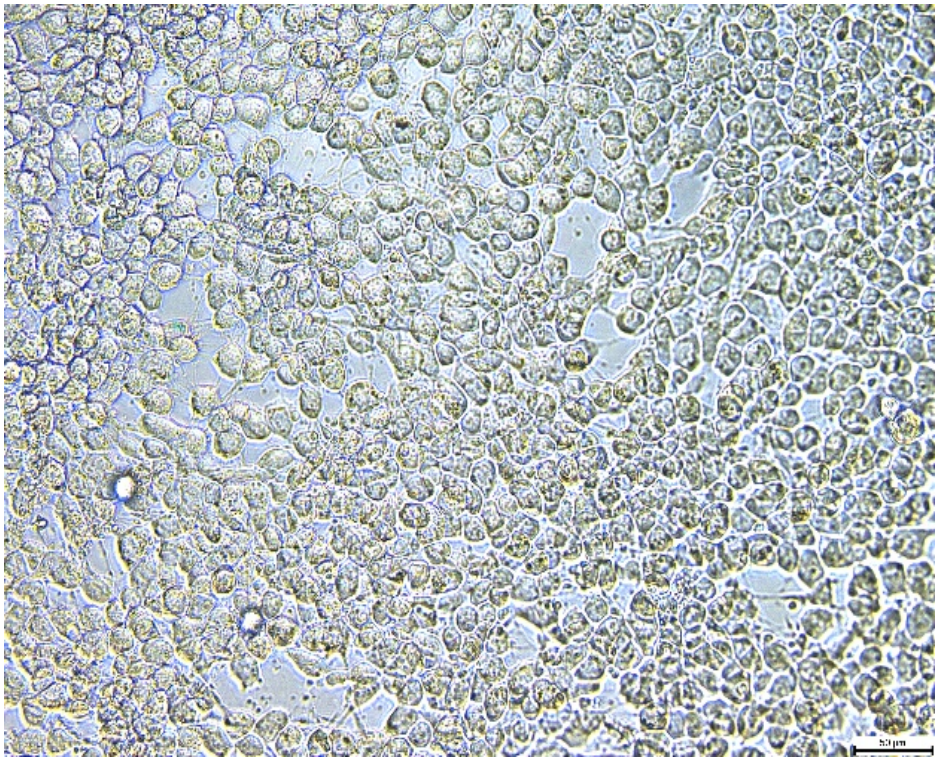

Figure 2. Growth status of A549/DDP in 300μM cisplatin-containing medium.

4.2 Drug sensitivity in different NSCLC cell lines to the effects of cisplatin, 740Y-P, and XL-765

To select the appropriate cisplatin concentration to stimulate different NSCLC cell lines in vitro, we used a series of cisplatin in a gradient of concentrations (1, 2, 4, 8, 16, 32, 64, 128, 200μM) to stimulate A549, HCC827 and H1975 cells for 36 h. The CCK-8 reagent was used to detect the cisplatin sensitivity of each cell line above. The survival rate of the three cell lines gradually decreased as the cisplatin concentration increased. We processed the data using Graphpad Prism 8.02 software and found that the IC50s of cisplatin in A549, HCC827 and H1975 cells were 11.39μM, 8.70μM and 11.48μM. In the same way, we used the same concentration gradient of XL-765 to stimulate the above three cell lines for 36 h. The IC50s of XL-765 in A549, HCC827 and H1975 cells were 26.18μM, 27.54μM and 28.10μM. As for the NSCLC/DDP cell lines, we used cisplatin concentration gradients (50, 100, 200, 300, 400, 500, 600, 800, and 1000μM) to stimulate them for 36 h. We used Graphpad prism 8.02 software to analyze the data, and the IC50s of cisplatin in A549/DDP, HCC827/DDP and H1975/DDP were 349.40μM, 429.20μM and 305.80μM.

To assess the effects of agonist 740Y-P in A549, HCC827 and H1975 cell lines, we stimulated them for 36 h using 740Y-P with concentration gradients (1, 2, 4, 8, 16, 32, 64, 128, 200μM). The EC50s of A549, HCC827 and H1975 cells were 7.47μM, 6.48μM and 7.39μM.

It could be seen that the survival rate of the three cell lines gradually decreased with increasing concentrations of cisplatin and XL-765 (Figure 3A-C,4A-C,5A-C). The survival rates of the three cell lines gradually increased with increasing concentrations of 740Y-P (Figure 3D,4D,5D). According to the drug sensitivity of the cells, cisplatin was set to another concentration gradients for subsequent experiments. The stimulating concentrations of cisplatin were 0μM, 2μM, 4μM, 6μM, 8μM and 16μM.

4.2.1 Drug sensitivity in A549 and A549/DDP cells

A

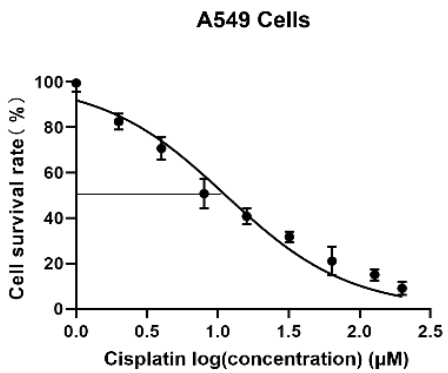

B

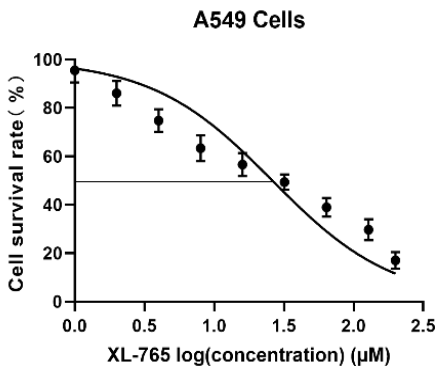

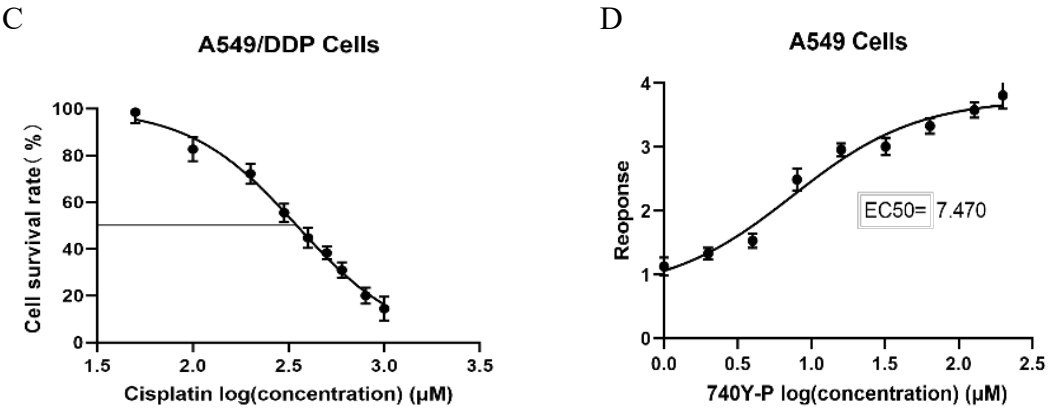

Figure 3. Drug sensitivity of A549 or A549/DDP cell line to cisplatin, XL-765, 740Y-P.
The A549 or A549/DDP cell line was stimulated with gradients of various concentrations of cisplatin, XL-765, and 740Y-P for 36 hours, and the survival rates of the above cells were detected with the CCK-8 kit.
(A). IC50=11.39μM; (B). IC50=26.18μM; (C). IC50=349.40μM; (D). EC50=7.47μM

4.2.2 Drug sensitivity in H1975 and H1975/DDP cells

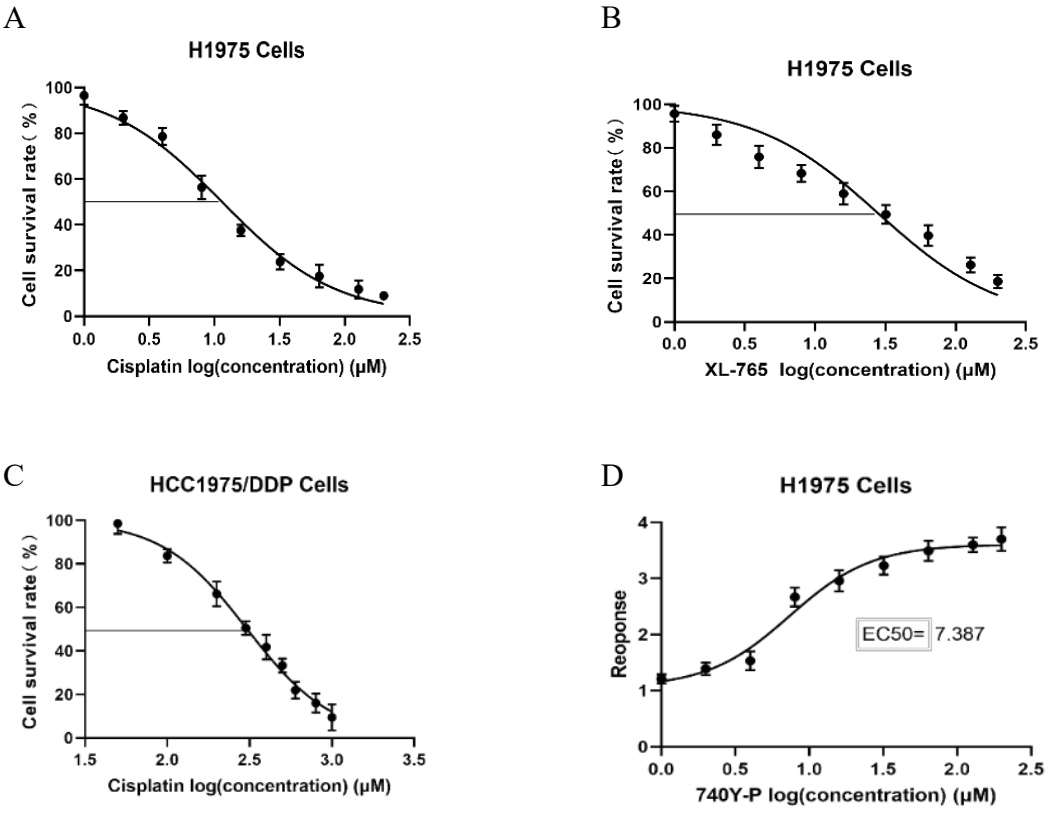

Figure 4. Drug sensitivity of H1975 or H1975/DDP cell line to cisplatin, XL-765, 740Y-P.
The H1975 or H1975/DDP cell line was stimulated with gradients of various concentrations of cisplatin, XL-765, and 740Y-P for 36 hours, and the survival rates of the above cells were detected with the CCK-8 kit.
(A). IC50=11.48μM; (B). IC50=28.10μM; (C). IC50=305.80μM; (D). EC50=7.39μM

4.2.3 Drug sensitivity in HCC827 and HCC827/DDP cells

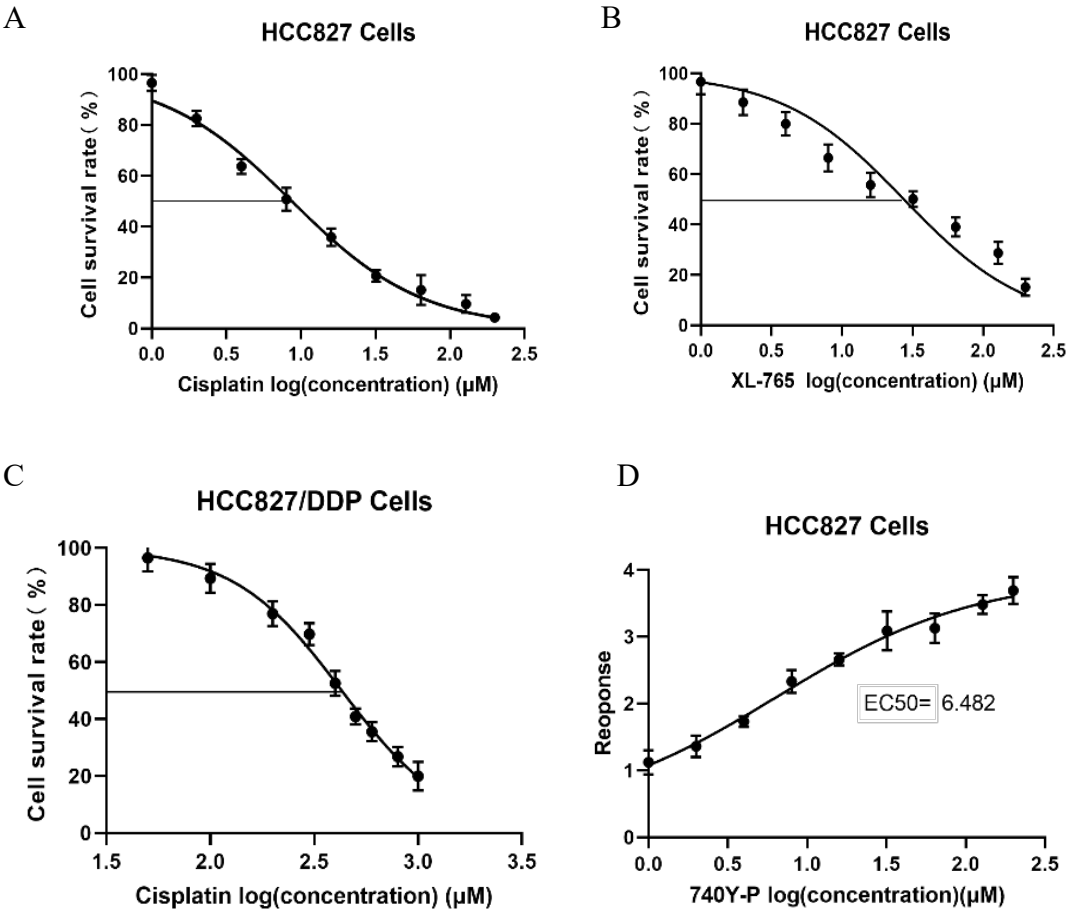

Figure 5. Drug sensitivity of HCC827 or HCC827/DDP cell line to cisplatin, XL-765, 740Y-P.
The HCC827 or HCC827/DDP cell line was stimulated with gradients of various concentrations of cisplatin, XL-765, and 740Y-P for 36 hours, and the survival rates of the above cells were detected with the CCK-8 kit.
(A). IC50=8.70μM; (B). IC50=27.54μM; (C). IC50=429.20μM; (D). EC50=6.48μM.

4.3 Invasion capabilities in different NSCLC cell lines to the effects of cisplatin, 740Y-P, and XL-765

To simulate the invasion capability of NSCLC cell lines in vivo after stimulation with cisplatin, XL-765, and 740Y-P, we performed Transwell experiments with A549, A549/DDP, HCC827, HCC827/DDP, H1975, and H1975/DDP cell lines. Before conducting the Transwell assay, NSCLC naïve cells were cultured in 20μM 740Y-P (NSCLC/740Y-P groups) for 8 hours and 6μM cisplatin medium for 12 hours (NSCLC/cisplatin groups); cisplatin-resistant strains were cultured in 10μM XL-765 medium for 8 hours (NSCLC/XL-765 groups). According to the pre-experiment of the Transwell assay, we selected the A549 cell line to be cultured in the incubator for 24

hours and the HCC827 and H1975 cell lines for 36 hours. The results showed that the invasion capability: A549<A549/DDP (Figure 6A), and the two groups had differences after statistical analysis (P<0.005, Figure 6B). The invasion capability of A549 after stimulation with 6μM cisplatin or 20μM 740Y-P was faster than that of the group with DMSO (Figure 6A), the two groups had differences after statistical analysis (P<0.05, Figure 6B). The invasion capability of A549/DDP after stimulation with 10μM XL-765 group>DMSO group (Figure 6A), the two groups had differences after statistical analysis (P<0.005, Figure 6B). Similar results were also observed in HCC827, HCC827/DDP, H1975 and H1975/DDP cell lines, as detailed in Figure 7A, Figure 7B and Figure 8A, Figure 8B. Each group of experiments was conducted independently for three times (*P<0.05, **P<0.01, ***P<0.005).

4.3.1 The invasion capabilities of A549 and A549/DDP cells

A

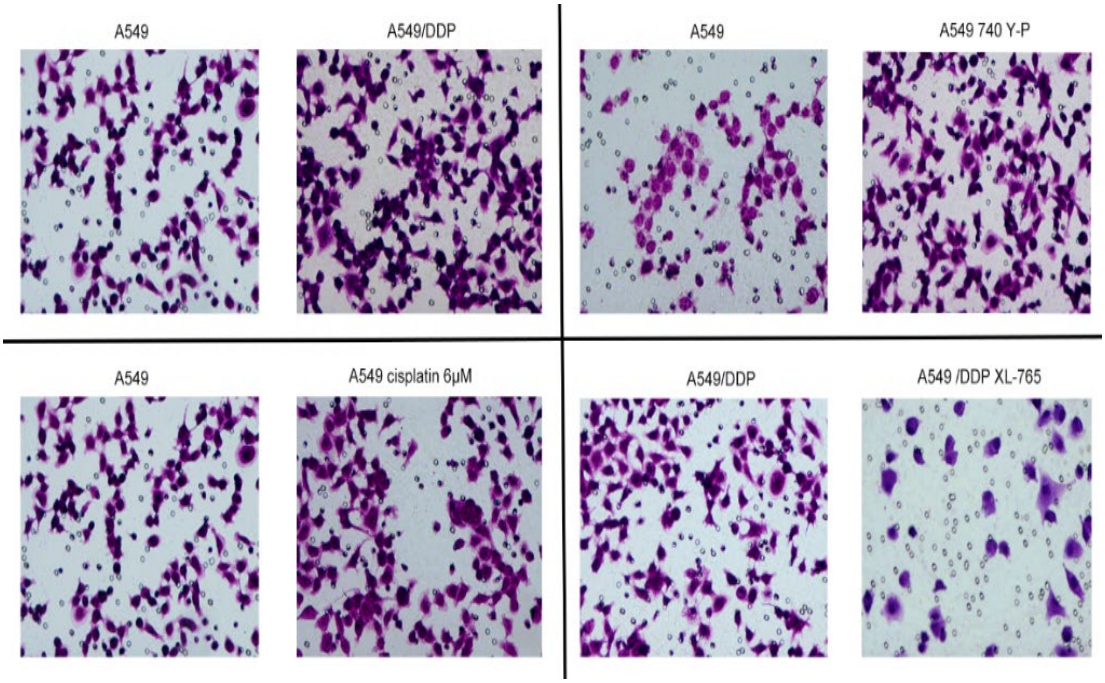

B

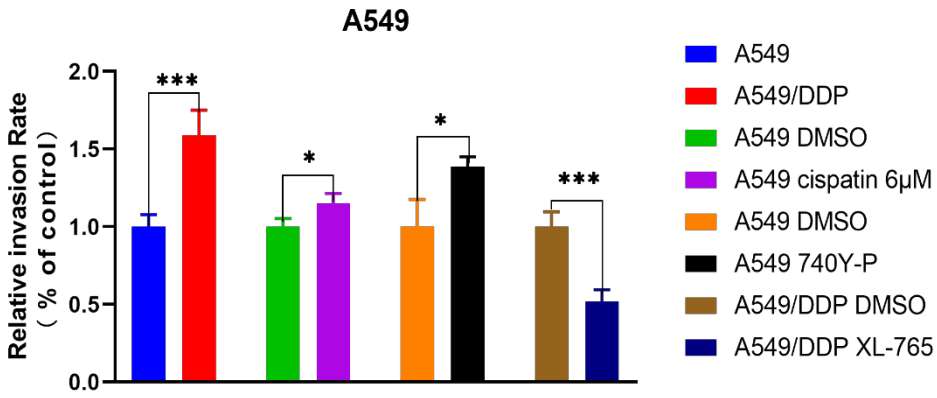

Figure 6. Comparison of the invasion capability of A549 and A549/DDP after stimulation with and without cisplatin, XL-765 and 740Y-P.

(A) Representative images of Transwell results are shown for each of the four quadrants. (B) This graph shows the fold differences in cell numbers between the treated and control groups. Statistically significant differences after independent samples t-test.

4.3.2 The invasion capabilities of HCC827 and HCC827/DDP cells

A

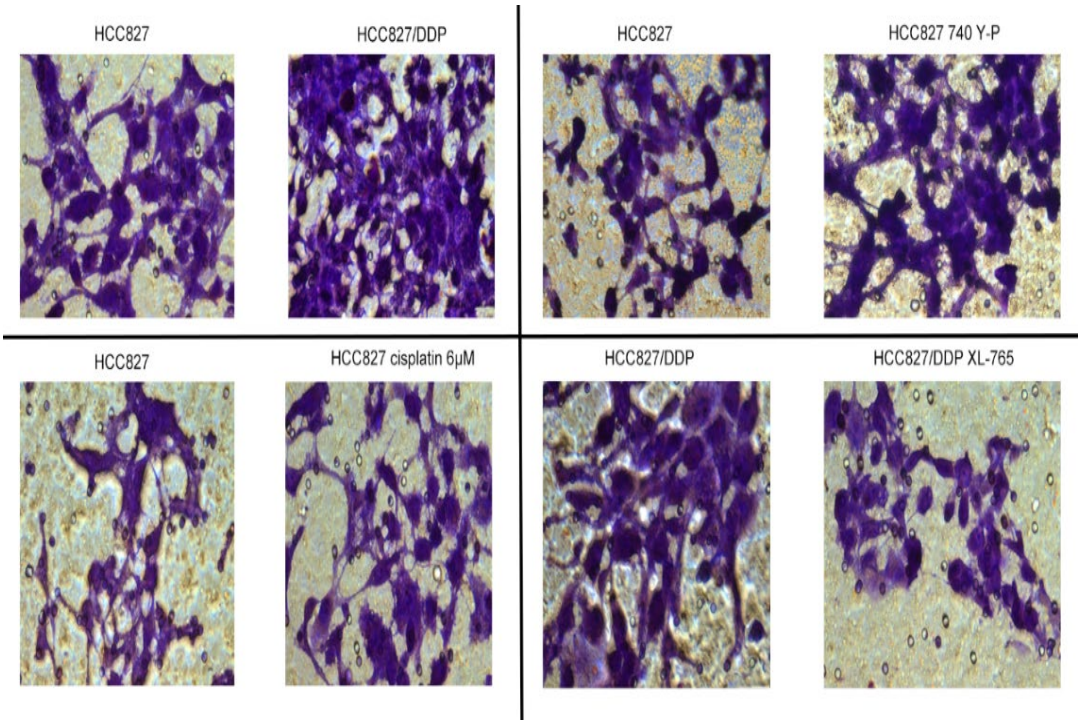

B

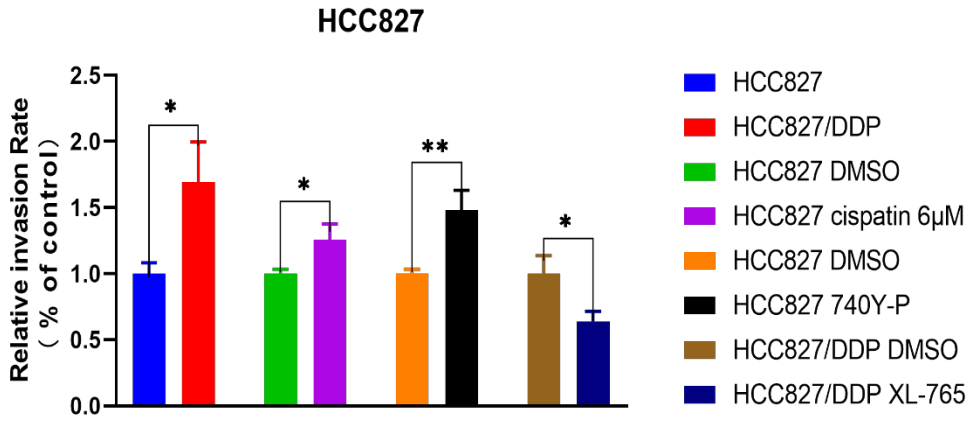

Figure 7. Comparison of the invasion capability of HCC827 and HCC827/DDP after stimulation with and without cisplatin, XL-765 and 740Y-P.
(A) Representative images of Transwell results are shown for each of the four quadrants. (B) This graph shows the fold differences in cell numbers between the treated and control groups. Statistically significant differences after independent samples t-test.

4.3.3 The invasion capabilities of H1975 and H1975/DDP cells

A

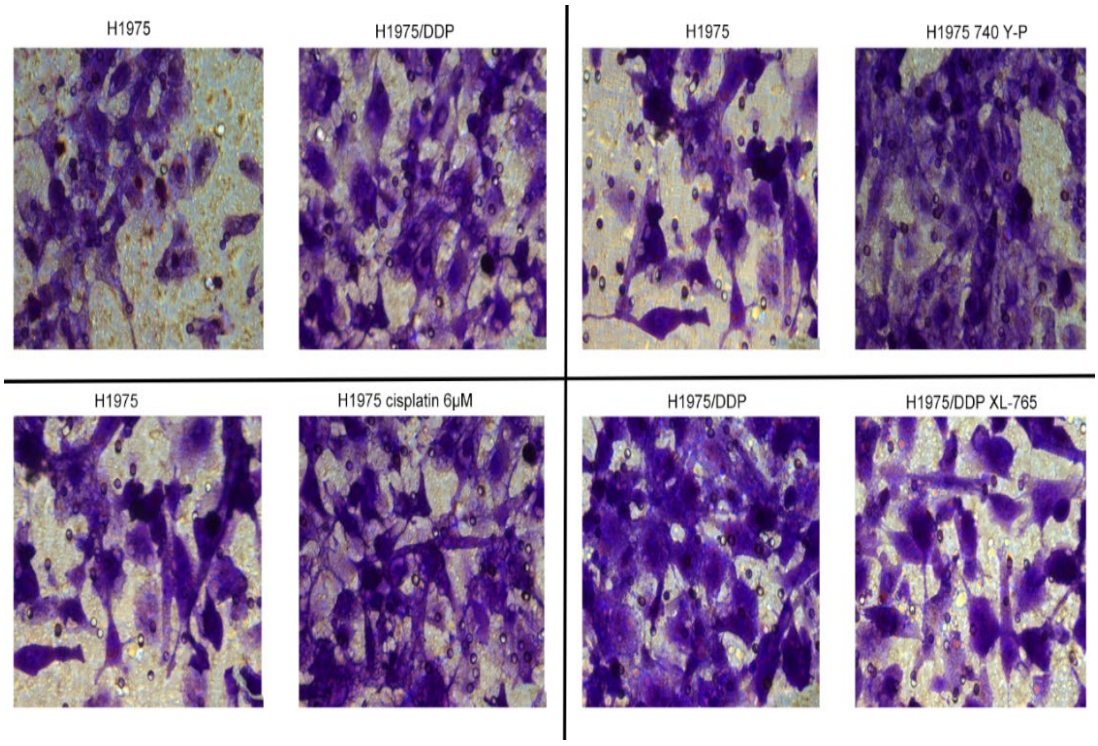

B

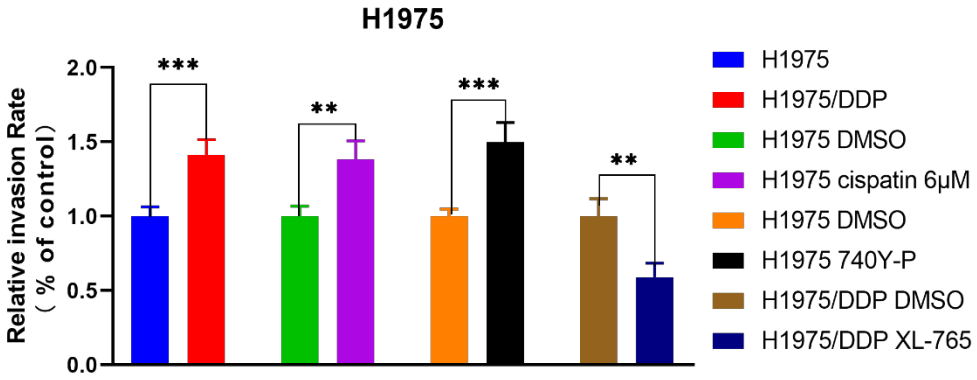

Figure 8. Comparison of the invasion capability of H1975 and H1975/DDP after stimulation with and without cisplatin, XL-765 and 740Y-P.

(A) Representative images of Transwell results are shown for each of the four quadrants. (B) This graph shows the fold differences in cell numbers between the treated and control groups. Statistically significant differences after independent samples t-test.

4. 4 Migration capabilities in different NSCLC cell lines to the effects of cisplatin, 740Y-P, and XL-765

We determined cell migration capability after stimulation with cisplatin, 740Y-P and XL-765 in A549, A549/DDP, HCC827, HCC827/DDP, H1975 and H1975/DDP cell lines. Naïve cell lines were separately incubated with 20μM 740Y-P for 8 hours and 6μM cisplatin for 12 hours before performing wound healing assay. Cisplatin-resistant strains were incubated with 10μM XL-765 for 8 hours. Three independent replicates were performed for each comparative experiment. We used the same 100μl pipette tip with a constant scratch spacing for the wound healing assay, then incubated together in the incubator for 48 h. After that we measured the scratch spacing on both sides. Our experimental data showed that the migration capability of A549/DDP was faster than that of A549 (Figure 9A), the two groups had differences after statistical analysis ($P<0.005$, Figure 9B). The migration capability of A549 group was faster after 6μM cisplatin stimulation than that of the DMSO group (Figure 9A), the two groups had differences after statistical analysis ($P<0.05$, Figure 9B). 20μM 740Y-P stimulation of A549 was faster than that of the DMSO group (Figure 9A), the two groups had differences after statistical analysis ($P<0.005$, Figure 9B). 10μM XL-765 stimulated A549/DDP had a slower migration capability than that of the DMSO group (Figure 9A), the two groups had differences after statistical analysis ($P<0.005$, Figure 9B). Similar results were observed in HCC827, HCC827/DDP, H1975 and H1975/DDP cell lines as detailed in Figure 10A, Figure 10B and Figure 11A, Figure 11B. (*$P<0.05$, **$P<0.01$, ***$P<0.005$).

4.4.1 The migration capabilities of A549 and A549/DDP cells

A

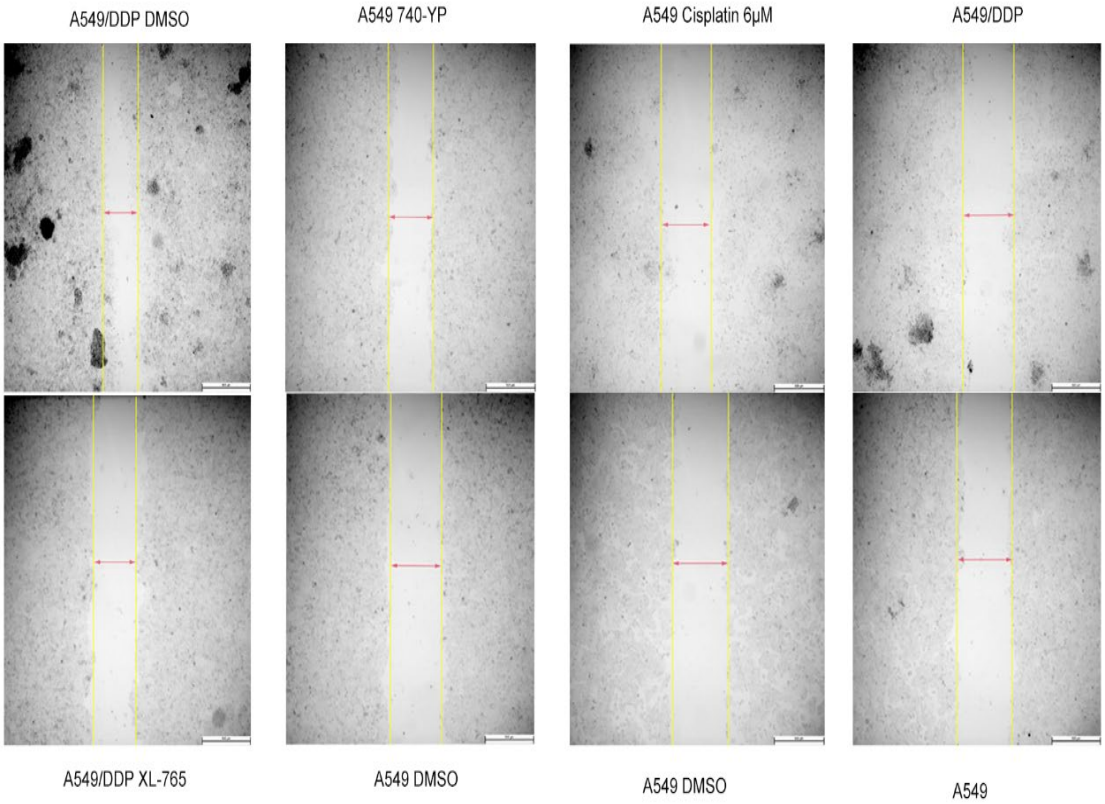

B

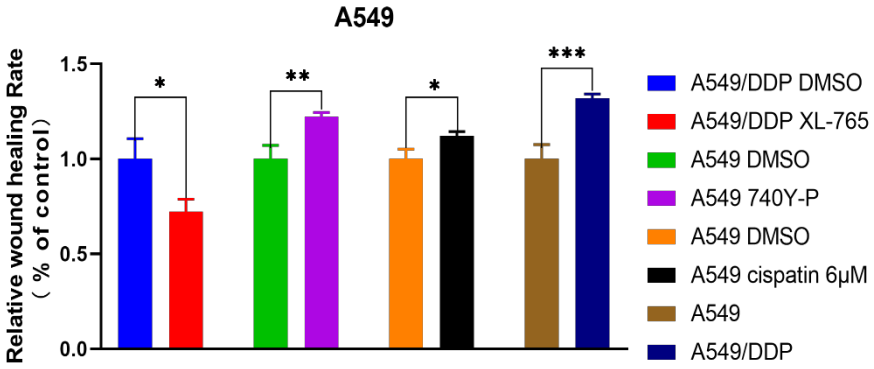

Figure 9. Detection of cell migration capability after cisplatin, 740Y-P, XL-765 stimulation of A549 and A549/DDP.

(A) Representative images of wound healing assay results. (B) This bar graph shows the fold differences in wound healing between treated and control groups. Statistically significant differences after independent samples t-test.

4.4.2 The migration capabilities of HCC827 and HCC827/DDP cells

A

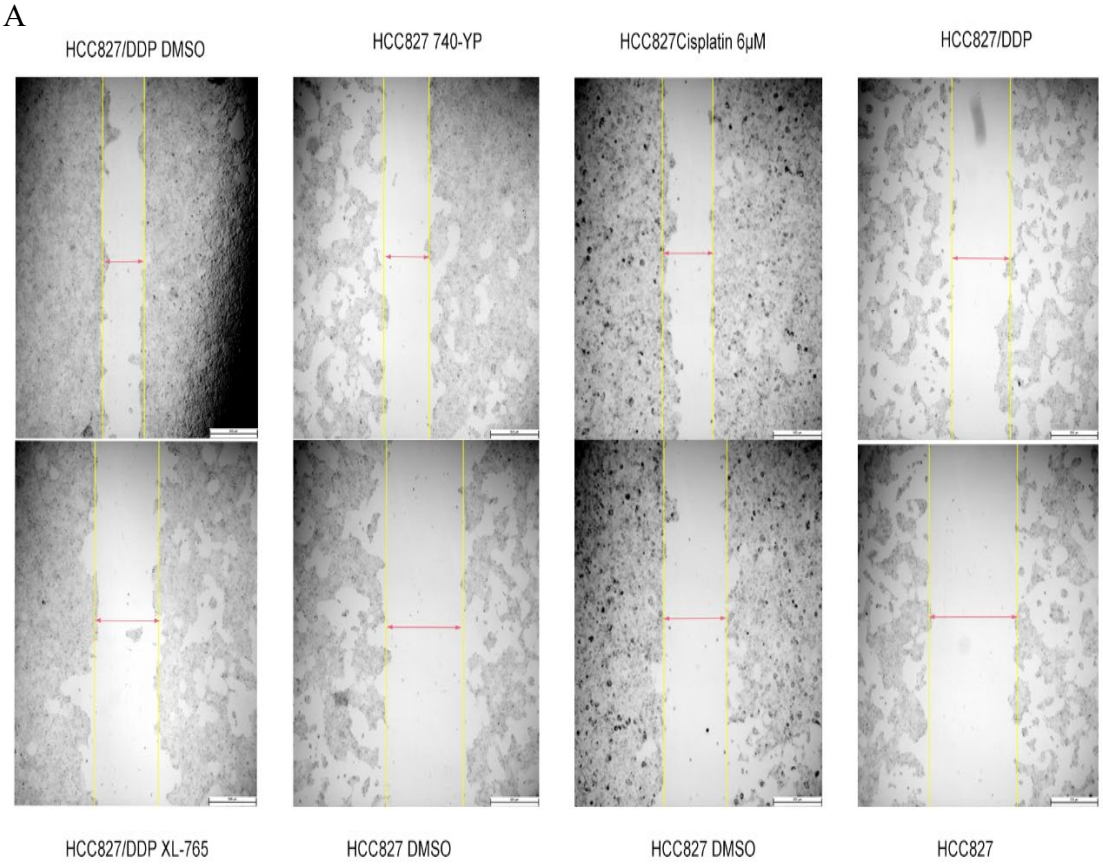

B

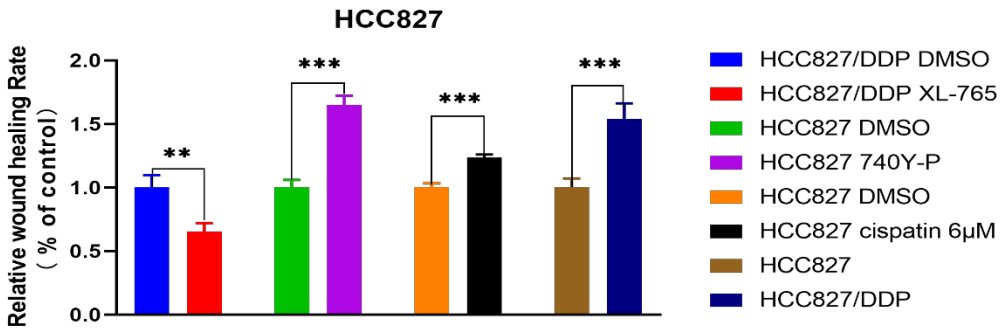

Figure 10. Detection of cell migration capability after cisplatin, 740Y-P, XL-765 stimulation of HCC827 and HCC827/DDP.

(A) Representative images of wound healing assay results. (B) This bar graph shows the fold differences in wound healing between treated and control groups. Statistically significant differences after independent samples t-test.

4.4.3 The migration capabilities of H1975 and H1975/DDP cells

A

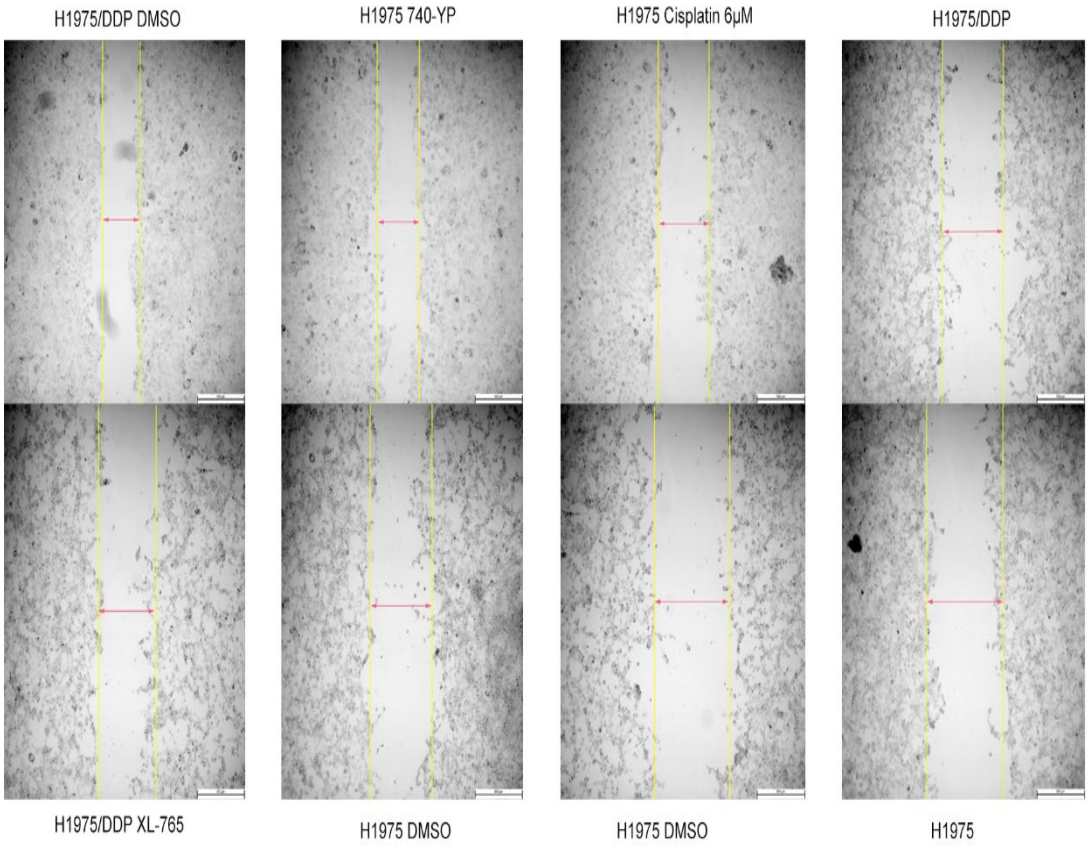

B

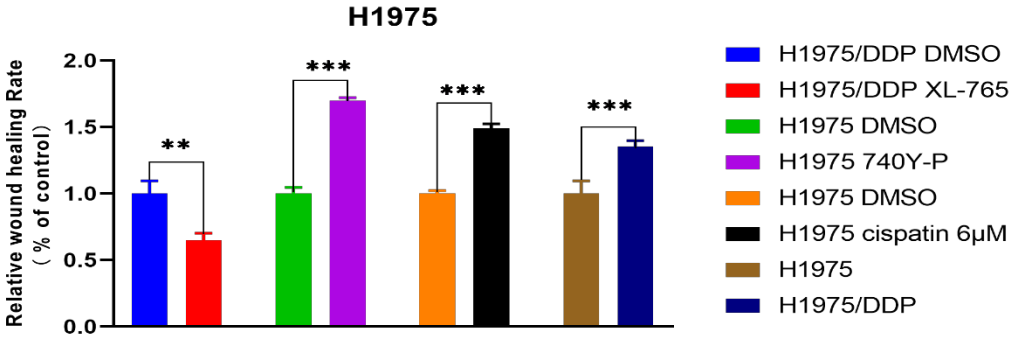

Figure 11. Detection of cell migration capability after cisplatin, 740Y-P, XL-765 stimulation of H1975 and H1975/DDP.

(A) Representative images of wound healing assay results. (B) This bar graph shows the fold differences in wound healing between treated and control groups. Statistically significant differences after independent samples t-test.

4.5 Cell viability of NSCLC cells treated with cisplatin, 740Y-P, XL-765

Cell viability is an important indicator for judging whether cells cultured in vitro can grow normally under certain conditions or not. In order to investigate the cell viability of A549, A549/DDP, HCC827, HCC827/DDP, H1975, H1975/DDP after treatment with cisplatin, 740Y-P, and XL-765, we used (0-16) μM cisplatin to stimulate A549, HCC827, and H1975 cells for 12h. A549, A549/DDP, HCC827, HCC827/DDP, H1975, H1975/DDP cells were stimulated with 20μM 740Y-P and 10μM XL-765 for (0-48) h. The data showed that the cell viability of NSCLC naïve cell lines gradually increased with increasing concentrations of cisplatin. The most significant increase in cell viability was observed at (4-8) μM cisplatin. This cisplatin concentration is lower than the IC50 concentration and well below the maximum concentration of cisplatin in human blood (149.261μM). When the naïve and cisplatin-resistant strains were stimulated with 740Y-P, the cell viability of each cell line was gradually increased at (0-48) h, and the increase in cell viability was most significant at (12-24) h. The cisplatin-resistant cells had higher cell viability than the naïve cells. When XL-765 was used to stimulate the above all cell lines, the cell activity of each cell line showed a downward trend. Within (0-48) h, the cell activity decreased significantly, and the cell activity of the NSCLC/DDP cells decreased significantly compared with the NSCLC naïve cells.

A

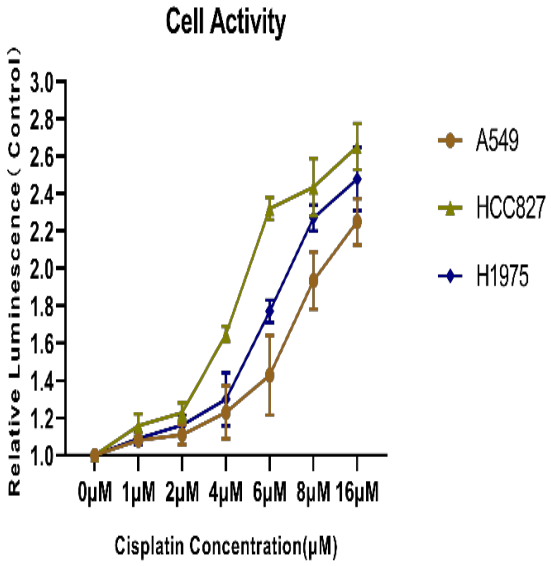

B

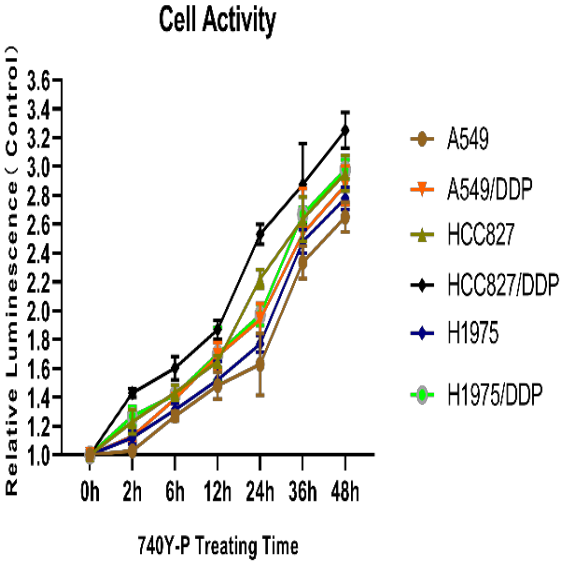

C

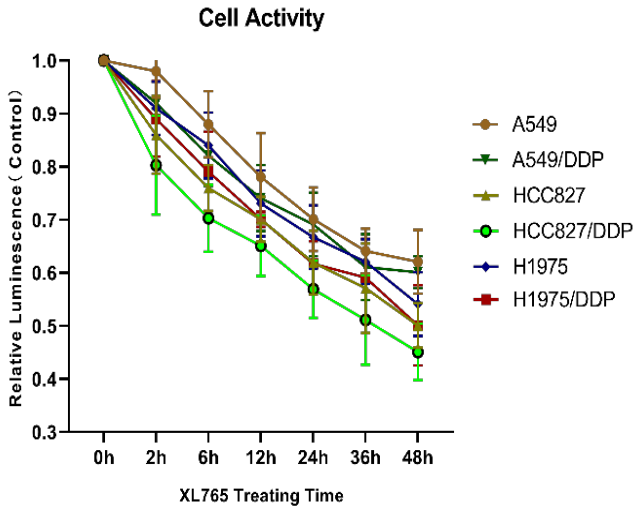

Figure 12. Effects of cisplatin, 740Y-P and XL-765 at different doses and times on cell viability.
(A) NSCLC naïve cells were cultured in medium containing (0-16) μM for 12 hours.
(B) A549, A549/DDP, HCC827, HCC827/DDP, H1975 and H1975/DDP cells were cultured in medium containing 20μM 740Y-P medium for (0-48) hours.
(C) A549, A549/DDP, HCC827, HCC827/DDP, H1975, H1975/DDP cells were cultured in medium containing 10μM XL-765 for (0-48) hours.
Cell viability assay was conducted with CellTiter-Glo® 2.0.

4.6 Apoptosis rates of NSCLC cell lines before and after stimulation with PI3K agonists and inhibitors

Apoptosis is an autonomous cell death process involving the expression and regulation of a series of genes after cells are stimulated. The purpose of detecting apoptosis rates is to investigate whether cellular signaling pathways that regulate PD-L1 expression can also influence apoptosis rates.
A549 and A549/DDP cells were cultured first, and then FCM was performed.
A549 cells was stimulated in medium containing 20μM 740Y-P for 4h, and then in normal medium for 20h, after that FCM was performed.
A549 cells was stimulated in medium containing 10μM XL-765 for 4h, and then in normal medium for 20h, after that FCM was performed.
The apoptosis rate of A549/DDP cells < A549 cells, and the 740Y-P stimulated A549 had a lower apoptosis rate than A549 cells, while the XL-765 stimulated A549/DDP cells had a higher apoptosis rate than A549/DDP cells (Figure 13A). This suggests that 740Y-P promotes cell growth, XL-765 promotes apoptosis, and cisplatin-resistant cells are less prone to apoptosis than naïve cells. Similar results were found in HCC827, HCC827/DDP, and H1975, H1975/DDP cell lines (Figure 14A, Figure 15A). Each group of experiments was conducted independently for three times (*P<0.05, **P<0.01, ***P<0.005).

4.6.1 The apoptosis rates of A549 and A549/DDP cells

A

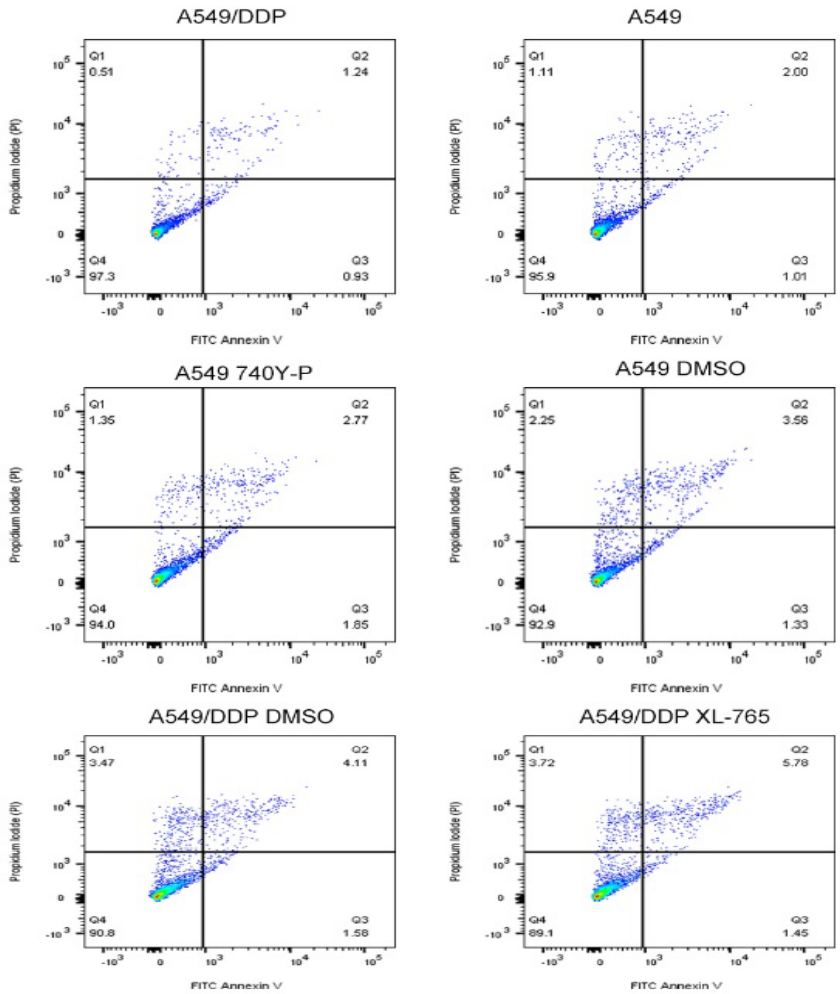

B

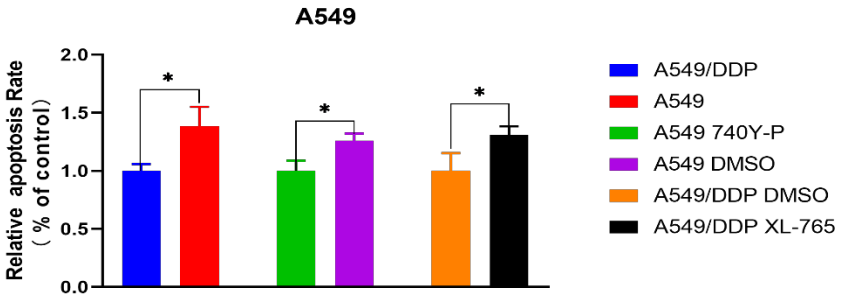

Figure 13. Apoptosis rates of A549 and A549/DDP after stimulation with 740Y-P, XL-765.
(A) Representative images of FCM results. The Annexin V-FITC Kit was used. (B) Histogram shows the fold differences in apoptosis rates (Q2+Q3) between the treated and control groups. Statistically significant differences after independent samples t-test.

4.6.2 The apoptosis rates of HCC827 and HCC827/DDP cells

A

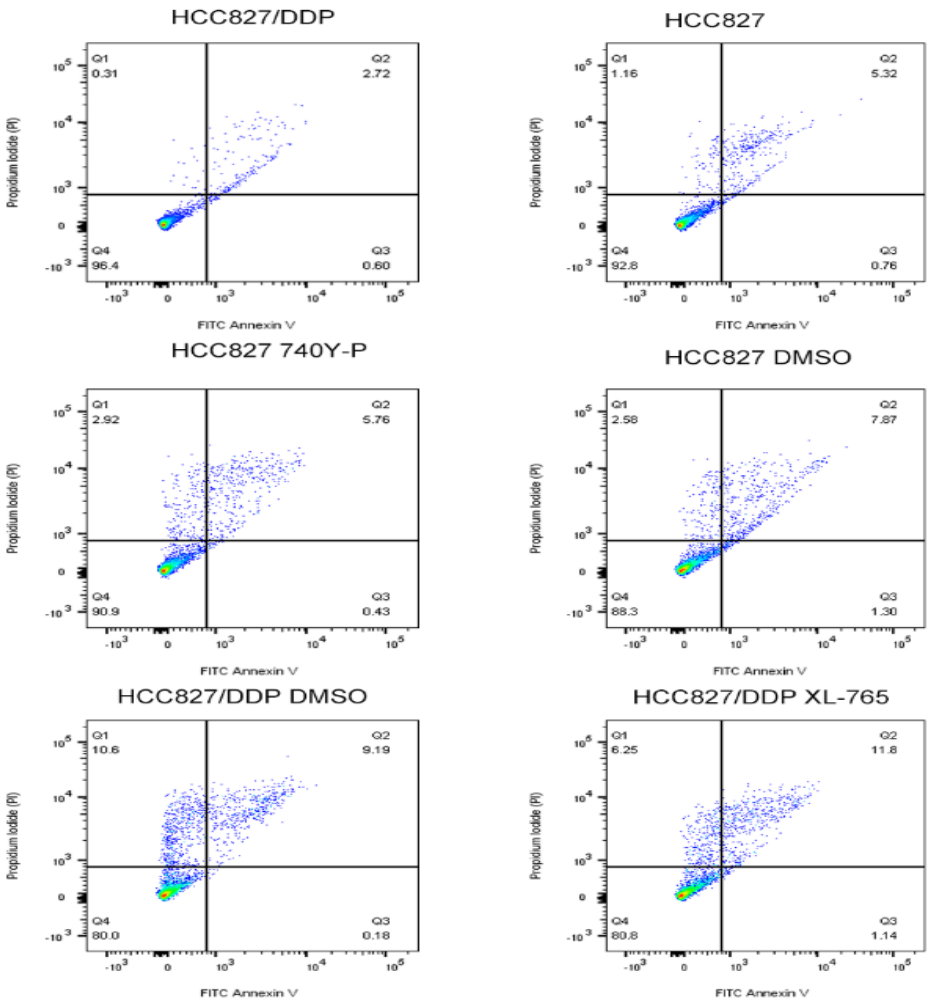

B

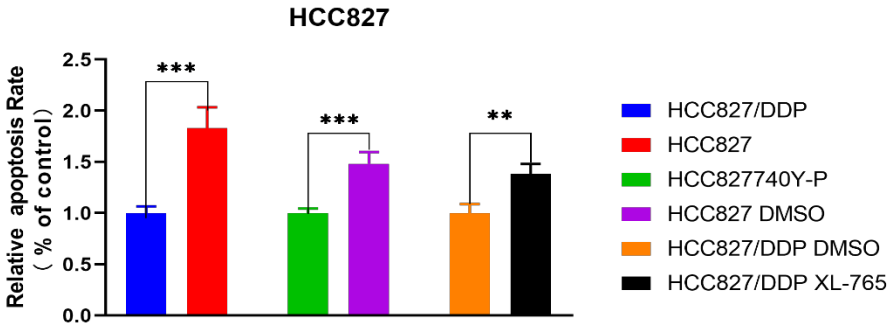

Figure 14. Apoptosis rates of HCC827 and HCC827/DDP after stimulation with 740Y-P, XL-765. (A) Representative images of FCM results. The Annexin V-FITC Kit was used. (B) Histogram shows the fold differences in apoptosis rates (Q2+Q3) between the treated and control groups. Statistically significant differences after independent samples t-test.

4.6.3 The apoptosis rates of H1975 and H1975/DDP cells

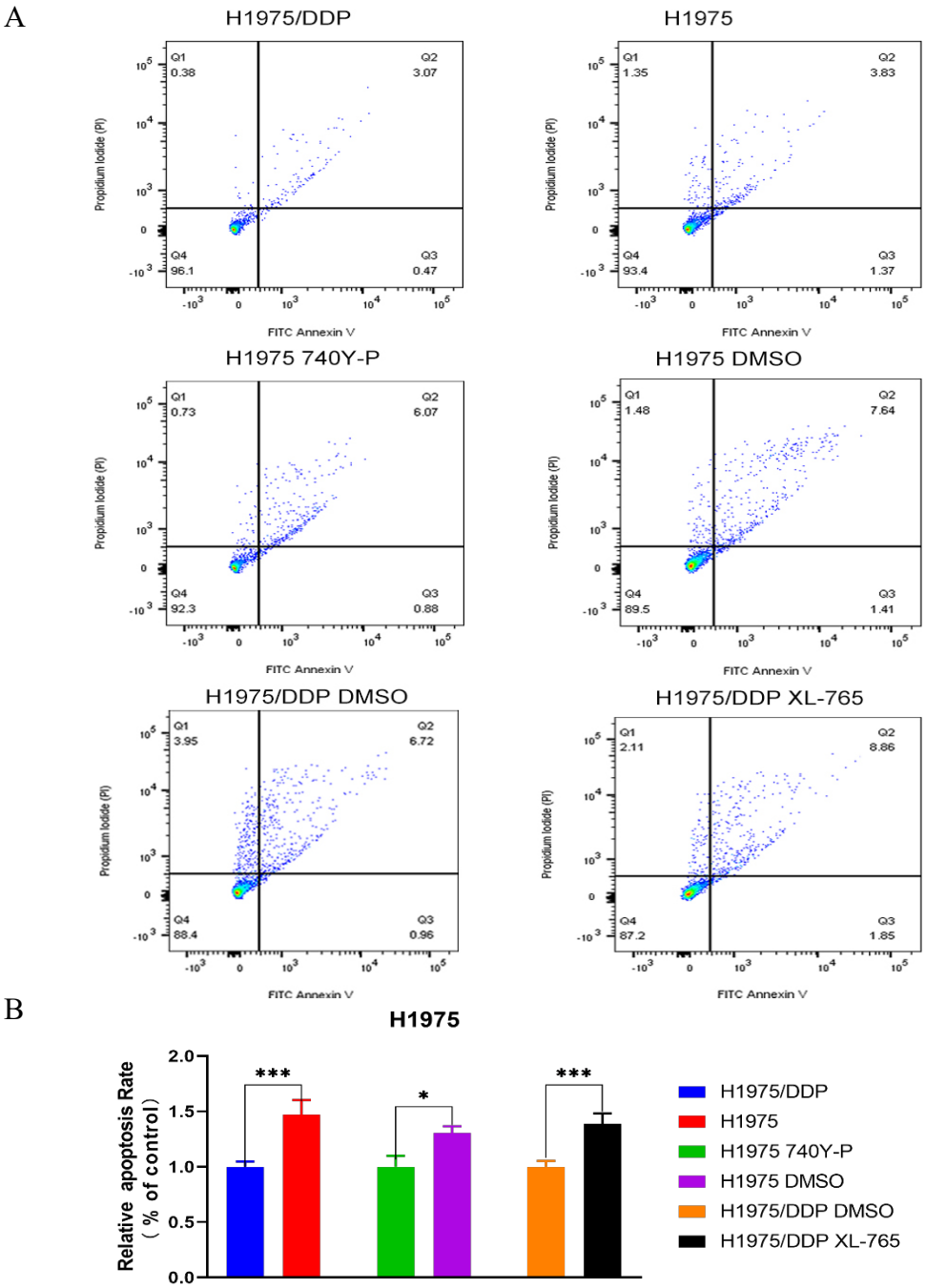

Figure 15. Apoptosis rates of H1975 and H1975/DDP after stimulation with 740Y-P, XL-765.
(A) Representative images of FCM results. The Annexin V-FITC Kit was used. (B) Histogram shows the fold differences in apoptosis rates (Q2+Q3) between the treated and control groups. Statistically significant differences after independent samples t-test.

4.7 PD-L1 expression in cisplatin-stimulated NSCLC, NSCLC and NSCLC/DDP cell lines

It has been learned from cell function experiments that cisplatin at a concentration lower than IC50 can enhance the cell activity, migration capability and invasion capability, and also reduce the apoptosis rates of NSCLC cell lines. Therefore, we further explored whether there were differences in PD-L1 expression in 8μM cisplatin-stimulated NSCLC naïve, NSCLC naïve and NSCLC/DDP cell lines. Immunohistochemistry staining was conducted with the staining kit on NSCLC/DDP cells, NSCLC naïve cells, and NSCLC naïve cells stimulated with 8μM cisplatin for 12h. The results showed that PD-L1 expression was higher in NSCLC/DDP cells than in NSCLC naïve cells, and PD-L1 expression in 8μM cisplatin-stimulated NSCLC naïve cells was in between. The two groups had differences after statistical analysis, when compared to NSCLC naïve cells ($P<0.005$, Figure 16D, 17D, 18D). As shown in Figures 16 (A-C), 17 (A-C), and 18 (A-C). The dark brown represents higher PD-L1 expression, and the purple or yellow represent negative cells. According to the immunohistochemistry results, it can be roughly seen that PD-L1 can be found in the cytoplasm and cell membrane.

We first used FCM to detect the difference in cell membrane PD-L1 expression and then used western blot to see the total PD-L1 expression in NSCLC cell lines. At the same time, we also explored the PD-L1 mRNA by qRT-PCR. Finally, we used 740Y-P and XL-765 to stimulate and inhibit the PATSP. Alterations in key proteins expression of this pathway were detected by western blot. (*$P<0.05$, **$P<0.01$, ***$P<0.005$).

4.7.1 Cisplatin up-regulates PD-L1 expression in A549 cells

A A549

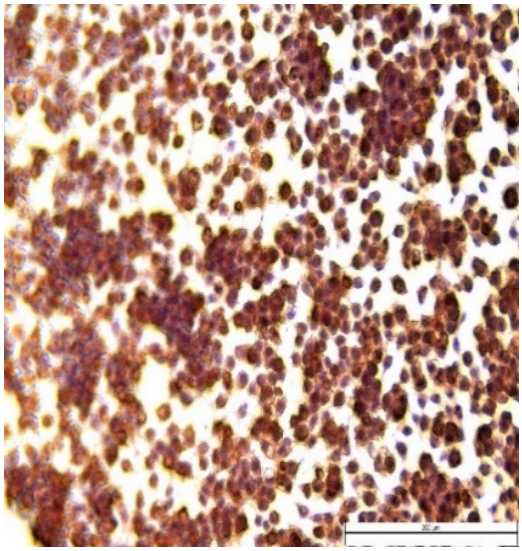

B A549/8μM

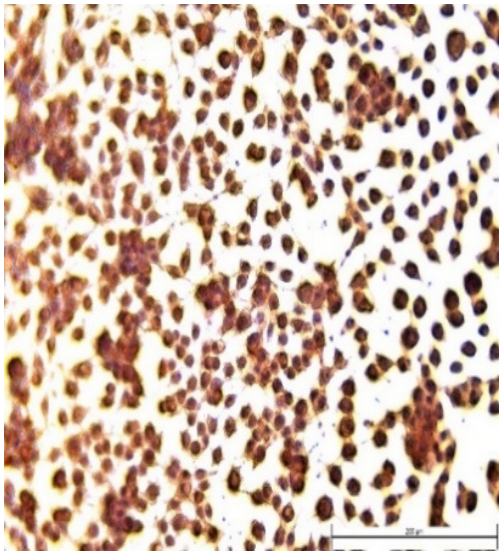

C A549/DDP

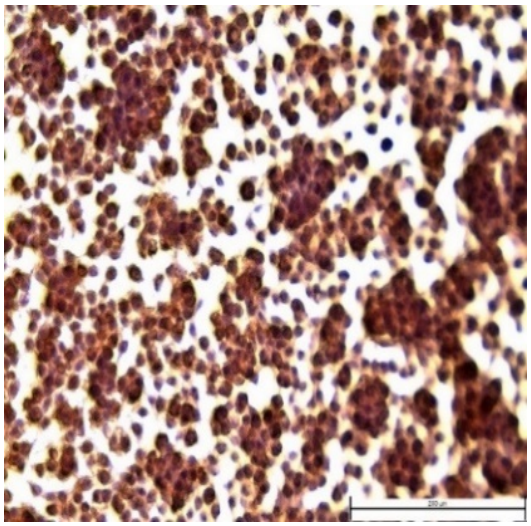

D

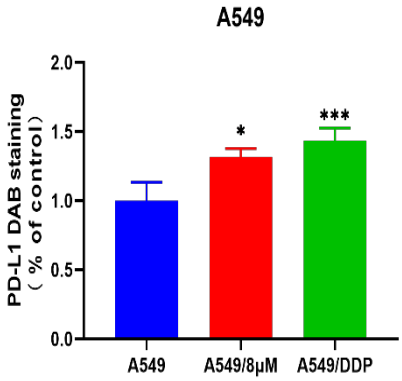

Figure 16. Differences in PD-L1 protein expression among A549/DDP, A549 and A549 stimulated with 8μM cisplatin.

(A-C) Representative images of the immunohistochemistry results. (D) Histogram shows the fold differences in staining intensity of A549/8μM (B) and A549/DDP cells (C) relative to A549 cells (A) in three independent experiments. Compared with the A549 group, the A549/8μM and A549/DDP groups underwent a one-way ANOVA, and the two groups had differences after statistical analysis.

4.7.2 Cisplatin up-regulates PD-L1 expression in HCC827 cells

A HCC827

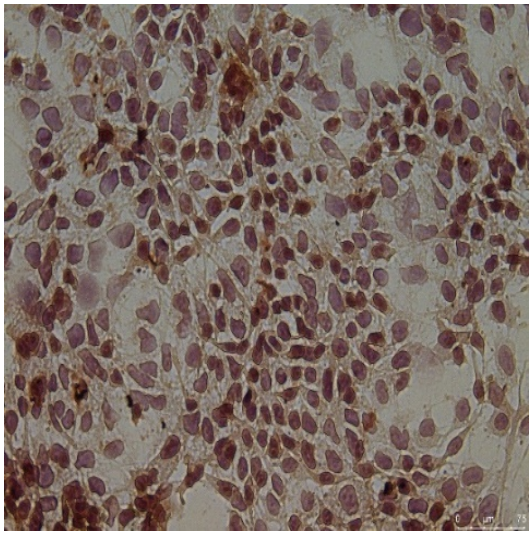

B HCC827/8μM

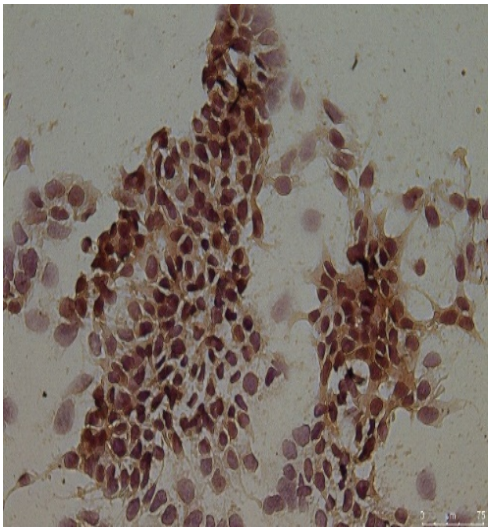

C HCC827/DDP

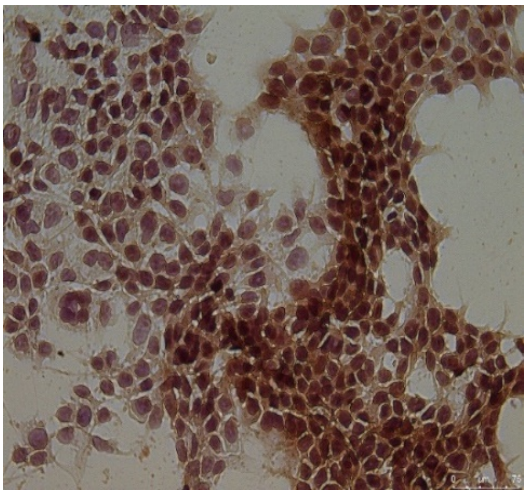

D

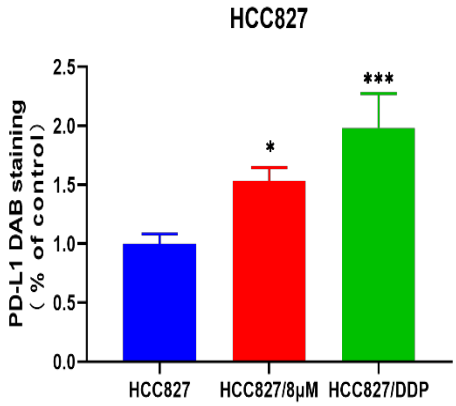

Figure 17. Differences in PD-L1 protein expression among HCC827/DDP, HCC827 and HCC827 stimulated with 8μM cisplatin.

(A-C) Representative images of the immunohistochemistry results. (D) Histogram shows the fold differences in staining intensity of HCC827/8μM (B) and HCC827/DDP cells (C) relative to HCC827 cells (A) in three independent experiments. Compared with the HCC827 group, the HCC827/8μM and HCC827/DDP groups underwent a one-way ANOVA, and the two groups had differences after statistical analysis.

4.7.3 Cisplatin up-regulates PD-L1 expression in H1975 cells

A H1975

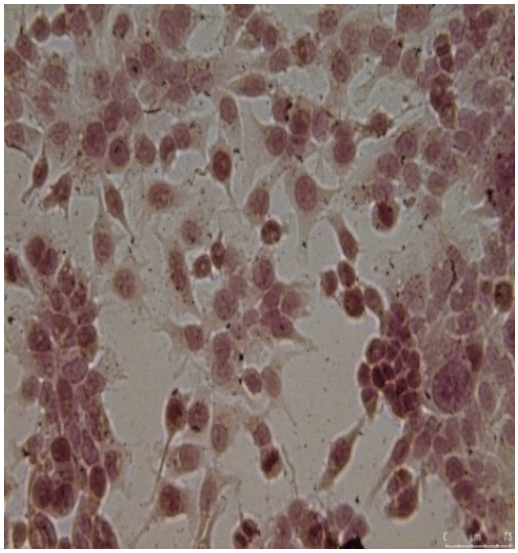

B H1975/8μM

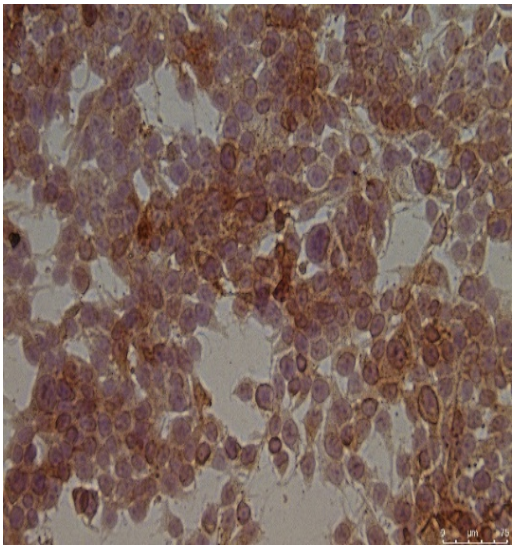

C H1975/DDP

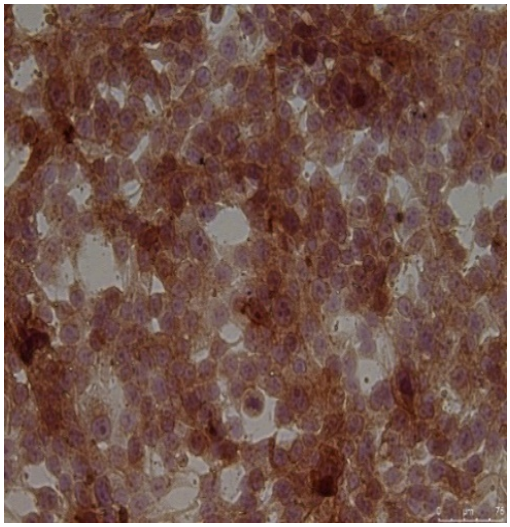

D

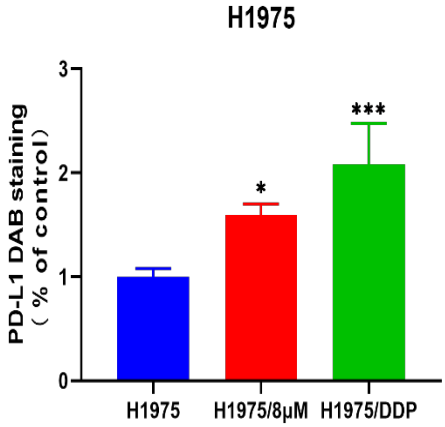

Figure 18. Differences in PD-L1 protein expression among H1975/DDP, H1975 and H1975 stimulated with 8μM cisplatin.

(A-C) Representative images of the immunohistochemistry results. (D) Histogram shows the fold differences in staining intensity of H1975/8μM (B) and H1975/DDP cells (C) relative to H1975 cells (A) in three independent experiments. Compared with the H1975 group, the H1975/8μM and H1975/DDP groups underwent a one-way ANOVA, and the two groups had differences after statistical analysis.

4.8 Cisplatin, XL-765 and 740Y-P regulate PD-L1 mRNA expression in NSCLC cell lines

To detect the effects of cisplatin, 740Y-P and XL-765 on PD-L1 mRNA expression in NSCLC cells, we established different subgroups with NSCLC naïve cells. For cisplatin stimulated groups, NSCLC naïve cells were cultured in vitro, stimulated with (0-16) μM cisplatin for 12 hours, and then performed qRT-PCR. For 740Y-P and XL-765 stimulated groups, A549, HCC827 and H1975 cells were stimulated with 20μM 740Y-P and 10μM XL-765 for (0-24) hours. Total RNAs were extracted from the above groups for qRT-PCR. PD-L1 mRNA expression was elevated in NSCLC cells in each cisplatin stimulated group compared to the non-cisplatin stimulated group. Details are in Figure 19 (A, D, G). With the time of 20μM 740Y-P stimulation increasing, PD-L1 mRNA expression in NSCLC naïve cells also increased. Details are in Figure 19 (B, E, H). The PD-L1 mRNA expression in NSCLC naïve cells showed a downward trend with the increase of 10μM XL-765 stimulation time. Details are in Figure 19 (C, F, I). The above results showed that (0-16)μM cisplatin and 740Y-P could promote the transcription of PD-L1 mRNA, while XL-765 could inhibit the transcription of PD-L1 mRNA.

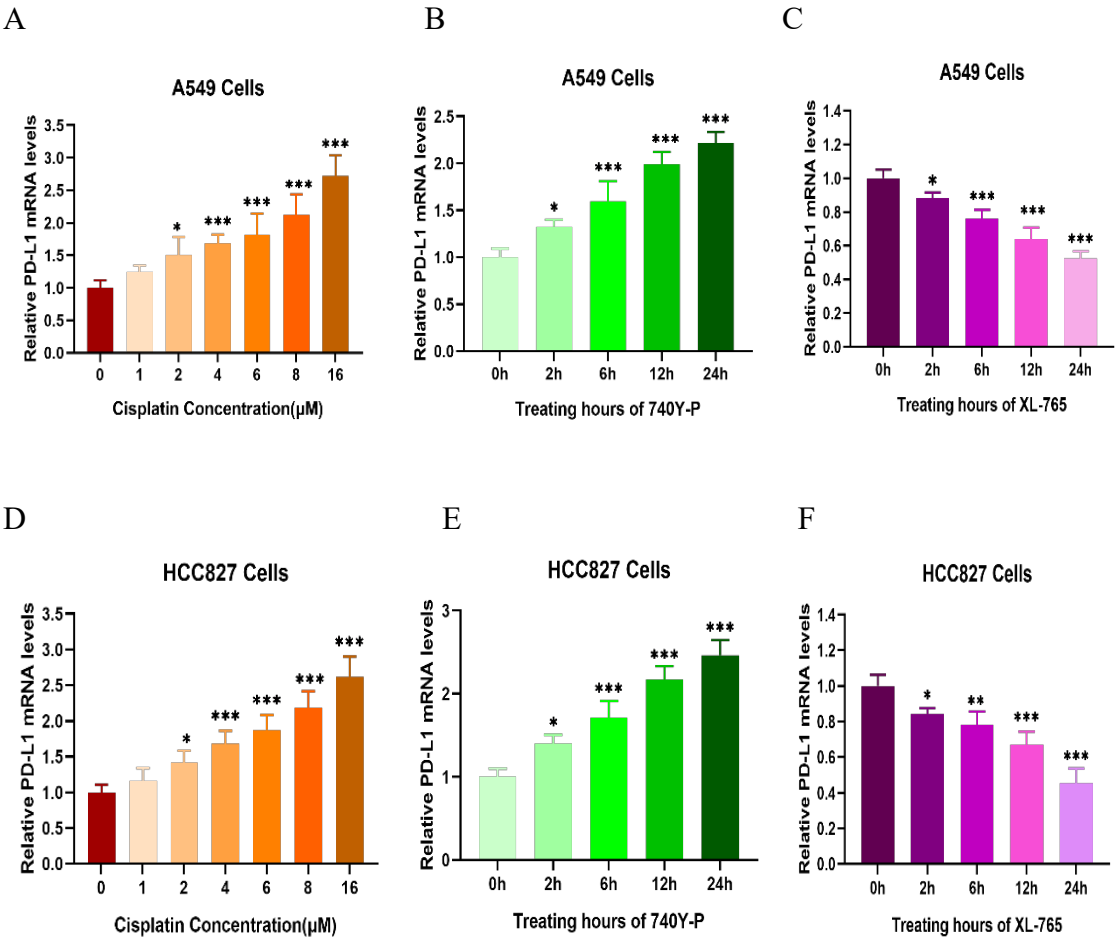

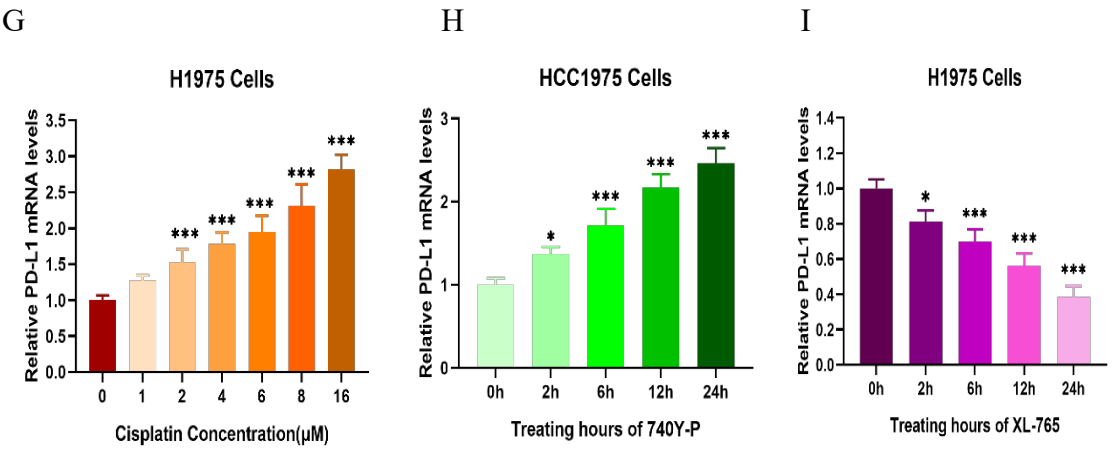

Figure 19. Up-and down-regulation of PD-L1 mRNA expression in NSCLC cell lines by cisplatin, 740Y-P and XL-765.

(A-C) Cisplatin up-regulated PD-L1 mRNA expression in A549 cells concerning concentration, while 740Y-P, XL-765 up- and down-regulated PD-L1 mRNA expression in A549 cells concerning time. (D-F) Cisplatin up-regulated PD-L1 mRNA expression in HCC827 cells concerning concentration, while 740Y-P, XL-76 up-and down-regulated PD-L1 mRNA expression in HCC827 cells concerning time. (G-I) Cisplatin up-regulated PD-L1 mRNA expression in H1975 cells concerning concentration, while 740Y-P, XL-765 up-and down-regulated PD-L1 mRNA expression in H1975 cells concerning time. (A-I) Histograms show the fold differences between the normalized average values of PD-L1 and the Ct values of β-Actin in cells in three independent replicate experiments. The groups were statistically different after one-way ANOVA compared with the control groups (*P<0.05, **P<0.01, ***P<0.005).

4.9 Cisplatin, XL-765 and 740Y-P regulate the membrane PD-L1 expression in NSCLC cell lines

As the above results described, cisplatin up-regulated PD-L1 protein and PD-L1 mRNA expression in NSCLC naïve cells. To further explore the effects of cisplatin on membrane PD-L1 expression in A549, HCC827, and H1975 cells, FCM assay was performed in our following experiments. Firstly, cell lines of A549, A549/DDP, HCC827, HCC827/DDP, H1975, H1975/DDP were cultured in vitro. When in well growth status, they were stimulated with 20μM 740Y-P and 10μM XL-765 for 4 hours, and then cultured for 48 h. After that, all the cell lines were collected and labeled with CD274 antibody and then FCM was performed. The results are shown in Figure 20A, Figure 21A, and Figure 22A. The relative expression levels of membrane PD-L1 in the NSCLC/DDP cells > the corresponding naïve cells. After stimulation with 740Y-P, the relative membrane PD-L1 expression of the naïve cells > the unstimulated naïve cells. After stimulation with XL-765, the expression levels of membrane PD-L1 protein in NSCLC/DDP cells were lower than that in unstimulated NSCLC/DDP cell lines. There were statistical differences after the comparison of the treatment groups and control

groups (Figure 20B, Figure 21B, Figure 22B). We can learn that membrane PD-L1 expression was affected by XL-765 and 740Y-P.

NSCLC naïve cells in well growth status were selected, and they were stimulated with (0-16) μM concentration gradients of cisplatin for 24h. Then the cells were labeled with CD274 antibody. The expression of membrane PD-L1 after stimulation with different concentration gradients of cisplatin were detected by FCM. The results are shown in Figure 23A, Figure 24A, and Figure 25A. Cisplatin significantly promoted membrane PD-L1 expression in NSCLC naïve cells. Compared with the DMSO group, membrane PD-L1 expression increased continuously after cells were stimulated with different cisplatin concentrations, and there were statistical differences (Figure 23B, Figure 24B, and Figure 25B).

The above results indicated that cisplatin and 740Y-P could up-regulate the membrane PD-L1 expression in NSCLC naïve cells, and (0-16)μM cisplatin up-regulated the membrane PD-L1 expression concerning concentration. XL-765 could inhibit the membrane PD-L1 expression. The differences were statistically significant after one-way ANOVA compared to the control group in three independent experiments (*P<0.05, **P<0.01, ***P<0.005).

4.9.1 XL-765 and 740Y-P regulate the membrane PD-L1 expression in A549 and A549/DDP cells

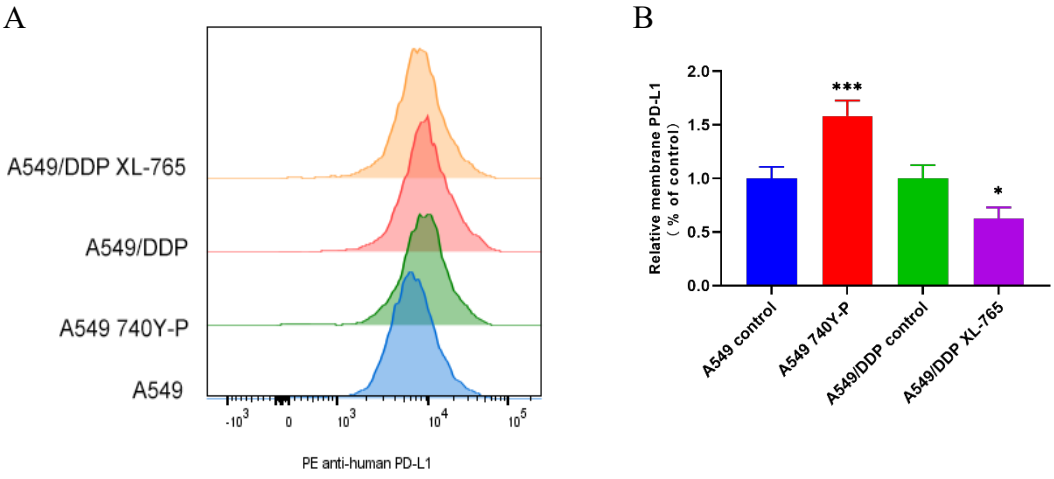

Figure 20. Effects of 740Y-P and XL-765 on membrane PD-L1 protein expression in A549 or A549/DDP cells.

(A) Four groups of cells were simultaneously prepared. A549 and A549/DDP cells were stimulated with 20μM 740Y-P and 10μM XL-765, respectively for 4 h, and then cultured for 48 h. FCM detected the average fluorescence intensity of PD-L1. This figure shows a representative flow cytometry image in each group; (B) Fold differences in the fluorescence intensity of PD-L1 after normalization in the experimental groups compared to the fluorescence intensity after normalization in the control groups. Statistically significant differences after independent samples t-test.

4.9.2 XL-765 and 740Y-P regulate the membrane PD-L1 expression in HCC827 and HCC827/DDP cells

A

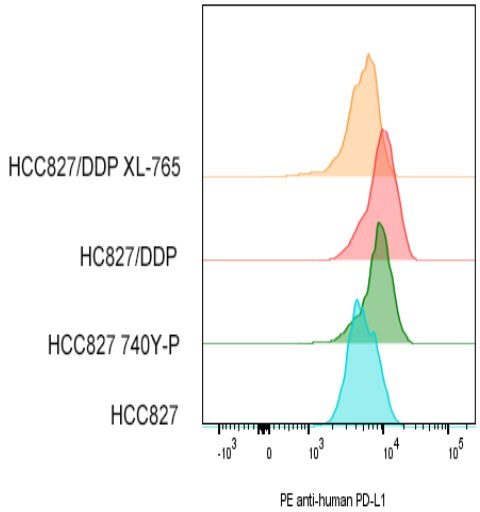

B

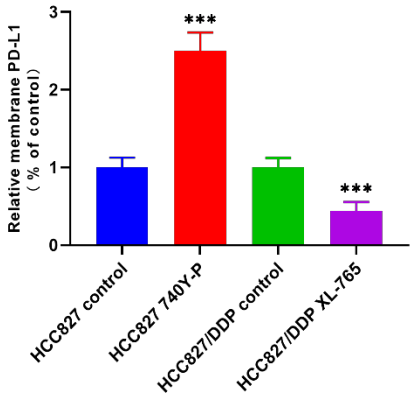

Figure 21. Effects of 740Y-P and XL-765 on membrane PD-L1 protein expression in HCC827 or HCC827/DDP cells.

(A) Four groups of cells were simultaneously prepared. HCC827 and HCC827/DDP cells were stimulated with 20μM 740Y-P and 10μM XL-765, respectively for 4 h, and then cultured for 48 h. FCM detected the average fluorescence intensity of PD-L1. This figure shows a representative flow cytometry image in each group; (B) Fold differences in the fluorescence intensity of PD-L1 after normalization in the experimental groups compared to the fluorescence intensity after normalization in the control groups. Statistically significant differences after independent samples t-test.

4.9.3 XL-765 and 740Y-P regulate the membrane PD-L1 expression in H1975 and H1975/DDP cells

A

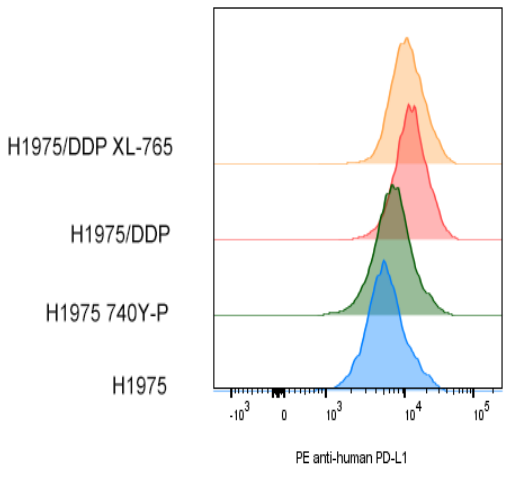

B

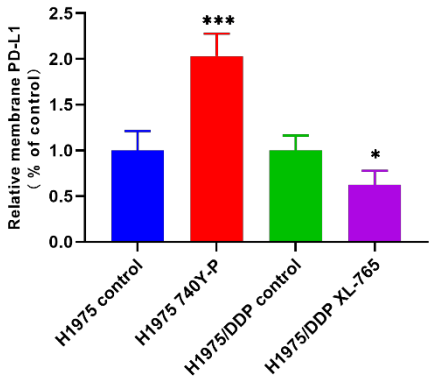

Figure 22. Effects of 740Y-P and XL-765 on membrane PD-L1 protein expression in H1975 or H1975/DDP cells.

(A) Four groups of cells were simultaneously prepared. H1975 and H1975/DDP cells were stimulated with 20μM 740Y-P and 10μM XL-765, respectively for 4 h, and then cultured for 48 h. FCM detected the average fluorescence intensity of PD-L1. This figure shows a representative flow cytometry image in each group; (B) Fold differences in the fluorescence intensity of PD-L1 after normalization in the experimental groups compared to the fluorescence intensity after normalization in the control groups. Statistically significant differences after independent samples t-test.

4.9.4 Cisplatin (0-16)μM up-regulates the membrane PD-L1 expression in A549 cells

A

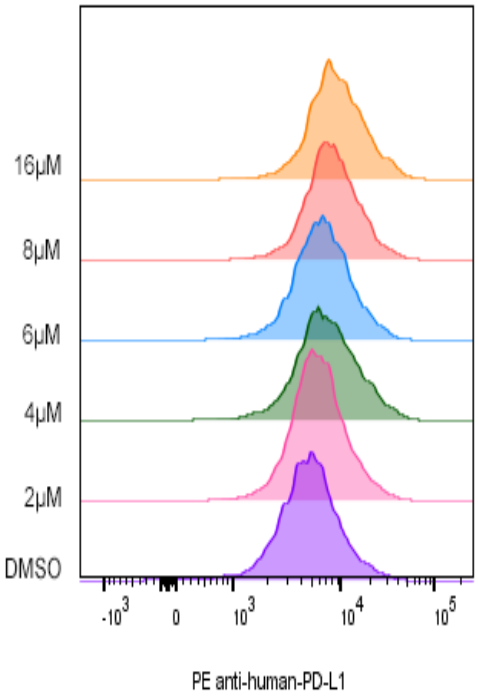

B

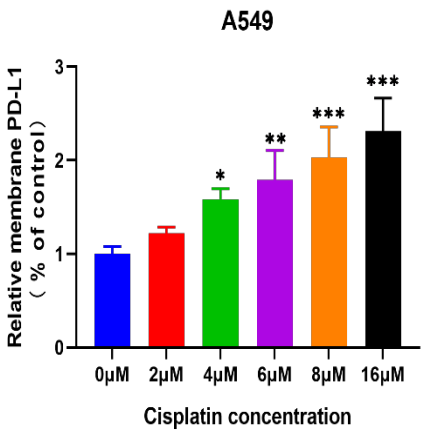

Figure 23. Concentration-dependent up-regulation of the expression of membrane PD-L1 by cisplatin in A549 cells.

(A) A549 cells were cultured for 24 h in medium containing (0μM, 2μM, 4μM, 6μM, 8μM, 16μM) cisplatin. FCM detected the mean fluorescence intensity of PD-L1. This figure shows a representative flow cytometry image in each group; (B) Fold differences in the fluorescence intensity of PD-L1 after normalization in the experimental groups compared to the fluorescence intensity after normalization in the control group. Statistically significant differences after one-way ANOVA.

4.9.5 Cisplatin (0-16)μM up-regulates the membrane PD-L1 expression in HCC827 cells

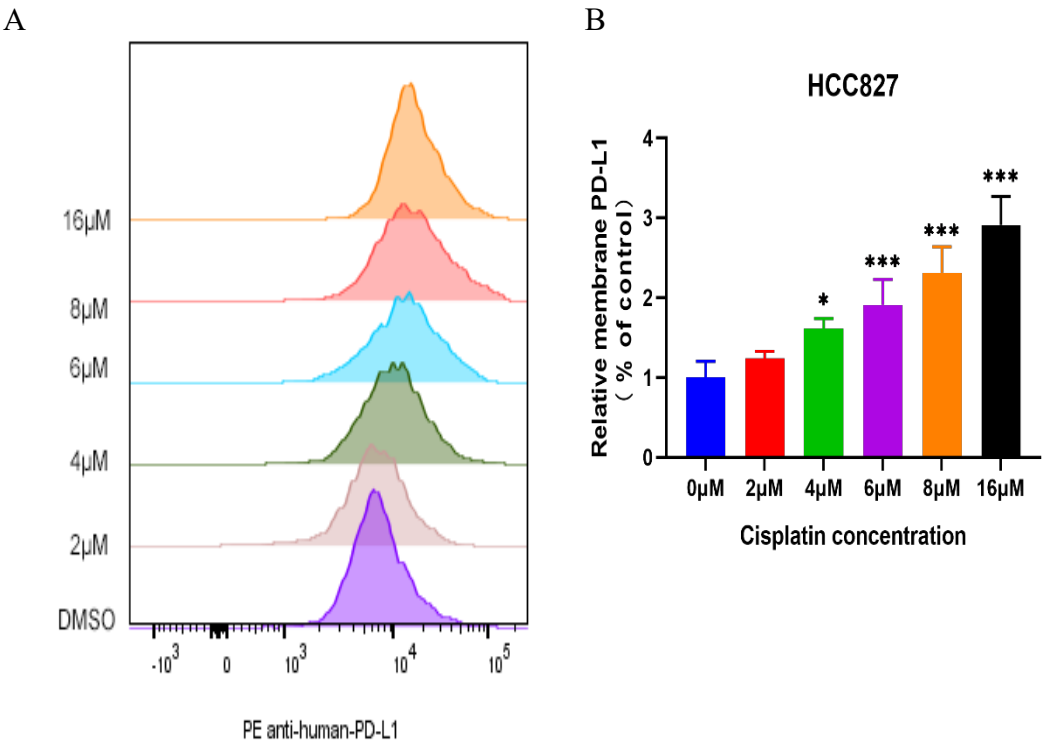

Figure 24. Concentration-dependent up-regulation of the expression of membrane PD-L1 by cisplatin in HCC827 cells.

(A) HCC827 cells were cultured for 24 h in medium containing (0μM, 2μM, 4μM, 6μM, 8μM, 16μM) cisplatin. FCM detected the mean fluorescence intensity of PD-L1. This figure shows a representative flow cytometry image in each group; (B) Fold differences in the fluorescence intensity of PD-L1 after normalization in the experimental groups compared to the fluorescence intensity after normalization in the control group. Statistically significant differences after one-way ANOVA.

4.9.6 Cisplatin (0-16)μM up-regulates the membrane PD-L1 expression in H1975 cells

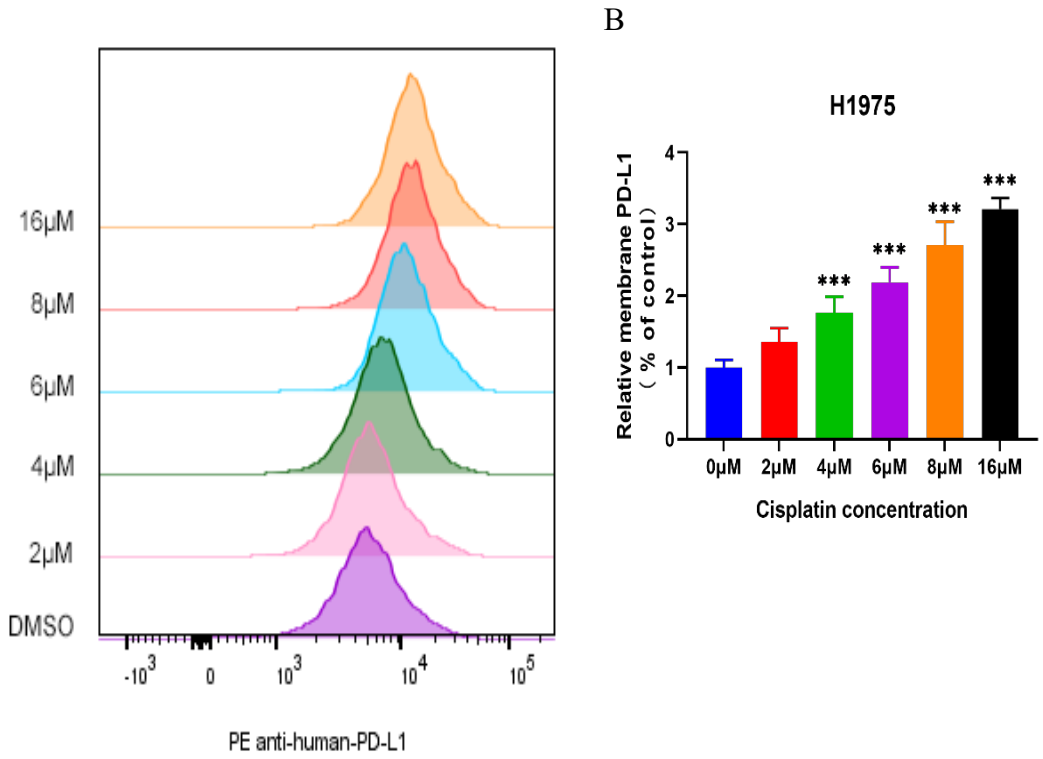

Figure 25. Concentration-dependent up-regulation of the expression of membrane PD-L1 by cisplatin in H1975 cells.

(A) H1975 cells were cultured for 24 h in medium containing (0μM, 2μM, 4μM, 6μM, 8μM, 16μM) cisplatin. FCM detected the mean fluorescence intensity of PD-L1. This figure shows a representative flow cytometry image in each group; (B) Fold differences in the fluorescence intensity of PD-L1 after normalization in the experimental groups compared to the fluorescence intensity after normalization in the control group. Statistically significant differences after one-way ANOVA.

4.10 Cisplatin up-regulates PD-L1 expression through activation of PATSP

In the above assays, the results of FCM, qRT-PCR and IHC showed that cisplatin significantly up-regulated PD-L1 expression in NSCLC cell lines. To clarify the possible causes of this phenomenon, we analyzed the cellular signaling pathways it may activate. Based on the results we had obtained, coupled with the extensive literature we have reviewed, different signaling pathways can affect PD-L1 expression, including PATSP [35,36]. So, we used western blot to detect PD-L1 expression in NSCLC naïve cells and NSCLC/DDP cells. It showed that PD-L1 expression in NSCLC/DDP cells > NSCLC naïve cells. PD-L1 expression gradually decreased after stimulation of NSCLC/DDP cell lines with 10μM XL-765 for 0h, 4h and 8h.

To know the role of the PATSP in regulating PD-L1 expression, we selected H1975 and H1975/DDP as the primary research cell lines. In order to determine the activation levels of each essential signaling pathway protein in the PATSP, we detected the differences in the expression of p-AKT, AKT, p-S6, and S6 proteins. We first stimulated H1975 cells with cisplatin (0-16) μM for 24h and then lysed the cell lines. After collecting the cell lysates of different concentrations, western blotting was conducted. The expression levels of p-AKT, AKT, p-S6 and S6 proteins increased with the cisplatin concentration. Second, we stimulated H1975 cells with 16μM cisplatin for (0-48) h. According to the results, it can be seen that the expression of p-AKT, AKT, p-S6 and S6 proteins showed an increasing trend after H1975 cells were cultured in medium containing 16μM cisplatin for 0, 2, 4, 6, 12, 24 and 48 hours. At the same time, we also detected the total PD-L1 expression in the same batch of samples after being stimulated with different concentrations and times. We found that the expression of total PD-L1 was proportional to the different concentrations and times of cisplatin treatment. The expression of p-AKT, AKT, p-S6, and S6 were also proportional to the concentrations and times.

Third, we stimulated H1975 cells with 10μM XL-765 for (0-8) h after them had been cultured in medium containing 16μM cisplatin for 48 h. The data told us that the expression of p-AKT, AKT, p-S6, and S6 were inversely proportional to the treatment time. We also stimulated H1975 cells with 20μM 740Y-P for (0-24) h after them had been cultured in medium containing 16μM cisplatin for 48 h. The results showed that the expression of p-AKT, AKT, p-S6, and S6 were proportional to the treatment time.

Finally, when H1975/DDP cells had been cultured in medium containing 16μM cisplatin for 48 h, we also stimulated H1975/DDP cells with 10μM XL-765 for (0-8) h. The data showed that the expression of p-AKT, AKT, p-S6 and S6 in H1975/DDP cells were also inversely proportional to time. The brightness of each band was analyzed using Image J software. The differences in all of the above results were statistically significant in three independent experiments (*$P<0.05$, **$P<0.01$, ***$P<0.005$).

Our results indicated that low concentrations of cisplatin could activate PD-L1 expression in NSCLC cell lines. PATSP was activated at different degrees with different

concentrations or times of cisplatin treatment. When PATSP was inhibited, PD-L1 expression in NSCLC cell lines was decreased. PATSP played a fundamental role in the molecular mechanism by which cisplatin promotes PD-L1 expression in NSCLC cell lines. When XL-765 inhibited the signaling pathway, the ability of reducing PD-L1 expression in NSCLC/DDP cell lines had important clinical implications.

4.10.1 The total PD-L1 expression in NSCLC naïve and NSCLC/DDP cell lines

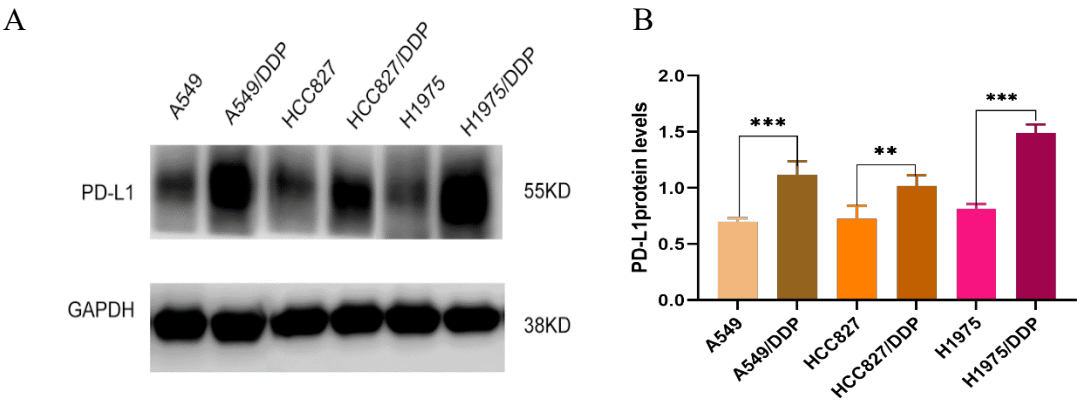

Figure 26. PD-L1 expression in NSCLC naïve cell lines and NSCLC/DDP cell lines.
(A) A549, A549/DDP, HCC827, HCC827/DDP, H1975 and H1975/DDP cell lines were cultured in normal medium for 48h. This figure shows each representative Western blotting image. (B) This bar chart shows the fold differences in the intensity of the mean PD-L1 bands after normalization compared to the intensity of the GAPDH bands. Statistically significant differences after independent samples t-test.

4.10.2 XL-765 reduced the total PD-L1 expression in NSCLC/DDP cell lines

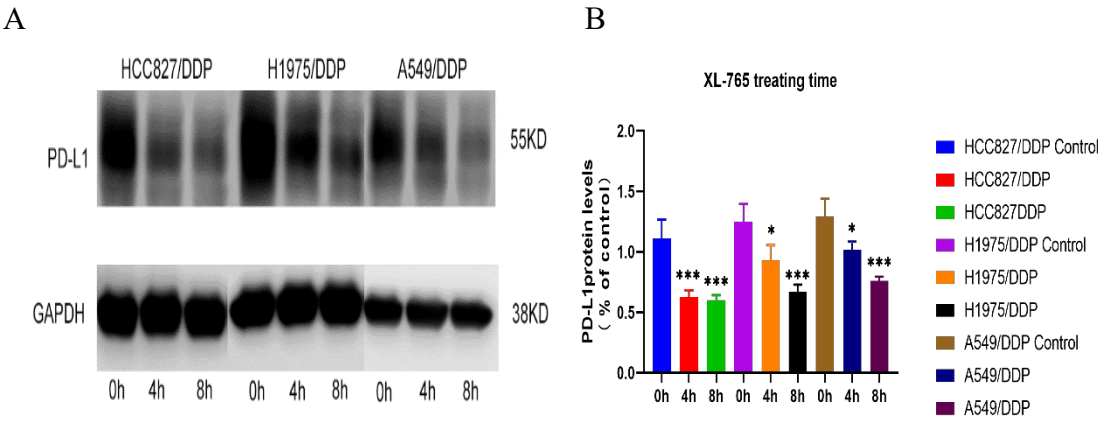

Figure 27. Differential expression levels of PD-L1 in NSCLC/DDP cell lines stimulated with XL-765.

(A) A549/DDP, H1975/DDP and HCC827/DDP cells were cultured in normal medium for 48 h, then they were treated with 10μM XL-765 for (0-8) h. This figure shows each representative Western blotting image. (B) This bar chart shows the fold differences in the intensity of the mean PD-L1 bands after normalization compared to the intensity of the GAPDH bands. Statistically significant differences after one-way ANOVA.

4.10.3 PD-L1 expression in the H1975 cell line was proportional to the cisplatin concentration

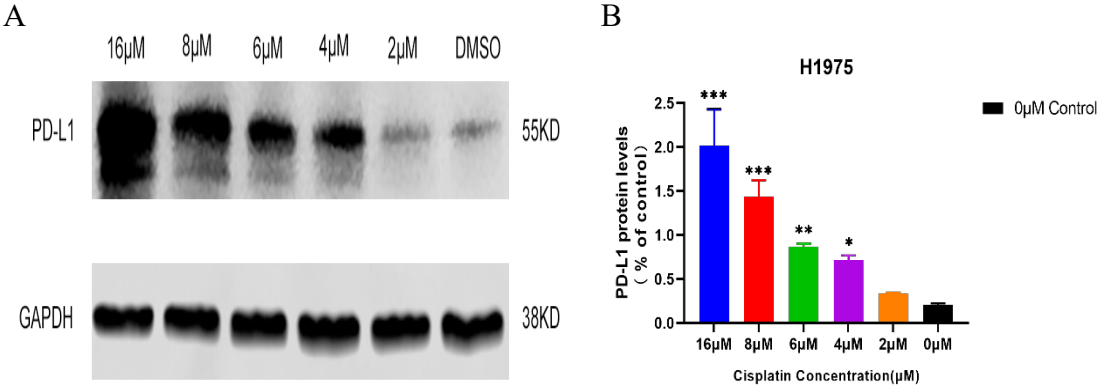

Figure 28. Differential expression levels of PD-L1 in H1975 cells stimulated with different cisplatin concentrations.

(A) H1975 cells were cultured in normal medium for 48 h, after that they were stimulated with (0-16) μM cisplatin for another 24 hours. This figure shows each representative Western blotting image. (B) This bar chart shows the fold differences in the intensity of the mean PD-L1 bands after normalization compared to the intensity of the GAPDH bands. Statistically significant differences after one-way ANOVA.

4.10.4 PD-L1 expression in the H1975 cell line was proportional to the time of cisplatin treatment

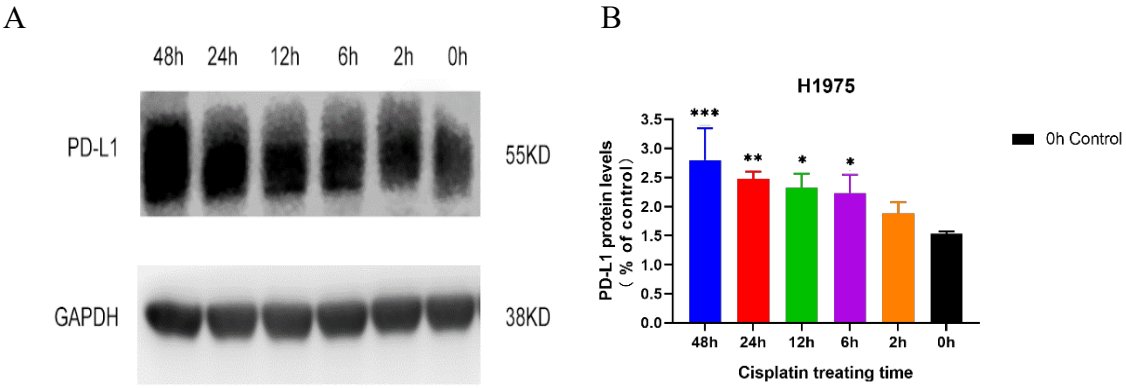

Figure 29. Differential expression levels of PD-L1 in H1975 cells were stimulated with different cisplatin treatment times.
(A) H1975 cells were cultured in normal medium for 48 hours, after that they were cultured in a 16μM cisplatin-containing medium for (0-48) h. This figure shows each representative Western blotting image. (B) This bar chart shows the fold differences in the intensity of the mean PD-L1 bands after normalization compared to the intensity of the GAPDH bands. Statistically significant differences after one-way ANOVA.

4.10.5 Expression levels of p-AKT, AKT, p-S6, S6 in the H1975 cell line were proportional to the cisplatin concentration

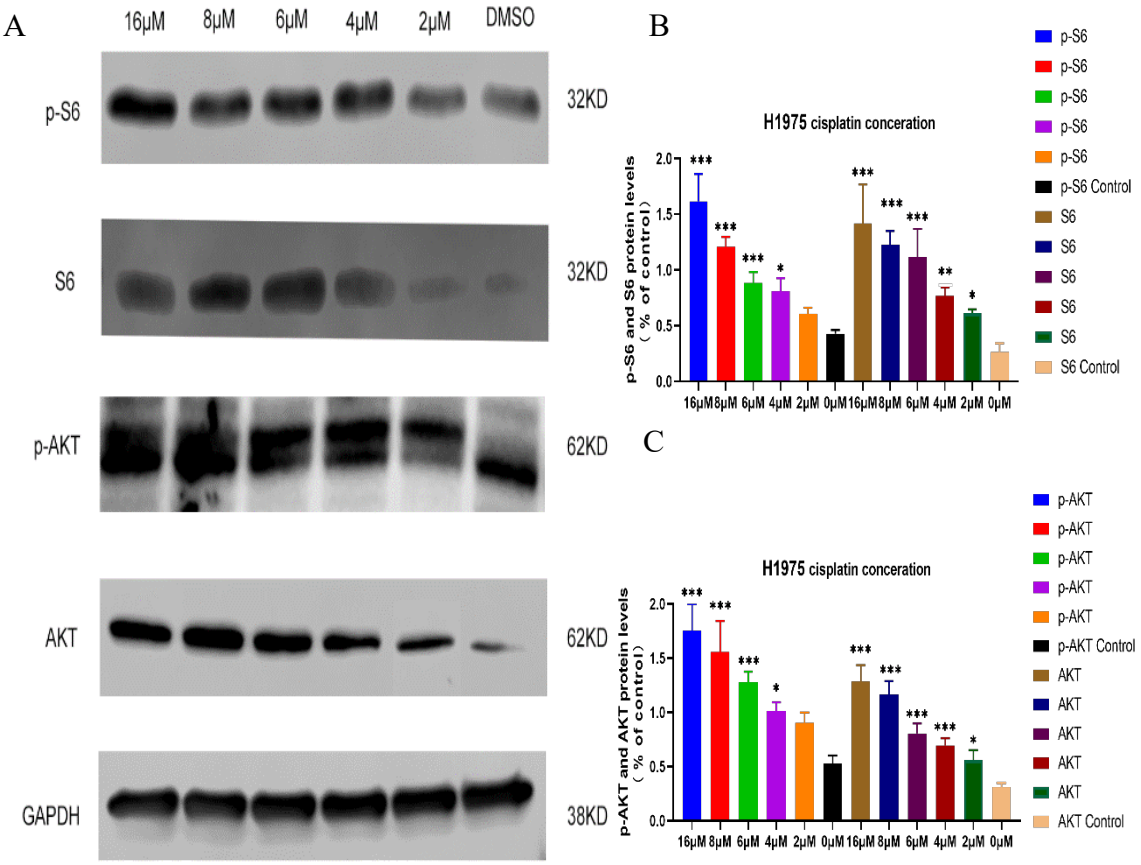

Figure 30. Differential expression levels of p-AKT, AKT, p-S6 and S6 in H1975 cells were stimulated with different cisplatin concentrations.

(A) H1975 cells were cultured in normal medium for 48 h and stimulated with (0-16) μM cisplatin for another 24 h. This figure shows each representative Western blotting image. (B-C) These bar charts show the fold differences in the intensity of the mean p-AKT, AKT, p-S6, S6 bands after normalization compared to the intensity of the GAPDH bands. Statistically significant differences after one-way ANOVA.

4.10.6 Expression levels of p-AKT, AKT, p-S6, S6 in the H1975 cell line were proportional to the time of cisplatin treatment

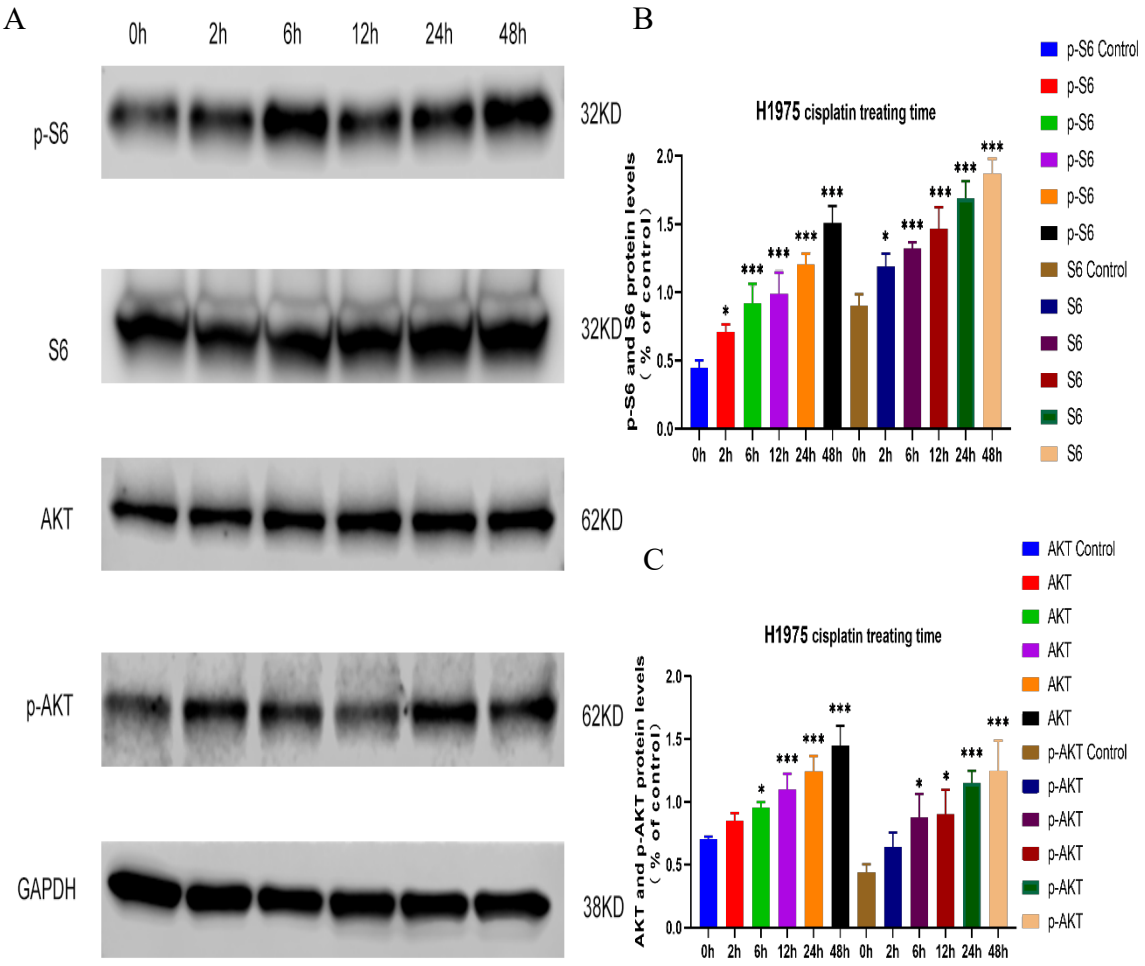

Figure 31. Differential expression levels of p-AKT, AKT, p-S6 and S6 in H1975 cells were stimulated with different cisplatin treatment times.

(A) H1975 cells were cultured in normal medium for 48h and then stimulated with 16μM cisplatin for another (0-48) hours. This figure shows each representative Western blotting image. (B-C) These bar charts show the fold differences in the intensity of the mean p-AKT, AKT, p-S6, S6 bands after normalization compared to the intensity of the GAPDH bands. Statistically significant differences after one-way ANOVA.

4.10.7 Expression levels of p-AKT, AKT, p-S6, and S6 in the H1975 cell line were inversely proportional to the time of XL-765 treatment

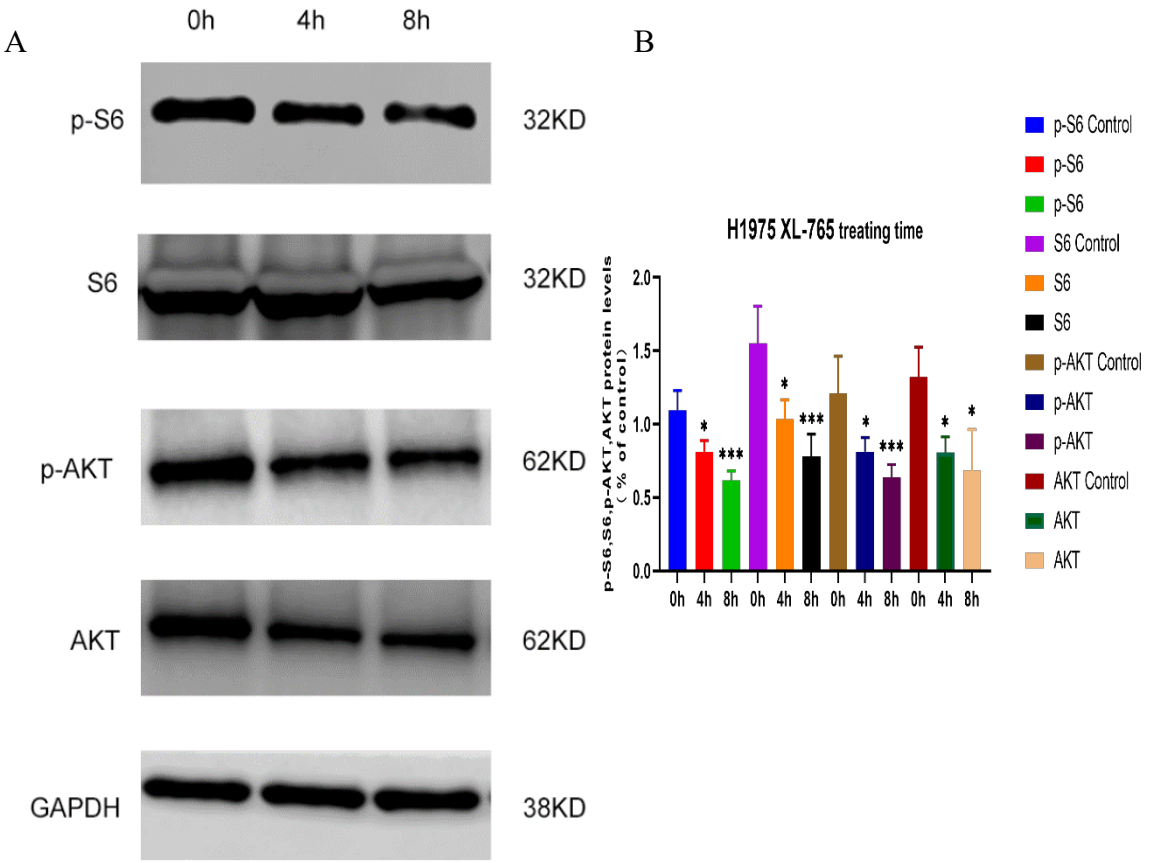

Figure 32. Differential expression levels of p-AKT, AKT, p-S6 and S6 in H1975 cells were stimulated with different XL-765 treatment times.
(A) H1975 cells were cultured in medium containing 16μM cisplatin for 48 h, after that they were stimulated with 10μM XL-765 for (0-8) h. This figure shows each representative Western blotting image. (B) This bar chart shows the fold differences in the intensity of the mean p-AKT, AKT, p-S6, S6 bands after normalization compared to the intensity of the GAPDH bands. Statistically significant differences after one-way ANOVA.

4.10.8 Expression levels of p-AKT, AKT, p-S6 and S6 in the H1975 cell line were proportional to the time of 740Y-P treatment

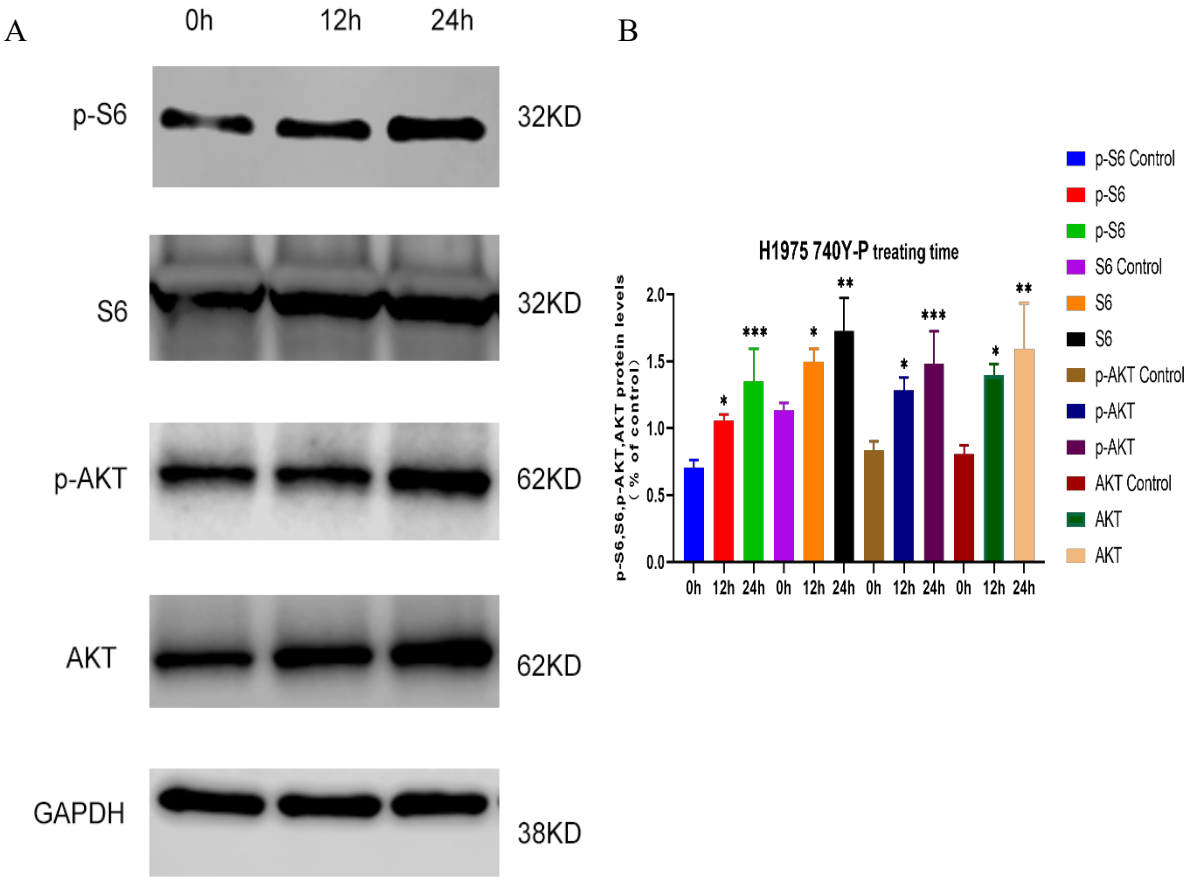

Figure 33. Differential expression levels of p-AKT, AKT, p-S6 and S6 in H1975 cells were stimulated with different 740Y-P treatment times.
(A) H1975 cells were cultured in medium containing 16μM cisplatin for 48 h and stimulated with 20μM 740Y-P for another (0-24) h. This figure shows each representative Western blotting image. (B) This bar chart shows the fold differences in the intensity of the mean p-AKT, AKT, p-S6, S6 bands after normalization compared to the intensity of the GAPDH bands. Statistically significant differences after one-way ANOVA.

4.10.9 Expression levels of p-AKT, AKT, p-S6, and S6 in the H1975/DDP cell line were inversely proportional to the time of XL-765 treatment

After stimulation of H1975/DDP cells with 20μM XL-765 for 0, 4, and 8h, the expression of p-AKT, AKT, p-S6, and S6 after normalization were negatively correlated with the treatment time. The decrease of p-AKT, AKT, p-S6 and S6 expression in H1975/DDP cells > H1975 cells.This indicates the PATSP is more active in H1975/DDP cells than in H1975 cells.

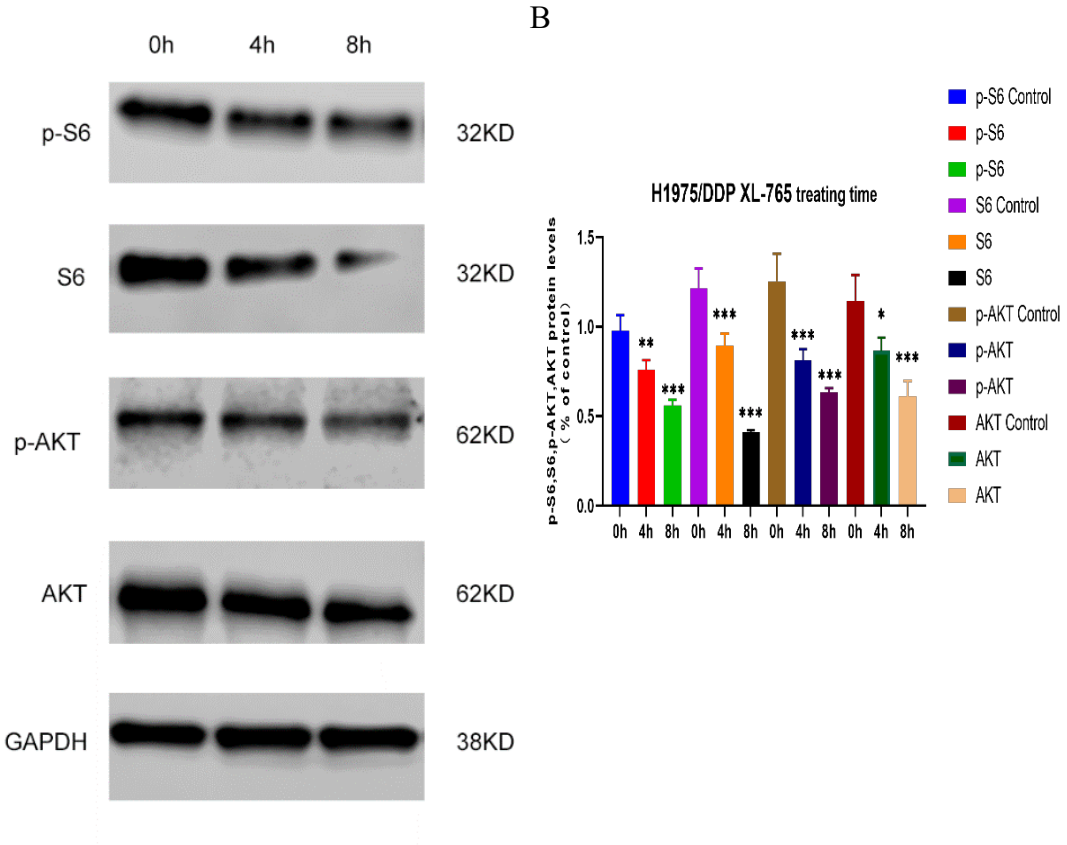

Figure 34. Differential expression levels of p-AKT, AKT, p-S6 and S6 in H1975/DDP cells were stimulated with different XL-765 treatment times.

(A) H1975/DDP cells were cultured in medium containing 16μM cisplatin for 48 h, after that they were stimulated with 10μM XL-765 for another (0-8) h. This figure shows each representative Western blotting image. (B) This bar chart shows the fold differences in the intensity of the mean p-AKT, AKT, p-S6, S6 bands after normalization compared to the intensity of the GAPDH bands. Statistically significant differences after one-way ANOVA.

5. DISCUSSION

5.1 Discussion of the methods

5.1.1 Establishment of A549/DDP cell line

In this subject, human-derived NSCLC cell lines A549, A549/DDP, HCC827, HCC827/DDP, H1975, H1975/DDP were used as experimental research cell lines. We applied the increment concentration gradient method to establish A549/DDP cell line that was not available in our laboratory. Sarin also obtained the A549/DDP cell line using this same method [107]. In this process, we also observed the change of cisplatin concentration during the establishment of A549/DDP cells and learned the growth characteristics of the cells. By inducing the A549/DDP in vitro, it provides a cell model for further study of the cisplatin resistance mechanism, which helps us explore the reasons for the failure of chemotherapy in clinical NSCLC patients. After successful induction of the A549/DDP cell line, we used cell proliferation and cytotoxicity assays to detect the sensitivity of NSCLC cell lines to cisplatin, 740Y-P and XL-765, which helped to select the appropriate drug concentration for subsequent experiments.

5.1.2 Cell functional assays

Cellular activity is an important indicator of whether cells cultured in vitro will grow well under certain conditions, such as drug stimulation, radiation or UV irradiation, and changes in culture conditions [108, 109]. ATP (adenosine triphosphate) releases more energy when it is hydrolyzed, and it is the direct source of energy in our body [110]. ATP luminescence is used to analyze cell activity and proliferation capacity by measuring the amount of intracellular ATP [111]. The Celltiter-Glo ® 2.0 reagent used in this study is based on a single reagent for detecting ATP in living cells and is highly stable. Therefore, it is helpful to accurately detect the activity changes of cell lines after drug stimulation. It can also indirectly represent the proliferation of NSCLC cell lines [112, 113]. The apoptosis rate of each cell line was determined by FCM with the theory of cell proliferation. Apoptosis is controlled by a series of intracellular switches that are switched on and off when the cell senses a corresponding signal stimulus. Different external environments generate different signal transduction to initiate apoptosis. The apoptosis rate also lays the foundation for later analysis of cellular pathways [114, 115]. The pore size of the membrane used in the Transwell experiment is 8μm. In the invasion experiment, the membrane pores are covered with Matrigel gel, and the cells cannot pass through freely. They must secrete hydrolase and deform to pass through the Matrigel-coated membrane, which is similar to the environment in vivo. The number of cells entering the lower chamber can be counted to determine the invasive ability of tumor cells [116]. In the experiment of studying the migration capability and invasion

capability of the A549 cell line promoted by CRTC2 in vitro, Shaoqing also used Transwell to measure the invasion capability of A549 cells, and the research results were very similar to ours. For monolayer adherent cells cultured in vitro, they were removed by scraping the area where the cells grew with a tip. After continuing to culture the cells for a while, they were observed under a microscope to see whether they migrated to the scratch area [117]. As for the wound healing assay, this method can be used to measure the movement of cells upon receiving a migratory signal or sensing a gradient of drugs. Our approach is the same as that de Araújo et al. used in their study of coumarin derivatives that exert anti-lung cancer activity. He also used the same two assays to evaluate the invasive and metastatic ability of coumarin derivatives against A549 and H2170 cell lines [118].

5.1.3 Detection of PD-L1 expression

With cell function assays as the basis of our study, we initially used the immunohistochemistry method to detect PD-L1 expression after cisplatin stimulation to determine changes in PD-L1 expression in naïve cell lines, cisplatin-stimulated cell lines, and cisplatin-resistant cell lines. We used more drugs to stimulate the above cell lines when this experiment was done. This design aimed to clarify the mechanism of elevated PD-L1 expression. Since PD-L1 can be expressed in the cell membrane and cytoplasm, we used Chen and Ikeda's method to detect expression differences in PD-L1 using FCM and western blot, respectively [119, 120]. Based on the immunohistochemistry results that PD-L1 expression was increased in NSCLC/DDP cells compared with NSCLC naïve cells, we further conducted qRT-PCR to clarify the PD-L1 mRNA expression and used western blot to detect the expression of cell membrane PD-L1 and total PD-L1. 740 Y-P is a PI3K phosphopeptide activator [121]. XL-765 is a PI3K/mTOR inhibitor, and its effective concentration is lower than that of PI3K selective inhibitors XL-147 and PIK90 [122]. In order to avoid accidental changes in PD-L1 expression, we also studied the differences in PD-L1 protein and PD-L1 mRNA expression after cisplatin, 740Y-P and XL-765 stimulation at different concentrations and at different times. To elucidate whether the PATSP is involved in the regulation of PD-L1 expression or not, we also used western blot to detect differences in p-AKT, AKT, p-S6, and S6 expression after stimulation with PI3K inhibitors and agonists. The results proved that this signaling pathway was indeed involved in PD-L1 expression. This process was consistent with the approach used by Annovazzi and Kanaizumi to study the PATSP.

5.2 Discussion of the results

5.2.1 Alteration of cellular activity

Yang and Casey observed migration ability was higher in NSCLC/DDP cells than in

parental cells [123, 124]. The results of Liu revealed that the cisplatin-resistant TNBC cell line exhibited EMT with enhanced ability in motility and invasion [125]. In our experiments, transwell and wound healing assays showed that cisplatin-resistant cell lines were also more invasive and metastatic than naïve cell lines. The invasive and metastatic abilities of NSCLC/DDP cells were diminished after stimulation with XL-765. After our continuous attempts, the naïve cell lines increased their invasive and metastatic capacity after stimulation with 6μM cisplatin. An increase in the metastatic capacity of the naïve cell lines also occurred after stimulation with the 20μM 740 Y-P. As for the NSCLC naïve cells, there were also differences in their responses to cisplatin. In the cell activity assay, we could learn that after stimulation with low concentrations of cisplatin, the activity of HCC827 cells > H1975 and A549 cells. In contrast, A549 cells showed the most negligible response to cisplatin. When stimulated with 740Y-P, HCC827/DDP showed the highest activity, H1975/DDP and A549/DDP had similar activity, and NSCLC/DDP cells were more active than the corresponding NSCLC naïve cell lines. This reflects that the PATSP is more involved in NSCLC/DDP cells than in NSCLC naïve cells, and the activation of this signaling pathway varies in different NSCLC cell lines. This matches Moon's findings in bladder cancer cells [126]. Based on these results, we also stimulated each cell line with the PATSP inhibitor XL-765. The data showed that the activity of HCC827 and HCC827/DDP cell lines decreased significantly, while the activity of A549 and A549/DDP cell lines decreased slightly. When comparing the cell activity of three cisplatin-treated NSCLC naïve cell lines, the cell lines affected to different degrees were HCC827 > H1975 > A549. This was consistent with the activation of the PATSP. More importantly, the cisplatin-resistant cell lines showed a higher decrease in activity than the corresponding NSCLC naïve cell lines.

5.2.2 Alteration of apoptosis

After completing the cell activity assays, we used FCM to detect the apoptosis rates of cisplatin-resistant and naïve cell lines, the apoptosis rates of naïve cell lines before and after stimulation with 740Y-P, and the apoptosis rates of cisplatin-resistant cells before and after stimulation with XL-765. The results showed that the apoptosis rate of NSCLC/DDP cell lines < NSCLC naïve cell lines. Barr also found a significant abrogation of cisplatin-induced apoptosis in NSCLC/DDP cells relative to their parental cells [127]. The apoptosis rates of cell lines stimulated with 740Y-P were lower than that of the untreated group. In contrast, the apoptosis rate of NSCLC/DDP cells treated with XL-765 was higher than that of the unstimulated group. These experimental results suggest that the PATSP is more active in NSCLC/DDP cells than NSCLC naïve cells and that low concentrations of cisplatin activate this pathway.

5.2.3 Alteration of PD-L1 expression

Based on the Immunohistochemistry results, PD-L1 expression was higher in

NSCLC/DDP cells than in NSCLC naïve cell lines. The data told us that PD-L1 expression gradually increased in the three NSCLC naïve cell lines after 8μM cisplatin stimulation, and the expression level was between the NSCLC/DDP and NSCLC naïve cell lines. The data suggested a correlation between PD-L1 expression and cisplatin concentration. Tran found in the results of a study on PD-1/PD-L1 that low doses of cisplatin may up-regulate PD-L1 expression [128]. In one subject, cisplatin modified antitumor immunity and synergistically inhibited the head and neck cancer [129]. Fournel also found that cisplatin increased PD-L1 expression and inhibited immune checkpoints in NSCLC [130]. In addition to immunohistochemistry, we further detected PD-L1 mRNA expression after stimulation of NSCLC naïve cell lines at different concentrations. We found that PD-L1 mRNA expression was proportional to cisplatin concentration in the range of 0 to 16μM. This indicated that low concentration cisplatin induced higher PD-L1 expression in NSCLC naïve cell lines. Current studies tell us that membrane PD-L1 plays a vital role in the immunosuppressive effect of tumor cells [131, 132]. Immunohistochemical results suggest that PD-L1 can be found in the cytoplasm and cell membrane.

5.2.3.1 Alteration of the membrane PD-L1 expression

We detected the cell membrane PD-L1 expression by FCM and the total PD-L1 expression by western blot. The FCM data showed that the cell membrane PD-L1 expression was higher in 740Y-P-stimulated NSCLC naïve cells than in unstimulated NSCLC naïve cells, and the NSCLC/DDP cells were higher than the 740Y-P-stimulated cell lines. Cell membrane PD-L1 expression was significantly reduced in NSCLC/DDP cell lines after XL-765 stimulation. Our research data suggested that the PATSP was also involved in the expression of membrane PD-L1. To elucidate whether membrane PD-L1 expression was dependent on a low concentration range of cisplatin concentrations, we set a series of cisplatin concentrations to stimulate NSCLC naïve cells. FCM results showed that the fluorescence intensity of cell membrane PD-L1 was proportional to the cisplatin concentration. We can learn that cisplatin stimulates the PD-L1 expression, which may be related to the activation of PATSP. This conclusion is the same as the results of Heavey's study [133]. In addition, this phenomenon is also present in bladder cancer, colorectal cancer, and gastric cancer [134-137].

5.2.3.2 Alteration of the total PD-L1 expression

To detect the total expression of PD-L1 in cells, we used western blot assays. The analyzed data revealed that PD-L1 expression in NSCLC/DDP cells > NSCLC naïve cells, and the expression level of PD-L1 gradually decreased after different times of XL-765 stimulation in each NSCLC/DDP cell line. To further clarify whether the PATSP is involved or not, we focus on H1975 cells and explore the expression levels of p-AKT, AKT, p-S6, and S6, which are all key proteins of this signaling pathway [138-141]. The expression levels of PD-L1, p-AKT, AKT, p-S6, and S6 in H1975 cells

after stimulation with various concentrations of cisplatin were proportional to the concentrations. The expression levels of PD-L1, p-AKT, AKT, p-S6, and S6 were proportional to time after stimulation with constant concentration of cisplatin for different times. When H1975 cells were stimulated with constant concentration of XL-765 and 740Y-P for different times, the expression of p-AKT, AKT, p-S6, and S6 were inversely and positively proportional to time, respectively. The results tell us that the PATSP is indeed involved in cell membrane PD-L1 and cytoplasmic PD-L1 expression in cells. Kim found that PD-L1 enhanced glycolysis in NSCLC cells through up-regulation of HK2, which might also suppress anti-tumor immunity [142]. The preliminary analysis of our findings suggests that the cause of this phenomenon may be related to the mechanism elaborated in Kim's study.

5.3 Current dilemmas in platinum-based chemotherapy

5.3.1 Cell resistance to platinum-based chemotherapeutics

In recent decades, many advances have been made in basic research, clinical trials, surgical treatment, radiotherapy, targeted therapy, immunotherapy and other comprehensive therapies [14, 143, 144]. However, the overall prognosis of NSCLC has not improved significantly. The recurrence, metastasis and chemotherapy resistance are important causes for treatment failure of lung cancer patients. Recurrence and metastasis of NSCLC are a highly complex multistep process affected by aberrant activation of multiple cellular signaling pathways [145]. Research teams around the world have been working to develop more and better chemotherapeutic drugs for different types of cancers. One of the representative chemotherapeutic agents is cisplatin, which has been in clinical use for about 40 years [146]. Despite significant advances in new targeted therapy in medical oncology, cisplatin and other platinum-based agents continue to play an irreplaceable role in many cancer treatment regimens [147]. Multiple clinical trials of platinum-containing chemotherapy regimens for NSCLC have shown that they are superior to standard supportive therapies in improving overall survival. In addition, first-line treatment with cisplatin chemotherapy agents remains the gold standard of medicine in the presence of metastasis [59, 148, 149]. Despite its remarkable success in treating NSCLC, cisplatin has apparent drawbacks. The major limitations to its use are its strict dose limits and multiple toxicities, especially in many NSCLC patients who are sensitive at first but develop severe resistance in the later stage of treatment [41, 150].

5.3.1.1 Mechanisms of cell resistance to platinum-based chemotherapeutics

Numerous clinical resistance studies on cisplatin or other platinum-based drugs focus on the following points. First, the transports of platinum drugs to cells are blocked so that platinum drugs cannot damage the DNA of target cells in sufficient concentrations.

Therefore, low concentrations of platinum drugs can lead to tumor resistance [151]. For example, alterations in cell membrane-associated proteins (P-glycoprotein) lead to reduced drug uptake or increased drug efflux. Second, mechanisms such as DNA repair mechanisms enhanced DNA repair capacity, and abnormal apoptosis regulatory systems lead to a relative decrease in cytotoxicity of cisplatin-based drugs [43]. In addition, we learned from literature reports that chemotherapeutic drugs may have systemic immunosuppressive effects [152]. Some chemotherapeutic drugs can affect the tumor's response to treatment by changing the local immune status of the body. Chemotherapeutic drugs commonly used in clinical treatment, such as paclitaxel and gemcitabine, can induce changes in the immune response [153]. These changes include the promotion of tumor antigen expression and the up-regulation of MHC molecules. Numerous research results have shown that the failure of tumor treatment is not only affected by the factors of chemotherapeutic drug resistance but also by the factors of tumor cell immune escape. These immunological side effects of chemotherapy are significant and further studies of them will be instructive in designing new combinations with improved clinical efficacy [154].

5.3.2 Platinum-based chemotherapeutics induce immune escape

Studies have shown that chemotherapeutic agents can modulate tumor immunity through various pathways, such as regulation of immune cells, modulation of immune molecule expression, and activation of cellular signaling pathways [155]. These regulatory mechanisms can promote or inhibit tumor immune responses to tumor cell lines or chemotherapeutic agents. For example, platinum-based drugs can up-regulate PD-L1 expression in breast and liver cancer cells. It shows that platinum-based drugs affect the expression of suppressive immune molecules. This reduces the efficacy of chemotherapy and leads to drug resistance [156]. Acquired resistance to platinum-based chemotherapeutics was shown to be directly related to elevated PD-L1 [157]. The phenomenon that chemotherapeutic drugs reduce the therapeutic effect by altering the body's anti-tumor immune response provides ideas for clinical guidance of chemotherapy combined with immunotherapy.

The main mechanisms of tumor immune escape are modification changes in the tumor cells themselves and alterations in the tumor immune microenvironment [158]. The modification changes of tumor cells include loss of tumor antigens and antigen regulation, low expression of MHC class I molecules, reduction of costimulatory signals in anti-tumor immune response, epigenetic changes of tumor cells, expression or secretion vesicles of immunosuppressive molecules, and changes in intracellular signaling pathways in tumor cells [159]. Changes in the TME include the assistance of immunosuppressive cells and the secretion of cytokines that promote tumor growth or inhibit tumor apoptosis. Many tumor cells are accompanied by persistent activation of NF-κB signaling, enabling tumor cells to avoid apoptosis while inducing chronic inflammatory responses in the TME [160]. In addition, changes in various signaling pathways, such as PI3K/AKT, BRAF-MAPK, are also involved in assisting or dominating tumor immune escape [161]. B7/CD28 are a pair of co-stimulatory signals

that stimulate the body's anti-tumor immune response. Lacking of expression of B7 molecules in tumor cells prevents the activation of T cells, resulting in a significant reduction in the body's anti-tumor effect [162]. PD-1/PD-L1 are a pair of co-inhibitory molecules that inhibit the activity of effector T cells [163]. The presence of both positive and negative stimulatory molecules on the surface of T cells allows the body to initiate/stop the immune response at an appropriate time. Upon activation, T cells can secrete IFN-γ, which increases the expression of PD-L1 in normal cells [164]. The binding of PD-L1 to PD-1 blocks the immune response and protects normal cells from attacking by immune cells.

5.4 The significance of this study to current literature

5.4.1 The phenomenon of immune escape induced by cisplatin is also present in NSCLC cell lines

PD-L1 is mainly expressed in tumor cells, which are essential immunosuppressive molecules [165]. PD-L1 can suppress the body's immune response to tumor cells and play a critical role in tumor immune escape which is associated with poor tumor prognosis [166, 167]. There are few studies on the effects of platinum drugs on PD-L1 expression in NSCLC cells, and the important intracellular regulatory mechanisms remain unclear [166]. Data from this study showed that low concentrations of cisplatin upregulated PD-L1 expression in NSCLC cells, with corresponding increases in cell activity, invasion and metastasis. Facts from the literature that cisplatin can up-regulate PD-L1 expression in ovarian cancer cells and hepatocellular carcinoma cells suggest the promotion of PD-L1 expression in tumor cells by platinum-based drugs may be universal [168, 169]. The drug concentrations of cisplatin in this study are all lower than the IC50 values of the corresponding cells. It indicates that when the concentration of chemotherapeutics is not enough to kill tumor cells directly, it may promote the expression of immunosuppressive molecules in tumor cells, thereby causing immune escape. One of the critical reasons for cisplatin resistance is the insufficient concentration of the drug that penetrates tumor cells. Studies have shown that the concentration of cisplatin in peripheral blood of patients resistant to platinum drug therapy is less than that of platinum-sensitive patients [170].

Combined with the results of our subject, we suggest that insufficient concentrations of cisplatin used to treat patients with NSCLC may not only cause drug resistance in tumor cells but also up-regulate the expression of immunosuppressive molecules in tumor cells and promote immune escape. Our subject also provides new evidence for the involvement of platinum-based drugs in tumor immune escape. In addition, preliminary results showed that patients receiving PD-1 or PD-L1 monoclonal antibodies plus conventional platinum had longer progression-free survival than patients receiving traditional platinum drugs alone [39, 57]. However, most studies have focused on the efficacy and side effects of combination therapy with PD-1 or PD-L1 monoclonal

antibodies and conventional platinum-based drugs. Still, the molecular mechanisms of combination therapy have not been reported. In this study, we found that platinum-based drugs induced elevated PD-L1 expression in NSCLC cell lines, and this process had aberrant activation of PATSP.

5.4.2 PD-L1 enhanced cisplatin resistance in NSCLC cell lines through PATSP

Multiple signaling pathways regulate the PD-L1 expression. We first explored the effects of cisplatin on the activation and expression levels of key proteins of PATSP in NSCLC cells (H1975). We found that cisplatin and 740Y-P up-regulated the expression of p-AKT, AKT, p-S6, S6 and PD-L1 proteins. Second, we further stimulated H1975 cells and H1975/DDP cells using the dual PI3K/mTOR inhibitor XL-765 and found that p-AKT, AKT, p-S6, S6 and PD-L1 proteins were inhibited at different degrees. What is more, the expression level of membrane PD-L1 protein was inhibited to varying degrees after XL-765 stimulated NSCLC cell lines. The inconsistent effect of the same signaling pathway inhibitor on PD-L1 expression in different NSCLC cells may be due to the various activities of the signaling pathways controlling PD-L1 expression.

5.5 Shortcomings of this subject

Due to various conditions and time constraints, our study still has several shortcomings. First, only three NSCLC lines were selected, and more representative NSCLC cell lines should be covered. Carboplatin was not used in this study. Carboplatin is a second-generation drug with similar effects to cisplatin but significantly less toxicity and side effects. In terms of mechanism research, we only selected H1975 and H1975/DDP cell lines as the focus cells to be studied, and other cell lines also need to carry out the same experiments. Second, the study of cisplatin on PD-L1 expression in NSCLC has only been conducted in vitro, without experiments in animals, which has limited value for clinical purposes. Third, there is still a lack of more comprehensive mechanism research and no exploration of gene regulation. Finally, we did not perform experiments on NSCLC cells cultured together with T cells, which is unconvincing for the immune escape mechanism. Nevertheless, our subject provides reference data on the combination of chemotherapeutics with immunosuppressants or PATSP inhibitors. The experimental data may provide new ideas for the management of NSCLC patients.

5.6 Further researches

In the follow-up study, we will make improvements to the following aspects. 1. Increase the number of NSCLC cell lines to verify the involvement of the PATSP in the up-regulation of PD-L1 expression by cisplatin. Furthermore, co-culture models should be

used. 2. Inoculate NSCLC cell lines into nude mice. The mice will be injected with cisplatin, XL-765,740Y-P, and then measure the tumor size and detect PD-L1 expression. 3. Explore more cellular signaling pathways involved in high PD-L1 expression.

5.7 Conclusion and Outlook

In conclusion, our findings suggested that cisplatin could regulate the expression of PD-L1 and alter the cellular function of NSCLC cell lines. The PATSP was involved in this process. Based on the effect of cisplatin on PD-L1 expression in NSCLC cell lines in our subject, we confirmed on the one hand, the prevalence of platinum-based chemotherapeutic agents with the ability to induce PD-L1 expression in tumor cells. On the other hand, it provides a new idea to explore the development of cisplatin resistance in NSCLC patients. Chemotherapeutic drugs induce the expression of PD-L1, which further inhibits the anti-tumor immune effect of T cells and makes tumor cells escape from the body's immune system, thus weakening the efficacy of chemotherapeutics. Therefore, the combination of chemotherapeutics with new immune checkpoint inhibitors or PATSP inhibitors may be more beneficial for patients.

6. REFERENCES

1. Barta, J.A., C.A. Powell, and J.P. Wisnivesky, *Global Epidemiology of Lung Cancer.* Ann Glob Health, 2019. **85**(1).
2. Sung, H., et al., *Global Cancer Statistics 2020: GLOBOCAN Estimates of Incidence and Mortality Worldwide for 36 Cancers in 185 Countries.* CA Cancer J Clin, 2021. **71**(3): p. 209-249.
3. Siegel, R.L., et al., *Cancer statistics, 2022.* CA: a cancer journal for clinicians, 2022.
4. D'addario, G., et al., *Metastatic non-small-cell lung cancer: ESMO Clinical Practice Guidelines for diagnosis, treatment and follow-up.* Annals of oncology, 2010. **21**: p. v116-v119.
5. Molina, J.R., et al., *Non-small cell lung cancer: epidemiology, risk factors, treatment, and survivorship.* Mayo Clin Proc, 2008. **83**(5): p. 584-94.
6. Lemjabbar-Alaoui, H., et al., *Lung cancer: Biology and treatment options.* Biochim Biophys Acta, 2015. **1856**(2): p. 189-210.
7. Collins, L.G., et al., *Lung cancer: diagnosis and management.* American family physician, 2007. **75**(1): p. 56-63.
8. Latimer, K. and T. Mott, *Lung cancer: diagnosis, treatment principles, and screening.* American family physician, 2015. **91**(4): p. 250-256.
9. Popper, H.H., *Progression and metastasis of lung cancer.* Cancer Metastasis Rev, 2016. **35**(1): p. 75-91.
10. Zappa, C. and S.A. Mousa, *Non-small cell lung cancer: current treatment and future advances.* Transl Lung Cancer Res, 2016. **5**(3): p. 288-300.
11. Board, P.A.T.E., *Non-Small Cell Lung Cancer Treatment (PDQ®)*, in *PDQ Cancer Information Summaries [Internet]*. 2021, National Cancer Institute (US).
12. Baskar, R., et al., *Cancer and radiation therapy: current advances and future directions.* Int J Med Sci, 2012. **9**(3): p. 193-9.
13. Calman, K.C., *Basic principles of cancer chemotherapy*. 2015: Macmillan International Higher Education.
14. Lemjabbar-Alaoui, H., et al., *Lung cancer: Biology and treatment options.* Biochimica et Biophysica Acta (BBA)-Reviews on Cancer, 2015. **1856**(2): p. 189-210.
15. Cai, W.-Q., et al., *The latest battles between EGFR monoclonal antibodies and resistant tumor cells.* Frontiers in Oncology, 2020. **10**: p. 1249.
16. Park, R., et al., *The value of immunotherapy for survivors of stage IV non-small cell lung cancer: patient perspectives on quality of life.* Journal of Cancer Survivorship, 2020. **14**(3): p. 363-376.
17. Xu, J., *Regulation of cancer immune checkpoints*. 2020: Springer.
18. Ohaegbulam, K.C., et al., *Human cancer immunotherapy with antibodies to the PD-1 and PD-L1 pathway.* Trends in molecular medicine, 2015. **21**(1): p. 24-33.

19. Francisco, L.M., P.T. Sage, and A.H. Sharpe, *The PD-1 pathway in tolerance and autoimmunity.* Immunological reviews, 2010. **236**(1): p. 219-242.
20. Pardoll, D.M., *The blockade of immune checkpoints in cancer immunotherapy.* Nature Reviews Cancer, 2012. **12**(4): p. 252-264.
21. Hudson, K., et al., *The extrinsic and intrinsic roles of PD-L1 and its receptor PD-1: implications for immunotherapy treatment.* Frontiers in immunology, 2020: p. 2362.
22. Vanneman, M. and G. Dranoff, *Combining immunotherapy and targeted therapies in cancer treatment.* Nat Rev Cancer, 2012. **12**(4): p. 237-51.
23. Pucci, C., C. Martinelli, and G. Ciofani, *Innovative approaches for cancer treatment: current perspectives and new challenges.* Ecancermedicalscience, 2019. **13**: p. 961.
24. Vaddepally, R.K., et al., *Review of Indications of FDA-Approved Immune Checkpoint Inhibitors per NCCN Guidelines with the Level of Evidence.* Cancers (Basel), 2020. **12**(3).
25. Available from: https://www.merck.com/news/european-commission-approves-mercks-keytruda-pembrolizumab-in-combination-with-pemetrexed-and-platinum-chemotherapy-for-the-first-line-treatment-of-patients-with-metastatic-nonsquamou/.
26. Botticella, A., et al., *Durvalumab for stage III non-small-cell lung cancer patients: Clinical evidence and real-world experience.* Therapeutic advances in respiratory disease, 2019. **13**: p. 1753466619885530.
27. Massarelli, E., et al., *Immunotherapy in lung cancer.* Transl Lung Cancer Res, 2014. **3**(1): p. 53-63.
28. Dammeijer, F., et al., *The PD-1/PD-L1-Checkpoint Restrains T cell Immunity in Tumor-Draining Lymph Nodes.* Cancer Cell, 2020. **38**(5): p. 685-700 e8.
29. Paik, P.K., et al., *Tepotinib in non–small-cell lung cancer with MET exon 14 skipping mutations.* New England Journal of Medicine, 2020. **383**(10): p. 931-943.
30. Markham, A., *Atezolizumab: first global approval.* Drugs, 2016. **76**(12): p. 1227-1232.
31. Krishnamurthy, A. and A. Jimeno, *Atezolizumab: A novel PD-L1 inhibitor in cancer therapy with a focus in bladder and non-small cell lung cancers.* Drugs of Today (Barcelona, Spain: 1998), 2017. **53**(4): p. 217-237.
32. Mathieu, L., et al., *FDA Approval Summary: Atezolizumab and Durvalumab in Combination with Platinum-Based Chemotherapy in Extensive Stage Small Cell Lung Cancer.* The Oncologist, 2021. **26**(5): p. 433-438.
33. Farina, M.S., K.T. Lundgren, and J. Bellmunt, *Immunotherapy in urothelial cancer: recent results and future perspectives.* Drugs, 2017. **77**(10): p. 1077-1089.
34. Vaddepally, R.K., et al., *Review of indications of FDA-approved immune checkpoint inhibitors per NCCN guidelines with the level of evidence.*

Cancers, 2020. **12**(3): p. 738.
35. Antonia, S.J., et al., *Durvalumab after chemoradiotherapy in stage III non–small-cell lung cancer.* New England Journal of Medicine, 2017. **377**(20): p. 1919-1929.
36. Verschraegen, C.F., et al., *Efficacy and safety of first-line avelumab in patients with advanced non-small cell lung cancer: results from a phase Ib cohort of the JAVELIN Solid Tumor study.* Journal for immunotherapy of cancer, 2020. **8**(2).
37. Hum, N., *An Examination of Dynamic Molecular Interactions in Triple Negative Breast Cancer Tumors Towards Improved Preclinical Approaches*. 2021: University of California, Merced.
38. Chen, Y.-Y., et al., *Risk factors of postoperative recurrences in patients with clinical stage I NSCLC.* World journal of surgical oncology, 2014. **12**(1): p. 1-8.
39. Yuan, M., et al., *The emerging treatment landscape of targeted therapy in non-small-cell lung cancer.* Signal transduction and targeted therapy, 2019. **4**(1): p. 1-14.
40. Rossi, A. and M. Di Maio, *Platinum-based chemotherapy in advanced non-small-cell lung cancer: optimal number of treatment cycles.* Expert review of anticancer therapy, 2016. **16**(6): p. 653-660.
41. Dasari, S. and P.B. Tchounwou, *Cisplatin in cancer therapy: molecular mechanisms of action.* European journal of pharmacology, 2014. **740**: p. 364-378.
42. Klein, A.V. and T.W. Hambley, *Platinum drug distribution in cancer cells and tumors.* Chemical reviews, 2009. **109**(10): p. 4911-4920.
43. Chen, S.-H. and J.-Y. Chang, *New insights into mechanisms of cisplatin resistance: from tumor cell to microenvironment.* International journal of molecular sciences, 2019. **20**(17): p. 4136.
44. Zitvogel, L., et al., *Mechanism of action of conventional and targeted anticancer therapies: reinstating immunosurveillance.* Immunity, 2013. **39**(1): p. 74-88.
45. Bracci, L., et al., *Immune-based mechanisms of cytotoxic chemotherapy: implications for the design of novel and rationale-based combined treatments against cancer.* Cell Death & Differentiation, 2014. **21**(1): p. 15-25.
46. Yang, H., et al., *Expression of PD-L1, PD-L2, PD-1 and CTLA4 in myelodysplastic syndromes is enhanced by treatment with hypomethylating agents.* Leukemia, 2014. **28**(6): p. 1280-1288.
47. Qin, X., et al., *Cisplatin induces programmed death-1-ligand 1 (PD-L1) over-expression in hepatoma H22 cells via Erk/MAPK signaling pathway.* Cellular and Molecular Biology, 2010. **56**(3): p. 1366-72.
48. Zhang, Z.S., et al., *HGF/c-MET pathway contributes to cisplatin-mediated PD-L1 expression in hepatocellular carcinoma.* Cell Biology International,

2021. **45**(12): p. 2521-2533.
49. Leonetti, A., et al., *Molecular basis and rationale for combining immune checkpoint inhibitors with chemotherapy in non-small cell lung cancer.* Drug Resistance Updates, 2019. **46**: p. 100644.
50. Opzoomer, J.W., et al., *Cytotoxic chemotherapy as an immune stimulus: a molecular perspective on turning up the immunological heat on cancer.* Frontiers in immunology, 2019. **10**: p. 1654.
51. Li, X.-F., et al., *The expression, modulation and use of cancer-testis antigens as potential biomarkers for cancer immunotherapy.* American Journal of Translational Research, 2020. **12**(11): p. 7002.
52. Alamoudi, M.K., et al., *CHA1: A New Combinatorial Therapy That Reciprocally Regulates Wnt and JAK/STAT/Interferon Signaling to Re-program Breast Tumors and the Tumor-Resident Landscape.* bioRxiv, 2022.
53. Cornel, A.M., I.L. Mimpen, and S. Nierkens, *MHC class I downregulation in cancer: Underlying mechanisms and potential targets for cancer immunotherapy.* Cancers, 2020. **12**(7): p. 1760.
54. Vinay, D.S., et al. *Immune evasion in cancer: Mechanistic basis and therapeutic strategies*. in *Seminars in cancer biology*. 2015. Elsevier.
55. Fournier, C., et al., *Immunotherapeutic properties of chemotherapy.* Current opinion in pharmacology, 2017. **35**: p. 83-88.
56. Nolan, E., et al., *Combined immune checkpoint blockade as a therapeutic strategy for BRCA1-mutated breast cancer.* Science translational medicine, 2017. **9**(393).
57. Englinger, B., et al., *Metal drugs and the anticancer immune response.* Chemical reviews, 2018. **119**(2): p. 1519-1624.
58. Gardner, A. and B. Ruffell, *Dendritic cells and cancer immunity.* Trends in immunology, 2016. **37**(12): p. 855-865.
59. MESOTHELIOMA, M.P., *INVITED ABSTRACTS Session PL03: Presidential Sympo-sium Including Top Rated Abstracts Tuesday, October 29, 2013.* Journal of Thoracic Oncology, 2013. **8**: p. 2.
60. Pfirschke, C., et al., *Immunogenic chemotherapy sensitizes tumors to checkpoint blockade therapy.* Immunity, 2016. **44**(2): p. 343-354.
61. Zakaria, C., *Exploring the effects and effectors of mTOR inhibition in oncolysis and TOP mRNA translation*. 2018: McGill University (Canada).
62. Vivanco, I. and C.L. Sawyers, *The phosphatidylinositol 3-kinase–AKT pathway in human cancer.* Nature Reviews Cancer, 2002. **2**(7): p. 489-501.
63. Yuan, T. and L. Cantley, *PI3K pathway alterations in cancer: variations on a theme.* Oncogene, 2008. **27**(41): p. 5497-5510.
64. Hassan, B., et al., *Targeting the PI3-kinase/Akt/mTOR signaling pathway.* Surgical Oncology Clinics, 2013. **22**(4): p. 641-664.
65. Chalhoub, N. and S.J. Baker, *PTEN and the PI3-kinase pathway in cancer.* Annual Review of Pathology: Mechanisms of Disease, 2009. **4**: p. 127-150.
66. Gonzalez, E. and T.E. McGraw, *The Akt kinases: isoform specificity in metabolism and cancer.* Cell cycle, 2009. **8**(16): p. 2502-2508.

67. Manning, B.D. and A. Toker, *AKT/PKB signaling: navigating the network.* Cell, 2017. **169**(3): p. 381-405.
68. Stander, X.X., *Philosophiae Doctor (Ph. D) in Human Physiology*. 2014, University of Pretoria.
69. Ballou, L.M. and R.Z. Lin, *Rapamycin and mTOR kinase inhibitors.* Journal of chemical biology, 2008. **1**(1): p. 27-36.
70. Wu, C.-W. and K.B. Storey, *mTOR Signaling in Metabolic Stress Adaptation.* Biomolecules, 2021. **11**(5): p. 681.
71. Jossé, L., et al., *mTORC1 signalling and eIF4E/4E-BP1 translation initiation factor stoichiometry influence recombinant protein productivity from GS-CHOK1 cells.* Biochemical Journal, 2016. **473**(24): p. 4651-4664.
72. Shamas-Din, A., et al., *Mechanisms of action of Bcl-2 family proteins.* Cold Spring Harbor perspectives in biology, 2013. **5**(4): p. a008714.
73. Simões, V.L.S., *DHT and E2 as modulators of apoptotic signaling in rat Sertoli cells*. 2012, Universidade da Beira Interior (Portugal).
74. Li, X., et al., *Overexpression of 4EBP1, p70S6K, Akt1 or Akt2 differentially promotes Coxsackievirus B3-induced apoptosis in HeLa cells.* Cell death & disease, 2013. **4**(9): p. e803-e803.
75. Van der Walt, N.B., *The medicinal plant Sutherlandia frutescens induces apoptotic cell death in malignant melanoma cells*. 2016: University of Johannesburg (South Africa).
76. Asghar, U., et al., *The history and future of targeting cyclin-dependent kinases in cancer therapy.* Nature reviews Drug discovery, 2015. **14**(2): p. 130-146.
77. Diehl, J.A., et al., *Glycogen synthase kinase-3β regulates cyclin D1 proteolysis and subcellular localization.* Genes & development, 1998. **12**(22): p. 3499-3511.
78. Scheffler, M., et al., *PIK3CA mutations in non-small cell lung cancer (NSCLC): genetic heterogeneity, prognostic impact and incidence of prior malignancies.* Oncotarget, 2015. **6**(2): p. 1315.
79. Yip, P.Y., *Phosphatidylinositol 3-kinase-AKT-mammalian target of rapamycin (PI3K-Akt-mTOR) signaling pathway in non-small cell lung cancer.* Translational lung cancer research, 2015. **4**(2): p. 165.
80. Balsara, B.R., et al., *Frequent activation of AKT in non-small cell lung carcinomas and preneoplastic bronchial lesions.* Carcinogenesis, 2004. **25**(11): p. 2053-2059.
81. Do, H., et al., *Detection of the transforming AKT1 mutation E17K in non-small cell lung cancer by high resolution melting.* BMC research notes, 2008. **1**(1): p. 1-5.
82. Guo, Y., J. Du, and D.J. Kwiatkowski, *Molecular dissection of AKT activation in lung cancer cell lines.* Molecular Cancer Research, 2013. **11**(3): p. 282-293.
83. David, O., et al., *Phospho-Akt overexpression in non–small cell lung cancer confers significant stage-independent survival disadvantage.* Clinical cancer research, 2004. **10**(20): p. 6865-6871.
84. Marinov, M., B. Fischer, and A. Arcaro, *Targeting mTOR signaling in lung*

cancer. Critical reviews in oncology/hematology, 2007. **63**(2): p. 172-182.
85. Dobashi, Y., et al., *Paradigm of kinase-driven pathway downstream of epidermal growth factor receptor/Akt in human lung carcinomas.* Human pathology, 2011. **42**(2): p. 214-226.
86. Dobashi, Y., et al., *Mammalian target of rapamycin: a central node of complex signaling cascades.* International journal of clinical and experimental pathology, 2011. **4**(5): p. 476.
87. Tan, A.C., *Targeting the PI3K/Akt/mTOR pathway in non-small cell lung cancer (NSCLC).* Thoracic cancer, 2020. **11**(3): p. 511-518.
88. Pisick, E., S. Jagadeesh, and R. Salgia, *Receptor tyrosine kinases and inhibitors in lung cancer.* TheScientificWorldJOURNAL, 2004. **4**: p. 589-604.
89. Grille, S.J., et al., *The protein kinase Akt induces epithelial mesenchymal transition and promotes enhanced motility and invasiveness of squamous cell carcinoma lines.* Cancer research, 2003. **63**(9): p. 2172-2178.
90. Fong, Y.-C., et al., *Transforming growth factor-β1 increases cell migration and β1 integrin up-regulation in human lung cancer cells.* Lung cancer, 2009. **64**(1): p. 13-21.
91. Phillips, R.J., et al., *Epidermal growth factor and hypoxia-induced expression of CXC chemokine receptor 4 on non-small cell lung cancer cells is regulated by the phosphatidylinositol 3-kinase/PTEN/AKT/mammalian target of rapamycin signaling pathway and activation of hypoxia inducible factor-1α.* Journal of Biological Chemistry, 2005. **280**(23): p. 22473-22481.
92. Zhang, D. and P. Brodt, *Type 1 insulin-like growth factor regulates MT1-MMP synthesis and tumor invasion via PI 3-kinase/Akt signaling.* Oncogene, 2003. **22**(7): p. 974-982.
93. Hu, L., et al., *Inhibition of phosphatidylinositol 3′-kinase increases efficacy of paclitaxel in in vitro and in vivo ovarian cancer models.* Cancer research, 2002. **62**(4): p. 1087-1092.
94. Ihle, N.T., et al., *Molecular pharmacology and antitumor activity of PX-866, a novel inhibitor of phosphoinositide-3-kinase signaling.* Molecular cancer therapeutics, 2004. **3**(7): p. 763-772.
95. Pospisilova, M., M. Seifrtova, and M. Rezacova, *Small molecule inhibitors of DNA-PK for tumor sensitization to anticancer therapy.* J Physiol Pharmacol, 2017. **68**(3): p. 337-344.
96. Sobolewski, C. and N. Legrand, *Celecoxib Analogues for Cancer Treatment: An Update on OSU-03012 and 2, 5-Dimethyl-Celecoxib.* Biomolecules, 2021. **11**(7): p. 1049.
97. Pruthi, R.S., et al., *Phase II trial of celecoxib in prostate-specific antigen recurrent prostate cancer after definitive radiation therapy or radical prostatectomy.* Clinical Cancer Research, 2006. **12**(7): p. 2172-2177.
98. Kattan, J., et al., *Phase II trial of weekly Docetaxel, Zoledronic acid, and Celecoxib for castration-resistant prostate cancer.* Investigational new drugs,

2016. **34**(4): p. 474-480.
99. Song, M., et al., *AKT as a therapeutic target for cancer.* Cancer research, 2019. **79**(6): p. 1019-1031.
100. Chen, K., et al., *Novel PI3K/Akt/mTOR pathway inhibitors plus radiotherapy: strategy for non-small cell lung cancer with mutant RAS gene.* Life Sciences, 2020. **255**: p. 117816.
101. Konstantinidou, G., et al., *Dual phosphoinositide 3-kinase/mammalian target of rapamycin blockade is an effective radiosensitizing strategy for the treatment of non–small cell lung cancer harboring K-RAS mutations.* Cancer research, 2009. **69**(19): p. 7644-7652.
102. Martelli, A.M., F. Buontempo, and J.A. McCubrey, *Drug discovery targeting the mTOR pathway.* Clinical Science, 2018. **132**(5): p. 543-568.
103. Calvo, E., et al., *Phase 1b study of oral dual-PI3K/mTOR inhibitor GDC-0980 in combination with carboplatin (carbo)/paclitaxel (pac)±bevacizumab (bev) and cisplatin (cis)/pemetrexed (pem) in patients (pts) with advanced solid tumors and NSCLC.* Annals of Oncology, 2014. **25**: p. iv429.
104. Available from: https://www.worlddata.info/average-bodyheight.php.
105. Du Bois, D. and E.F. Du Bois, *Clinical calorimetry: tenth paper a formula to estimate the approximate surface area if height and weight be known.* Archives of internal medicine, 1916. **17**(6_2): p. 863-871.
106. Nadler, S.B., J.U. Hidalgo, and T. Bloch, *Prediction of blood volume in normal human adults.* Surgery, 1962. **51**(2): p. 224-232.
107. Sarin, N., et al., *Cisplatin resistance in non-small cell lung cancer cells is associated with an abrogation of cisplatin-induced G2/M cell cycle arrest.* PLoS One, 2017. **12**(7): p. e0181081.
108. Aslantürk, Ö.S., *In vitro cytotoxicity and cell viability assays: principles, advantages, and disadvantages.* Genotoxicity-A predictable risk to our actual world, 2018. **2**: p. 64-80.
109. Fulda, S., et al., *Cellular stress responses: cell survival and cell death.* International journal of cell biology, 2010. **2010**.
110. Bodin, P. and G. Burnstock, *Purinergic signalling: ATP release.* Neurochemical research, 2001. **26**(8): p. 959-969.
111. Crouch, S., et al., *The use of ATP bioluminescence as a measure of cell proliferation and cytotoxicity.* Journal of immunological methods, 1993. **160**(1): p. 81-88.
112. Kim, H., et al., *Olfactory Receptor OR7A17 Expression Correlates with All-Trans Retinoic Acid (ATRA)-Induced Suppression of Proliferation in Human Keratinocyte Cells.* International Journal of Molecular Sciences, 2021. **22**(22): p. 12304.
113. Lo, M.K., et al., *GS-5734 and its parent nucleoside analog inhibit Filo-, Pneumo-, and Paramyxoviruses.* Scientific reports, 2017. **7**(1): p. 1-7.
114. Mak, T.W. and W.-C. Yeh, *Signaling for survival and apoptosis in the immune system.* Arthritis Research & Therapy, 2002. **4**(3): p. 1-10.
115. Fadeel, B. and S. Orrenius, *Apoptosis: a basic biological phenomenon with*

wide-ranging implications in human disease. Journal of internal medicine, 2005. **258**(6): p. 479-517.
116. Anguiano, M., et al., *The use of mixed collagen-Matrigel matrices of increasing complexity recapitulates the biphasic role of cell adhesion in cancer cell migration: ECM sensing, remodeling and forces at the leading edge of cancer invasion.* PLoS One, 2020. **15**(1): p. e0220019.
117. Shi, S., et al., *CRTC2 promotes non-small cell lung cancer A549 migration and invasion in vitro.* Thorac Cancer, 2018. **9**(1): p. 136-141.
118. de Araújo, R.S.A., et al., *Coumarin Derivatives Exert Anti-Lung Cancer Activity by Inhibition of Epithelial–Mesenchymal Transition and Migration in A549 Cells.* Pharmaceuticals, 2022. **15**(1): p. 104.
119. Chen, S., et al., *Mechanisms regulating PD-L1 expression on tumor and immune cells.* Journal for immunotherapy of cancer, 2019. **7**(1): p. 1-12.
120. Ikeda, S., et al., *PD-L1 is upregulated by simultaneous amplification of the PD-L1 and JAK2 genes in non–small cell lung cancer.* Journal of Thoracic Oncology, 2016. **11**(1): p. 62-71.
121. Tang, J., et al., *miR-27a promotes osteogenic differentiation in glucocorticoid-treated human bone marrow mesenchymal stem cells by targeting PI3K.* Journal of Molecular Histology, 2021. **52**(2): p. 279-288.
122. Zhao, H., G. Chen, and H. Liang, *Dual PI3K/mTOR Inhibitor, XL765, suppresses glioblastoma growth by inducing ER stress-dependent apoptosis.* OncoTargets and therapy, 2019. **12**: p. 5415.
123. Yang, L., et al., *A FASN-TGF-β1-FASN regulatory loop contributes to high EMT/metastatic potential of cisplatin-resistant non-small cell lung cancer.* Oncotarget, 2016. **7**(34): p. 55543.
124. Pate, K.M., et al., *8th IAS Conference on HIV Pathogenesis, Treatment & Prevention 19â 22 July 2015, Vancouver, Canada.* 2015.
125. Liu, J., et al., *Combined niclosamide with cisplatin inhibits epithelial-mesenchymal transition and tumor growth in cisplatin-resistant triple-negative breast cancer.* Tumor Biology, 2016. **37**(7): p. 9825-9835.
126. Moon, D.G., et al., *NVP-BEZ235, a dual PI3K/mTOR inhibitor synergistically potentiates the antitumor effects of cisplatin in bladder cancer cells.* International journal of oncology, 2014. **45**(3): p. 1027-1035.
127. Barr, M.P., et al., *Generation and characterisation of cisplatin-resistant non-small cell lung cancer cell lines displaying a stem-like signature.* PloS one, 2013. **8**(1): p. e54193.
128. Tran, L., et al., *Cisplatin alters antitumor immunity and synergizes with PD-1/PD-L1 inhibition in head and neck squamous cell carcinoma.* Cancer immunology research, 2017. **5**(12): p. 1141-1151.
129. Tran, L., et al., *Cisplatin Alters Antitumor Immunity and Synergizes with PD-1/PD-L1 Inhibition in Head and Neck Squamous Cell Carcinoma.* Cancer Immunol Res, 2017. **5**(12): p. 1141-1151.
130. Fournel, L., et al., *Cisplatin increases PD-L1 expression and optimizes*

immune check-point blockade in non-small cell lung cancer. Cancer letters, 2019. **464**: p. 5-14.
131. Ricklefs, F.L., et al., *Immune evasion mediated by PD-L1 on glioblastoma-derived extracellular vesicles.* Science advances, 2018. **4**(3): p. eaar2766.
132. Kantekure, K., et al., *Expression patterns of the immunosuppressive proteins PD-1/CD279 and PD-L1/CD274 at different stages of cutaneous T-cell lymphoma (CTCL)/mycosis fungoides (MF).* The American Journal of dermatopathology, 2012. **34**(1): p. 126.
133. Heavey, S., K.J. O'Byrne, and K. Gately, *Strategies for co-targeting the PI3K/AKT/mTOR pathway in NSCLC.* Cancer treatment reviews, 2014. **40**(3): p. 445-456.
134. Sathe, A. and R. Nawroth, *Targeting the PI3K/AKT/mTOR pathway in bladder cancer.* Urothelial carcinoma, 2018: p. 335-350.
135. Hermanowicz, J.M., et al., *MM-129 as a Novel Inhibitor Targeting PI3K/AKT/mTOR and PD-L1 in Colorectal Cancer.* Cancers, 2021. **13**(13): p. 3203.
136. Wu, L., et al., *PD-1/PD-L1 enhanced cisplatin resistance in gastric cancer through PI3K/AKT mediated P-gp expression.* International Immunopharmacology, 2021. **94**: p. 107443.
137. Zhang, R., et al., *PD-L1 Mediates Triple Negative Breast Cancer Evolution by Regulating TAM/M2 Polarization.* 2022.
138. Iwenofu, O.H., et al., *Phospho-S6 ribosomal protein: a potential new predictive sarcoma marker for targeted mTOR therapy.* Modern pathology, 2008. **21**(3): p. 231-237.
139. Lu, T., et al., *DRAM1 regulates autophagy and cell proliferation via inhibition of the phosphoinositide 3-kinase-Akt-mTOR-ribosomal protein S6 pathway.* Cell Communication and Signaling, 2019. **17**(1): p. 1-15.
140. Chen, N., et al., *Upregulation of PD-L1 by EGFR activation mediates the immune escape in EGFR-driven NSCLC: implication for optional immune targeted therapy for NSCLC patients with EGFR mutation.* Journal of Thoracic Oncology, 2015. **10**(6): p. 910-923.
141. Yunokawa, M., et al., *Efficacy of everolimus, a novel m TOR inhibitor, against basal-like triple-negative breast cancer cells.* Cancer science, 2012. **103**(9): p. 1665-1671.
142. Kim, S., et al., *Programmed cell death ligand-1-mediated enhancement of hexokinase 2 expression is inversely related to T-cell effector gene expression in non-small-cell lung cancer.* Journal of Experimental & Clinical Cancer Research, 2019. **38**(1): p. 1-14.
143. Society, A., *Cancer Treatment & Survivorship Facts & Figures 2019–2021*. 2019, American Cancer Society Atlanta GA.
144. Herbst, R.S., D. Morgensztern, and C. Boshoff, *The biology and management of non-small cell lung cancer.* Nature, 2018. **553**(7689): p. 446-454.
145. Osada, H. and T. Takahashi, *Genetic alterations of multiple tumor suppressors*

and oncogenes in the carcinogenesis and progression of lung cancer. Oncogene, 2002. **21**(48): p. 7421-7434.
146. LOEHRER, P.J. and L.H. EINHORN, *Cisplatin.* Annals of internal medicine, 1984. **100**(5): p. 704-713.
147. Kenny, R.G. and C.J. Marmion, *Toward multi-targeted platinum and ruthenium drugs—a new paradigm in cancer drug treatment regimens?* Chemical reviews, 2019. **119**(2): p. 1058-1137.
148. Fennell, D., et al., *Cisplatin in the modern era: the backbone of first-line chemotherapy for non-small cell lung cancer.* Cancer treatment reviews, 2016. **44**: p. 42-50.
149. Del Alba, A.G., et al., *SEOM clinical guideline for treatment of muscle-invasive and metastatic urothelial bladder cancer (2018).* Clinical and Translational Oncology, 2019. **21**(1): p. 64-74.
150. Zhou, J., et al., *The drug-resistance mechanisms of five platinum-based antitumor agents.* Frontiers in pharmacology, 2020. **11**: p. 343.
151. Makovec, T., *Cisplatin and beyond: molecular mechanisms of action and drug resistance development in cancer chemotherapy.* Radiology and oncology, 2019. **53**(2): p. 148.
152. Zitvogel, L., O. Kepp, and G. Kroemer, *Immune parameters affecting the efficacy of chemotherapeutic regimens.* Nature reviews Clinical oncology, 2011. **8**(3): p. 151-160.
153. Peng, J., et al., *Chemotherapy induces programmed cell death-ligand 1 overexpression via the nuclear factor-κB to foster an immunosuppressive tumor microenvironment in ovarian cancer.* Cancer research, 2015. **75**(23): p. 5034-5045.
154. Galluzzi, L., et al., *Immunological effects of conventional chemotherapy and targeted anticancer agents.* Cancer cell, 2015. **28**(6): p. 690-714.
155. Pai, S.G., et al., *Wnt/beta-catenin pathway: modulating anticancer immune response.* Journal of hematology & oncology, 2017. **10**(1): p. 1-12.
156. Rébé, C., et al., *Platinum derivatives effects on anticancer immune response.* Biomolecules, 2019. **10**(1): p. 13.
157. Testa, U., G. Castelli, and E. Pelosi, *Lung cancers: molecular characterization, clonal heterogeneity and evolution, and cancer stem cells.* Cancers, 2018. **10**(8): p. 248.
158. Kim, J. and D.S. Chen, *Immune escape to PD-L1/PD-1 blockade: seven steps to success (or failure).* Annals of Oncology, 2016. **27**(8): p. 1492-1504.
159. Dhatchinamoorthy, K., J.D. Colbert, and K.L. Rock, *Cancer Immune Evasion Through Loss of MHC Class I Antigen Presentation.* Frontiers in immunology, 2021. **12**: p. 469.
160. Xia, Y., S. Shen, and I.M. Verma, *NF-κB, an active player in human cancers.* Cancer immunology research, 2014. **2**(9): p. 823-830.
161. Bhatia, A. and Y. Kumar, *Cellular and molecular mechanisms in cancer immune escape: a comprehensive review.* Expert review of clinical immunology, 2014. **10**(1): p. 41-62.

162. Guinan, E.C., et al., *Pivotal role of the B7: CD28 pathway in transplantation tolerance and tumor immunity.* 1994.
163. Liu, H., et al., *A Novel Small Cyclic Peptide-Based 68Ga-Radiotracer for Positron Emission Tomography Imaging of PD-L1 Expression in Tumors.* Molecular pharmaceutics, 2021.
164. Taube, J.M., et al., *Differential expression of immune-regulatory genes associated with PD-L1 display in melanoma: implications for PD-1 pathway blockade.* Clinical Cancer Research, 2015. **21**(17): p. 3969-3976.
165. Chen, H., et al., *Multiplex Immunohistochemistry Applies to Examination of PD-1/PD-L1 on Immune Cells for Prognosis Prediction in Non-Small Cell Lung Cancer.* 2021.
166. Salmaninejad, A., et al., *PD-1/PD-L1 pathway: Basic biology and role in cancer immunotherapy.* Journal of cellular physiology, 2019. **234**(10): p. 16824-16837.
167. Ding, R., et al., *Single-cell transcriptome analysis of the immunosuppressive effect of differential expression of tumor PD-L1 on responding TCR-T cells.* bioRxiv, 2020.
168. Zhu, X. and J. Lang, *Programmed death-1 pathway blockade produces a synergistic antitumor effect: combined application in ovarian cancer.* Journal of gynecologic oncology, 2017. **28**(5).
169. Xue, Y., et al., *Platinum-based chemotherapy in combination with PD-1/PD-L1 inhibitors: preclinical and clinical studies and mechanism of action.* Expert Opinion on Drug Delivery, 2021. **18**(2): p. 187-203.
170. Kelland, L., *The resurgence of platinum-based cancer chemotherapy.* Nature Reviews Cancer, 2007. **7**(8): p. 573-584.

7. APPENDIX

7.1 Acknowledgements

First of all, I would like to thank my supervisor Rudolf Maria Huber for interviewing me remotely in 2018 and accepting me as his student for the Doctor degree at LMU. Prof. Rudolf Maria Huber played a very important role in the overall planning of the experimental content of my project. He is very kind to me and teaches me how to get along with others and how to act pragmatically. I wish Rudolf Maria Huber a long and healthy life. I would also like to thank Amanda Tufman, the director of the Lung Oncology Center in Munich. She guided me from the selection of the topic and the research methodology to the completion of this thesis. I am deeply impressed by her profound knowledge, rigorous scholarship, scientific acumen, dedication and professional ethics, and moved by her concern for students, which will serve as a model for my future study, research and work in my life.

Secondly, I would like to thank Rosemarie Kiefl, who helped me a lot during the whole process of my project and helped me to finish every order of reagents and cisplatin in time. She was able to solve every difficulty I encountered promptly. Without her help, my experiments could not have been completed successfully. I would like to extend my sincere thanks to Diego Kaufman-Guerrero for patiently guiding me through the design and completion of my thesis, which has greatly benefited me. I would also like to thank my colleague, Dong Liu, who has been very helpful in my study and life. I would also like to thank Tian Fei, Zhixiao Jiang, Chunfang Zan, and Qinlin Tang for their help in conducting my experiments.

Finally, I would like to thank my parents and friends who gave me a lot of encouragement and support during the COVID-19 epidemic. I would like to thank my sweetheart, whose kindness and wisdom made her unpretentious character. Her hard work, patience and perseverance have helped me achieve a lot. I would also like to thank my country and CSC for providing me with a scholarship so that I don't have to worry about the cost. I will always love you all.

7.2 Affidavit

Affidavit

Xu, Yinhui

Surname, first name

I hereby declare, that the submitted thesis entitled

PD-L1 enhanced cisplatin resistance in Non-Small Cell Lung Cancer through PI3K/AKT/mTOR

is my own work. I have only used the sources indicated and have not made unauthorised use of services of a third party. Where the work of others has been quoted or reproduced, the source is always given.

I further declare that the dissertation presented here has not been submitted in the same or similar form to any other institution for the purpose of obtaining an academic degree.

Shanghai, China 26.10.2022

Place, Date

Xu Yinhui

Signature doctoral candidate